
Reports

5-21-2018

Simple Parameterized Models for Predicting Mobility, Burial and re-exposure of underwater munitions. SERDP Final Report MR-2224

Carl Friedrichs
Virginia Institute of Marine Science

Sarah E. Rennie
Johns Hopkins University Applied Physics Laboratory

Alan Brandt
Johns Hopkins University Applied Physics Laboratory

Follow this and additional works at: <https://scholarworks.wm.edu/reports>



Part of the [Environmental Engineering Commons](#), and the [Oceanography Commons](#)

Recommended Citation

Friedrichs, C., Rennie, S. E., & Brandt, A. (2018) Simple Parameterized Models for Predicting Mobility, Burial and re-exposure of underwater munitions. SERDP Final Report MR-2224. Virginia Institute of Marine Science, William & Mary. <https://doi.org/10.25773/gk95-bb88>

This Report is brought to you for free and open access by W&M ScholarWorks. It has been accepted for inclusion in Reports by an authorized administrator of W&M ScholarWorks. For more information, please contact scholarworks@wm.edu.

REPORT DOCUMENTATION PAGE

Form Approved
OMB No. 0704-0188

Public reporting burden for this collection of information is estimated to average 1 hour per response, including the time for reviewing instructions, searching existing data sources, gathering and maintaining the data needed, and completing and reviewing this collection of information. Send comments regarding this burden estimate or any other aspect of this collection of information, including suggestions for reducing this burden to Department of Defense, Washington Headquarters Services, Directorate for Information Operations and Reports (0704-0188), 1215 Jefferson Davis Highway, Suite 1204, Arlington, VA 22202-4302. Respondents should be aware that notwithstanding any other provision of law, no person shall be subject to any penalty for failing to comply with a collection of information if it does not display a currently valid OMB control number. **PLEASE DO NOT RETURN YOUR FORM TO THE ABOVE ADDRESS.**

1. REPORT DATE (DD-MM-YYYY) 21-05-2018		2. REPORT TYPE Final		3. DATES COVERED (From - To) March 2012 – May 2018	
4. TITLE AND SUBTITLE Simple Parameterized Models for Predicting Mobility, Burial and Re-Exposure of Underwater Munitions				5a. CONTRACT NUMBER W912HQ-12-P-0022	
				5b. GRANT NUMBER	
				5c. PROGRAM ELEMENT NUMBER	
6. AUTHOR(S) ¹ Friedrichs, Carl T. ² Rennie, Sarah E. ² Brandt, Alan				5d. PROJECT NUMBER MR-2224	
				5e. TASK NUMBER	
				5f. WORK UNIT NUMBER	
7. PERFORMING ORGANIZATION NAME(S) AND ADDRESS(ES) ¹ Virginia Institute of Marine Science Box 1346, 1375 Greate Road Gloucester Point, VA 23062 ² Johns Hopkins University Applied Physics Laboratory 11100 Johns Hopkins Road Laurel, MD 20723				8. PERFORMING ORGANIZATION REPORT NUMBER	
9. SPONSORING / MONITORING AGENCY NAME(S) AND ADDRESS(ES) Strategic Environmental Research and Development Program (SERDP) 4800 Mark Center Drive Suite 17D08 Alexandria, VA 22350-3600				10. SPONSOR/MONITOR'S ACRONYM(S) SERDP	
				11. SPONSOR/MONITOR'S REPORT NUMBER(S)	
12. DISTRIBUTION / AVAILABILITY STATEMENT Approved for public release; distribution is unlimited					
13. SUPPLEMENTARY NOTES N/A					
14. ABSTRACT A compilation of 761 observations of scour-induced burial and 406 observations of initiation of motion of UXO-like objects are presented. The main factors that increase the scour-induced burial-to-diameter ratio (B/D) under (i) currents and (ii) waves are the (i) Shields parameter (θ) and (ii) Keulegan-Carpenter number. For cylinders under waves, B/D additionally increases as the current component parallel to wave orbitals decreases, as θ increases, and as the angle between wave orbitals and a cylinder's axis increases. Cylinders bury most, then spheres, and conical frustums bury least. Simple models dependent on these variables explain 85% of observed variance in B/D. Onset of motion is parameterized by $f_1 \Theta_{Ucrit}$, where Θ_{Ucrit} is the critical object mobility parameter, and f_1 accounts for inertia forces from time-varying pressure gradients. Θ_{Ucrit} is observed to decrease systematically as D/k increases, where k is the bed roughness. Theory combined with observations lead to $f_1 \Theta_{Ucrit} = a_1 (D/k)^{b_1}$. Observations give $a_1 = 1.75$ and $b_1 = -0.72$, which explains 89% of the observed variance in $f_1 \Theta_{Ucrit}$.					
15. SUBJECT TERMS underwater munitions, unexploded ordnance, scour-induced burial, initiation of motion					
16. SECURITY CLASSIFICATION OF:			17. LIMITATION OF ABSTRACT SAR	18. NUMBER OF PAGES 72	19a. NAME OF RESPONSIBLE PERSON Carl T. Friedrichs
a. REPORT U	b. ABSTRACT U	c. THIS PAGE U			19b. TELEPHONE NUMBER (include area code) (804) 684-7303

Table of Contents

Table of Contents.....	i
List of Tables.....	i
List of Figures.....	ii
List of Acronyms.....	ii
Key Words.....	iii
Acknowledgements.....	iii
1 Abstract.....	1
1.1 Objectives.....	1
1.2 Technical Approach.....	1
1.3 Results.....	1
1.4 Benefits.....	2
2 Objective.....	3
2.1 SERDP Relevance.....	3
2.2 Technical Objectives.....	3
3 Background.....	4
3.1 Self-burial of Objects on Sandy Beds by Scour.....	4
3.2 Initiation of Motion of Objects on Sandy Beds.....	6
4 Materials and Methods.....	9
4.1 Compilation and Analysis Methods for Self-Burial of Objects by Scour.....	9
4.1.1 Self-burial of Objects Under Mean Currents Only.....	10
4.1.2 Self-burial of Objects Under Waves Only.....	11
4.1.3 Self-burial of Objects Under Waves Plus Mean Currents.....	12
4.2 Compilation and Analysis Methods for Initiation of Motion of Objects.....	12
5 Results and Discussion.....	15
5.1 Results and Discussion for Self-Burial of Objects by Scour.....	15
5.1.1 Self-burial by Scour Under Mean Currents Only.....	15
5.1.2 Self-burial by Scour Under Waves and Under Waves Plus Currents.....	18
5.2 Results and Discussion for Initiation of Motion of Objects.....	24
6 Conclusions and Implications for Future Research.....	26
7 Literature Cited.....	28
Appendix A. Data Compilation for Equilibrium Self-Burial of Objects by Scour.....	32
Appendix B. Data Compilation for Initiation of Motion of Objects.....	54
Appendix C. List of Scientific/Technical Publications.....	68

List of Tables

Table 1. Properties of cylinders and pipe segments used in self-burial by scour experiments.....	9
Table 2. Properties of additional shapes used in scour burial experiments.....	10
Table 3. Environmental properties associated with observations of equilibrium burial depth.....	10
Table 4. Properties at initiation of motion of objects with $D > 0.5$ cm on beds composed of objects or roughness elements smaller than D	13
Table A1. Individual observations of self-burial of objects by scour, including object and environmental properties.....	32

Table A2. Notes regarding sources of individual parameters in Table A1.....	51
Table B1. Observations of initiation of motion of gravel clasts and spheres in steady flow.....	54
Table B2. Laboratory observations from William (2001) of initiation of motion of cylinders on a smooth bed under waves.....	60
Table B3. Laboratory observations of initiation of motion of cylinders placed on smooth and rough beds under currents in the absence of waves.....	62
Table B4. Notes regarding sources of individual parameters in Tables B1 to B3.....	66

List of Figures

Figure 1. Schematic of an object of diameter, D , that has buried to an equilibrium depth, B , below the mean height of the far field sand bed.....	4
Figure 2. Mobilizing forces on an object resting on the seabed.....	6
Figure 3. All observations of B/D plotted as a function of θ and KC	14
Figure 4. All observations of B/D under steady currents in the absence of waves plotted as a function of θ	16
Figure 5. B/D for steady currents normalized by the power-law relations from Fig. 4 and plotted as a function of ρ_o/ρ for large cylinders.....	17
Figure 6. All available observations of B/D for currents in the absence of waves, plotted as a function the final parameterized model for B/D under steady flow.....	18
Figure 7. All observations of B/D that include waves, plotted as a function of KC	19
Figure 8. (a) B/D normalized by the power-law relations from Fig. 7 and plotted as a function of $U_{c }/U_m$. (b) B/D additionally normalized by the exponential relation from Fig. 8a and plotted as a function of $\cos \alpha$	20
Figure 9. B/D normalized by the functional relationships from Fig. 7 and Fig. 8, and plotted as a function of θ for all cases that include waves.....	21
Figure 10. B/D normalized by the functional relationships from Fig. 7 through Fig. 9, for all non-fluidized live-bed data from Fig. 9 available within the range $1.7 < \rho_o/\rho < 3.3$	22
Figure 11. All available, non-fluidized, live-bed observations of B/D under waves (including cases with waves plus currents), plotted as a function of the final parameterized model for B/D under waves.....	23
Figure 12. Threshold for the initiation of motion of underwater objects.....	25

List of Acronyms

APL: Applied Physics Laboratory
DoD: Department of Defense
ESTCP: Environmental Security Technology Certification Program
JHU: Johns Hopkins University
SERDP: Strategic Environmental Research and Development Program
UnMES: Underwater Munitions Expert System
UXO: unexploded ordnance
VIMS: Virginia Institute of Marine Science

Keywords

underwater munitions, scour burial, initiation of motion, parameterized models

Acknowledgements

Funding was provided by the Munitions Response program area of SERDP. We thank the investigators and program managers associated with the underwater munitions burial and mobility component of Munitions Response for their insights and feedback, including Joe Calantoni, Diane Foster, Marcelo Garcia, Blake Landry, Herb Nelson, Meg Palmsten, Jack Puleo, Mike Richardson, and Peter Traykovski.

1 Abstract

1.1 Objectives

The objectives of this project were: (i) to identify and compile existing quantitative data from the scientific literature and from the coastal engineering, geology and Department of Defense (DoD) communities regarding the mobility, burial and re-exposure of unexploded ordnance (UXO) and UXO-like objects; (ii) to utilize these data to further develop and constrain simple, rational, parameterized models for UXO mobility, burial and re-exposure; and (iii) to provide these data and improved parameterized model formulations to SERDP investigators for use within a more sophisticated Underwater Munitions Expert System (UnMES) as well as providing them to the larger SERDP, DoD, coastal engineering, and scientific communities.

1.2 Technical Approach

Relevant data were identified and compiled through searches of academic journals, thesis and dissertation databases, DoD reports, interlibrary loan, and the internet. SERDP colleagues also provided new data through targeted laboratory experiments designed to fill crucial gaps in parameter space. Development of parameterized models for (a) initiation of motion and (b) scour-induced burial were guided most directly by (a) geological literature on the motion of gravel and cobbles in streams and (b) coastal engineering literature addressing seabed pipelines. Data and improved parameterizations were provided to SERDP investigators through an iterative approach such that gaps in the data supporting parameterized model development were used to guide new lab experiments. Results were provided to the larger community via two peer-reviewed articles: Friedrichs et al. (2016), which concentrated on object burial by scour, and Rennie et al. (2017), which focused additionally on the initiation of object motion. The findings of Friedrichs et al. (2016) and Rennie et al. (2017) that are most relevant to the objectives of MR-2224 are provided in this report. In addition, extensive tables in appendices to this report contain a tabular version of data synthesized by Friedrichs et al. (2016) and Rennie et al. (2017) and provide more detailed explanations of the sources of the individual data points.

1.3 Results

A compilation of 761 observations of scour-induced burial and 406 observations of initiation of motion of UXO-like objects are presented. The main factors that increase scour-induced burial-to-diameter ratios (B/D) under steady currents without waves are found to be an increased Shields parameter (θ) and small D (< 3 cm). For larger D , greater cylinder density also increases B/D under steady currents. The main factor that increases scour-induced B/D under wave-dominated conditions is an increased Keulegan-Carpenter number (KC). B/D additionally increases as the mean current component parallel to wave orbitals decreases. For cylinders under waves, B/D also increases as θ increases and as the angle between wave orbitals and a cylinder's axis increases. All else being equal, cylinders bury most, then spheres, and conical frustums bury least. Parameterized models dependent on the above variables explain 85% of observed variance in B/D . The force balance for onset of motion is parameterized by the mobility criteria, $f_1 \Theta_{Ucrit}$ where Θ_{Ucrit} is the critical object mobility parameter, and f_1 accounts for the possible effect of a time-varying horizontal pressure gradient. The threshold mobility parameter for an object on a

rigid seabed is observed to systematically decrease as D/k increases, where k is the bed roughness. Theory combined with observations suggested a power law relationship of the form $f_I \Theta_{Ucrit} = a_1(D/k)^{b_1}$. Using all compiled data with $D > 1$ cm, the best-fit power-law coefficients at 95% confidence is determined here to be $a_1 = 1.75 \pm 0.16$ and $b_1 = -0.72 \pm 0.03$, which explains 89% of the observed variance in $f_I \Theta_{Ucrit}$.

1.4 Benefits

This project (MR-2224) led to a highly successful collaboration between the Virginia Institute of Marine Science (VIMS) and the Johns Hopkins University Applied Physics Laboratory (JHU/APL) (via SERDP MR-2227, led by S. Rennie and A. Brandt) in support of the Underwater Munitions Expert System (UnMES). Via this project and its collaboration with MR-2227, simple parameterized process models for initiation of motion and scour-induced burial of seabed UXO by waves and currents were incorporated into the initial version of UnMES by Rennie and Brandt. Before this effort, existing data on the initiation of motion and scour-induced burial of UXO-like objects had not been as thoroughly compiled and synthesized. The lack of simple, robust parameterizations based on a sufficiently wide range of lab and field data may have limited the ability of DoD to efficiently determine the potential for underwater UXO burial and/or migration. Through the results of this project, a better understanding and predictive ability regarding the initiation of motion and scour-induced burial of UXO has been made possible, potentially enhancing the ability of DoD to productively detect, characterize and remediate UXO-related safety hazards. The scientific and engineering communities has also benefited from a better and more unified understanding of fundamental controls on the interaction of sediment with UXO-like objects, based on a synthesis encompassing a wide range of object sizes, shapes and densities.

2 Objective

2.1 SERDP Relevance

As a result of past military training and weapons testing activities, many former DoD military bases and test sites are contaminated with abandoned underwater munitions that need to be remediated (SERDP, 2010). These unexploded ordnance (UXO) may have been displaced from their original locations due to local water currents and often are buried under sediment making them difficult to locate during cleanup efforts. Better understanding and predictive ability regarding the mobility, burial and re-exposure of UXO will enhance the ability of DoD to productively detect and thus characterize and remediate these environmental and safety hazards. Topics of interest to the Munitions Response Program within SERDP explicitly include, “...predicting the location of munitions relative to the sea floor: whether they are found proud of the sea bottom, partially buried, or completely buried in the sediment as a function of historical use and site conditions” (SERDP, 2011).

In order to be useful under real-world conditions, a spatially large yet locally-resolved modeling effort aimed at helping determine the likely location of munitions relative to the sea floor must be reasonably accurate and reliable, but also simple and cost-effective enough to practically execute in a timely fashion. Furthermore, some dynamic aspects of UXO interaction with the sea bed are, at this point in time, simply too complicated to predict from “first principles”. Parameterized models utilize rationally-based physical scales to search for robust, site-independent empirical relationships between independent forcings and dependent physical behavior of interest. Parameterized modeling has a long history of success in numerous disciplines within science and engineering, including coastal processes and sediment dynamics.

2.2 Technical Objectives

The objectives of this project were:

- (i) To identify and compile existing quantitative data from the scientific literature and from the coastal engineering, geology and DoD communities regarding the mobility, burial and re-exposure of UXO and UXO-like objects;
- (ii) To utilize these data to further develop and constrain simple, rational, parameterized models for UXO mobility, burial and re-exposure; and
- (iii) To provide these data and improved parameterized model formulations to SERDP/ESTCP investigators for use within a more sophisticated Underwater Munitions Expert System (UnMES) as well as providing them to the larger DoD, coastal engineering and scientific communities.

3 Background

3.1 Self-burial of Objects on Sandy Beds by Scour

When an object sitting on the bed extends above the surrounding bed roughness, the object will alter the local flow pattern relative to the far field boundary layer. Such perturbations increase the velocities and stresses impinging on surface sediment immediately adjacent to the object. Nearby grains tend to be dispersed, resulting in a scour pit or pits that deepen until the tendency for sediment to be dispersed is balanced by a tendency for sediment to fall back into the pit(s). The difference in pressure at the bed upstream and downstream of the object may also drive seepage flow that can cause piping and tunnel erosion under the object (Whitehouse 1998, Sumer & Fredsøe, 2002, Voropayev et al., 2003).

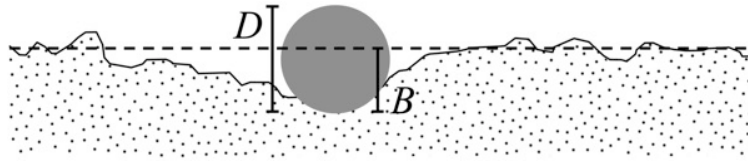


Figure 1. Schematic of an object of diameter, D , that has buried to an equilibrium depth, B , below the mean height of the far field sand bed. Modified from Cataño-Lopera et al. (2007).

As a result of the above processes, the object may eventually become unstable and settle into the scoured depression, reducing the object's exposure height (Fig. 1). For a given object, surrounding sediment, and far field hydrodynamics, an equilibrium value for the depth of scour-induced self-burial (B) is anticipated to be a function of the far field waves and currents, the properties of the surrounding sediment, and the size, shape and density of the object (Sumer & Fredsøe, 2002, Cataño-Lopera et al., 2007, 2011).

Two parameters have been identified most often in the literature as fundamental, overarching controls on the equilibrium depth of self-burial by scour for objects on sandy beds: the Shields parameter and the Keulegan-Carpenter number.

The sediment Shields parameter (θ), which is a dimensionless representation of bed shear stress (τ_b), is given by:

$$\theta = \tau_b / [(\rho_s - \rho) g d_{50}] \quad (1)$$

where ρ_s is grain density (2.65 g/cm³ for quartz sand), ρ is fluid density (taken here to be 1.0 g/cm³), g is acceleration due to gravity (9.81 m²/s), and d_{50} is the median bed grain size. The Shields parameter is proportional to the drag force acting on a sand grain, which tends to mobilize the grain, divided by the immersed weight of the sand grain, which tends to keep the grain stationary.

If an object enhances turbulence enough to initiate local sediment motion, but far-field θ is below its critical value for sediment motion (θ_{cr}), then scour around the object is known as clear-

water scour. For $\theta > \theta_{cr}$, (where $\theta_{cr} \approx 0.03$ to 0.06 for well-sorted sand with $(\tau_b/\rho)^{1/2}d_{50}/\nu^3 \geq 4$, and ν is kinematic viscosity), scour around an object is known as live-bed scour (Whitehouse, 1998).

The Keulegan-Carpenter number (KC), is given by:

$$KC = U_m T D \quad (2)$$

where U_m is maximum near-bed wave plus current velocity, T is wave period, and D is object diameter. KC is proportional to the ratio of the maximum orbital particle excursion distance, $A = U_m T / (2\pi)$, to the object diameter, such that $KC = 2\pi A / D$. (Note that $U_m \geq U_w$, where U_w is the amplitude of the wave orbital velocity alone; i.e., U_m includes the near-bed mean current, U_c , while U_w does not.)

If KC is small, vortices are more likely to be concentrated closer to the object, while if KC is large, vortices will be swept farther from the object. Thus narrower, steeper scour pits may be expected at small KC , while wider, more gently sloped scour pits may be expected at larger KC . Wider scour pits may then, in turn, shelter an object from ambient flow less, exposing the object to higher near-bed velocities and ultimately lead to deeper scour (Sumer & Fredsøe, 2002). KC is also proportional to the ratio of the wave boundary thickness (δ) to object diameter, and it has previously been found that the depth of scour tends to increase with greater δ . (Sumer & Fredsøe, 2002).

Based on the existing literature, it is not immediately clear if θ or KC is typically more important, or if both are usually needed to successfully predict B/D . For individual sets of observed data describing the self-burial of objects by scour on sandy beds, several authors have previously found θ to be the dominant parameter (Whitehouse, 1998; Cataño-Lopera et al., 2007, Demir & García, 2007, Friedrichs 2007). Some have found only KC to be necessary (Sumer et al., 2001; Truelsen et al., 2005; Cataño-Lopera et al., 2011); and others have argued that both are needed (Stansby & Starr, 1992; Voropayev et al., 2003; Cataño-Lopera & García, 2006.)

When the direction of a relatively weak mean current is parallel to wave orbital velocity, the depth of scour under pipelines and self-burial of cylinders has been found to decrease as the strength of the near-bed mean current (U_c) increases (up to $U_c/U_m \approx 0.5$) (Sumer & Fredsøe, 2002, Cataño-Lopera & García, 2006). This occurs because, if U_c and U_w are parallel, the wave and current oppose each other during half of wave cycle, reducing the intensity of the lee wake on one side.

Depth of scour under pipelines and self-burial of cylinders has also been found to decrease if the angle (α) between maximum velocity and a pipeline or cylinder's axis remains small throughout the scour process (Sumer & Fredsøe, 2002, Cataño-Lopera & García, 2007).

The density of the object (ρ_o) can further affect B/D . Under conditions of a liquefied sand bed, pipelines tend to rise through the bed for $\rho_o < \rho_{cr}$, and sink for $\rho_o > \rho_{cr}$, where ρ_{cr} is the critical density for object flotation (Sumer, 2014). In the absence of liquefaction, Cataño-Lopera & García (2006) still observed a tendency for heavy cylinders to bury deeper. Cataño-Lopera et al.

(2007) found bed fluidization rather than classic scour to dominate burial of cylinders in sand for $\theta > \sim 0.7$ to 0.8.

Far-field geological affects, including bedform migration (Voropayev et al., 1999), subsurface resistant layers (McNinch et al., 2006), and large-scale erosion or deposition (Jenkins et al., 2007), can also affect the burial depth of objects subject to scour on a sandy bottom. Since bedform height and length both scale with grain size, and objects settle at least to the base of troughs if bedform wavelengths are large compared to D (Voropayev et al., 1999), one may expect B/D to increase as d_{50}/D increases (after accounting for the inverse effect of d_{50} in θ).

Finally, the shape of the object is likely to affect the depth of scour-induced burial. For example, Cataño-Lopero et al. (2011) found that conical frustums produce significantly less scour and self-burial than cylinders of similar D under similar wave forcing. This is likely because cone shapes offer less resistance to flow than cylinders and thus shed weaker vortices (Sumer & Fredsøe, 2002).

3.2 Initiation of Motion of Objects on Sandy Beds

The underwater initial movement of various objects, including gravel, cobbles and spheres, has been parameterized in the past by considering the competing forces of fluid drag (F_D), lift (F_L), immersed weight (F_W), and inertia (F_I), the magnitudes of which are reasonably well represented by the following equations and schematically shown in Fig. 2a (Wiberg & Smith, 1987).

$$F_D = \frac{1}{2} C_D \rho A_D U^2 \quad (3)$$

$$F_L = \frac{1}{2} C_L \rho A_L U^2 \quad (4)$$

$$F_W = (\rho_o - \rho) g V_T \quad (5)$$

$$F_I = C_I \rho V_I \partial U / \partial t \quad (6)$$

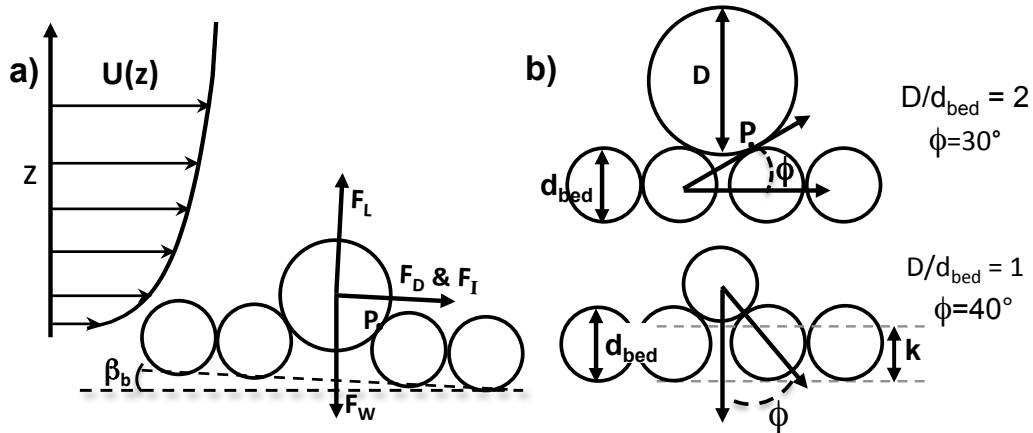


Figure 2. Mobilizing forces on an object resting on the seabed. (a) Object on a rough bed subject to a steady current and the presence of a bottom slope β ; (b) Object of diameter D partially blocked by neighboring objects of diameter d_{bed} with effective roughness length scale k , and friction angle ϕ about pivot point P . In this hypothetical example, the Nikuradse effective roughness $k \approx 0.75 d_{bed}$ for spheres. Diagram adapted from Kirchner et al. (1990) and Wiberg & Smith (1987).

In Eq. (3) to (6), ρ_o is the object density; C_D , C_L and C_I are drag, lift and inertia coefficients; A_D and A_L are the projected vertical and horizontal cross-sectional areas of the object exposed to drag and lift; and V_T and V_I are the total object volume and the object volume exposed to flow. (Note that F_I/C_I is equal to the inertial response of an object-sized volume of water responding to a time-varying horizontal pressure gradient. Thus F_I is a measure of the time-varying horizontal pressure gradient force acting on the object.) Following James (1993), U is defined to be the far field velocity at a height near the top of the object. In this context, U is defined as the instantaneous velocity, averaged over turbulent scales but not averaged over waves.

The threshold of motion condition occurs when the sum of mobilizing forces acting on the object just exceeds the sum of stabilizing forces. If initial motion occurs by rotation about a single pivot point, P , then it is appropriate to evaluate the moments of force about P , where the pivot angle, ϕ , is the angle between the horizontal (x) axis and a line tangential to P (see Fig. 2b) (Komar & Li, 1988, James, 1993). If the distance from P to the line of action for each force is about the same, then the threshold condition is given simply by balancing the sum of forces in the horizontal and vertical directions:

$$(\cos \phi) (F_D + F_I + F_W \sin \beta_b) = (\sin \phi) (F_W \cos \beta_b - F_L) \quad (7)$$

where β_b is the slope of the bed and ϕ is also known as the angle of repose. Under conditions of no flow, $F_D = F_L = F_I = 0$, and incipient motion occurs when $\phi = \beta_b$. For homogeneous gravel-sized particles, the angle of repose measured in laboratory experiments ranges from 20° to 40° (Li & Komar, 1986), depending on particle shape and pivot geometry.

If initial motion occurs by more complex motion than pivoting (e.g. sliding), ϕ can be operationally defined by Eq. (7) (i.e. independent of pivoting), such that $\tan \phi$ is set equal to the ratio of the net force in the horizontal direction relative to the net force in the vertical when incipient motion occurs (Garcia, 2008). With that logic mind, ϕ is also known as the friction angle (Kirchner et al., 1990) and $\mu = \tan \phi$ is known as the friction coefficient (Garcia, 2008). In this context, μ can be used to quantify frictional resistance to initiation of motion whether an object initially moves by pivoting, by sliding, or by some more complex motion.

To highlight the role of fluid drag relative to submerged weight, one can re-express F_I and F_L in terms of F_D , and place the ratio of F_D to F_W to the left hand side of the balance. Doing so for threshold conditions then yields

$$f_I \Theta_{Ucrit} = \alpha_t \gamma [\mu (\cos \beta_b) - (\sin \beta_b)] / [1 + \mu (f_L/f_I)] \quad (8)$$

where $f_I = |F_D + F_I|/F_D$; $\gamma = (2 V_T)/(C_D D A_D)$; $f_L = F_L/F_D$; and

$$\Theta_U = U^2/[g D (\rho_o/\rho - 1)] \quad (9)$$

where Θ_U is the object's mobility number (Nielsen, 1992), and the subscript "crit" in Eq. (8) indicates the critical value for initiation of object motion. The parameter α_t , where $\alpha_t \leq 1$, is

introduced in Eq. (8) to allow for the role of turbulent fluctuations in U causing brief peaks in the mobilizing forces, which reduces Θ_{Ucrit} (Komar & Li, 1988).

Additional simplifications to Eq. (8) are common when considering the initiation of motion of objects such as gravel or cobbles. Often, the far-field bed is considered to be effectively horizontal ($\beta_b \approx 0$) although it is simple to reintroduce bed slope when relevant. If flow is steady, or for a situation where surface waves are present and the wave orbital excursion distance is much larger than D , then $f_l \approx 1$. In that case Eq. (8) reduces to

$$\Theta_{Ucrit} = \alpha_t \gamma \mu / (1 + \mu f_L) \quad (10)$$

Studies of mixed sediment sizes as well as mixed sizes of ellipsoids and spheres (Miller & Byrne, 1966; Li & Komar, 1986) suggest that the friction coefficient, $\mu = \tan \phi$, for individual objects sitting atop a non-cohesive sediment bed is a systematically decreasing function of the diameter of the object, D , relative to the roughness of the surrounding bed, k , expressed in terms of the ratio D/k . The physical basis for a decrease in μ as D/k increases is that the larger D is relative to k , the larger the protrusion of the object into the flow, and the easier it is for an object to pivot or slide over the underlying bed roughness. Conversely, the smaller D is relative to k , the more likely the underlying bed roughness will prevent object motion. In sediment dynamics (Soulsby, 1997), the roughness of the sea bed is characterized by the roughness length z_0 , which is defined by the structure of the velocity profile within the bottom boundary layer, where $U(z) \approx (u^*/0.41) \log(z/z_0)$, and $u^* = (\tau_b/\rho)^{1/2}$. Alternately, z_0 is estimated by the Nikuradse roughness, which gives $k = 30 z_0$ under fully rough turbulence (Soulsby, 1997).

For the case of spheres of various sizes, a complete solution for $\gamma \mu / (1 + \mu f_L)$ for the right hand side of Eq. (10) as a function of D/k can be obtained from existing literature values. For a sphere placed atop a closely packed bed of similar underlying spheres, geometry (with $V_T = (4/3)\pi(D/2)^3$ and $A_D = \pi(D/2)^2$), gives $\gamma = 4/(3 C_D)$. For the present focus on UXO-like objects, the range of object Reynolds numbers is $Re = DU/\nu \approx 10^3$ to 10^5 (with $D \approx 1$ to 20 cm, $U \approx 10$ to 50 cm/s, and $\nu \approx 10^{-2}$ cm²/s). For that range of Re , spheres have $C_D \approx 0.4$ (Schlichting & Gersten, 2000), therefore $\gamma = 3.33$, and $f_L \approx 0.8$. Laboratory measurements of the angle of repose for spheres, Li & Komar (1986) found a good fit to ϕ in degrees of $\phi = 20.4^\circ (D/d_{bed})^{-0.75}$ where d_{bed} is the bed sphere diameter. Defining k as the bed Nikuradse roughness (Garcia, 2008), such that $k = 30 z_0$ in rough turbulence, then the results of Schlichting & Gersten (2000) for a bed of close-packed spheres gives $k = 0.75 d_{bed}$, so that $\phi = (25.3 (D/k)^{-0.75})^\circ$. Putting these all together, we then have for spheres:

$$\Theta_{Ucrit} = 3.3 \alpha_t \tan[(25.3(D/k)^{-0.75})^\circ] \{ 1 + 0.8 \tan[(25.3(D/k)^{-0.75})^\circ] \}^{-1} \quad (11)$$

Given the explicit dependence of Eq. (11) on D/k , $\mu / (1 + \mu f_L)$ in Eq. (10) is expected to be a function of D/k for UXO-like objects, and therefore the critical object mobility number will depend on the ratio of the object diameter to the bed roughness. Translating degrees to radians and solving for the asymptote for (11) at large D/k gives $\Theta_{Ucrit} \approx 1.46 \alpha_t (D/k)^{-0.75}$.

For bottom-sitting objects subjected to short period waves, the inertial response to time-varying pressure gradients, F_I , can be a significant contributor relative to the drag force, F_D . For a near-bed wave orbital described by $U = U_W \sin(2\pi t/T)$, it follows from the definitions of f_I , F_D , and F_I that the maximum value for f_I over the wave cycle in the absence of a mean current is approximately

$$f_I = (F_D^2 + F_I^2)^{1/2}/F_D \approx (1 + 16\pi^2 (C_I/C_D)^2 (KC)^{-2})^{1/2} \quad (12)$$

Sumer & Fredsoe (2006) indicate that for a cylinder on a bed, $C_I/C_D \approx 2$ for $KC < \sim 30$. (As $KC \rightarrow \infty$, the flow becomes effectively steady; F_D dominates F_I , and $f_I \rightarrow 1$.) Thus, to compare Θ_{Ucrit} for conditions where the ambient flow is oscillatory or otherwise accelerating to those where the flow is steady, the values of Θ_{Ucrit} for the former can be divided by f_I to account for the role of the time-varying pressure gradient.

4 Materials and Methods

4.1 Compilation and Analysis Methods for Self-Burial of Objects by Scour

Sufficiently complete data on the equilibrium self-burial depth of objects on sandy beds, associated object and sand properties, and wave and current forcing were identified in 18 papers, reports, theses and dissertations (see Tables 1 to 3). A total of 761 data points for B/D were compiled, including 667 measurements for self-buried cylinders, 58 for conical frustums, 25 for spheres, and 11 for tapered cylinders. The data include 379 cases measured under waves only, 256 under waves plus mean currents, and 126 under steady currents; 694 are laboratory measurements, while 67 are field measurements. The compiled data sets are provided in detailed tabular form in Appendix A of this report.

Table 1. Properties of cylinders and pipe segments used in self-burial by scour experiments. N = reference number, D = diameter (vertical dimension), L = length (horizontal dimension), ρ_o = object density. Dashes indicate range of values reported.

N	Reference	D cm	L cm	ρ_o g/cm ³
1	Carstens & Martin (1963)	1.3-8.8	5.1-35.1	2.7
2	Starr (1989)*	1.3-2.5	15.0-45.0	1.8-10.6
3	Sumer & Fredsøe (1994)*	11.0	198	1.3-6
4	Sumer et al. (2001)*	2.0-10.0	59.4-198	1.3-6
5	Cataño-Lopera (2005)	5.1-25.4	20.3-102	2.0-7.8
6	Demir & García (2007)	7.5-12.5	20.0-34.4	2.3-7.8
7	Cataño-Lopera et al. (2007)	8.6-10.0	20.0-34.4	2.3-2.7
8-14	ONR-MBP ⁺	47.0-53.3	150-203	2.0-2.4
15	Rennie et al. (2017)	2.5-10.5	9.9-32.0	1.2-7.9

*Cylinders horizontally fixed; others free to move horizontally.

⁺Office of Naval Research Mine Burial Program data sources are (8) Bower et al. (2007), (9) Bradley et al. (2007), (10) Mayer et al. (2007), (11) Traykovski et al. (2007), (12) Trembanis et al. (2007), (13) Wolfson (2005), and (14) Wolfson et al. (2007).

Table 2. Properties of additional shapes used in scour burial experiments. Symbols as in Table 1.

<i>N</i>	Reference	<i>D</i> cm	<i>L</i> cm	ρ_o g/cm ³
16	Truelsen et al. (2005) (spheres)	3.0-7.3	3.0-7.3	2.0-4.0
17	Cataño-Lopera et al. (2011) (conical frustums)	7.5-25.0	15.0-50.0	2.0
18	Pang & Liu (2014) (tapered cylinders)	5.0	22.0	2.7
19	Rennie et al. (2017) (tapered cylinders)	7.9	31.8	2.4

Table 3. Environmental properties associated with observations of equilibrium burial depth, including range of values. *N* = reference number, d_{50} = median bed grain size, U_w = wave orbital velocity amplitude, T = wave period, U_c = current velocity, h = water depth, B/D = burial depth/object diameter.

<i>N</i>	d_{50} mm	U_w cm/s	T sec	U_c cm/sec	h m	B/D
1*	0.30-0.59	27-76	3.6	0	0.30	0.29-1.59
2	0.22	0-29	1.6-2.6	0-37	0.25	0.04-0.81
3-4	0.18-0.20	0-50	1.5-3.5	0-54	0.20-0.33	0.19-0.82
5	0.25	15-55	1.4-6.9	0-17	0.56	0.02-0.77
6-7*	0.25	0-80	3.0-12.0	0-45	0.60	0.15-1.00
8-14 ⁺	0.14-0.65	50-128	6.1-9.6	10-40	12-13	0.02-1.17
15	0.42	0	∞	20-60	0.46	0.02-2.27
16	0.18	0-42	1.1-480	0-40	0.30-0.54	0.02-0.57
17	0.25	20-65	1.5-5.7	0-15	0.60	0.02-0.15
18	0.12-0.21	25-39	1.5-2.0	0	0.30	0.58-1.06
19	0.42	0	∞	30-58	0.46	0.12-1.17

*U-tube; +field observations ($U_w = U_{w1/3}$); others lab flumes.

4.1.1 Self-burial of Objects Under Mean Currents Only: The far-field bed stress ($\tau_b/\rho = u_*^2$) under mean currents in the absence of waves was calculated following Yalin (1992) as presented in García (2008). The mean current, U_{obs} , observed at height z_{obs} above the far-field mean bed elevation was used to solve for shear velocity, u_* , in

$$\frac{U_{obs}}{u_*} = \frac{1}{\kappa} \log\left(\frac{z_{obs}}{k}\right) + B_s \quad (13)$$

where B_s is an empirical function of the roughness Reynolds number, $Re_* = u_*k/\nu$, which is given by

$$B_s = 8.5 + [2.5 \log(Re_*) - 3] e^{-0.12 |\log(Re_*)|^{2.42}} \quad (14)$$

In the above, ν is kinematic viscosity of water (set to 10^{-6} m²/s), $\kappa = 0.41$ is the von Karman constant, and $k = 2.5d_{50}$ is the bed roughness height. An advantage of Eqs. (13) – (14) is that they simultaneously represent hydraulically smooth and rough turbulence, as well as the transitional range between them (García, 2008).

The Shields parameter under mean currents was calculated via Eq. (1) using the value of $\tau_b/\rho = u_*^2$ determined from Eqs. (13) – (14). In applying Eqs. (13) – (14) in our analysis, u_* represents skin friction, and we do not adjust u_* to compensate for the possible effects of bedforms. Under steady currents in the absence of waves, the value assigned to the Keulegan-Carpenter number is $KC = \infty$.

4.1.2 Self-burial of Objects Under Waves Only: Bed stress under waves in the absence of currents was calculated via the equation

$$\tau_b = 0.5\rho f_w U_w^2 \quad (15)$$

where f_w is the wave friction factor, and U_w is the amplitude of the near-bed wave orbital velocity. All the wave-only data identified for this analysis was collected in lab flumes, and U_w is taken to be equal to the amplitude of the near-bed orbital velocity as reported in the references or as calculated from observed wave height assuming linear wave theory. No further adjustment of U_w was made to account for the elevation of the observation relative to the bed.

The wave friction factor was calculated using the formulation of Myrhaug & Slaattelid (1990) as presented by Demir & García (2007):

$$\frac{0.32}{f_w} - 1.64 = \left\{ \log(6.36 f_w^{0.5} A / k) - \log \left[1 - \exp \left(-0.262 \frac{R_w f_w^{0.5}}{(A/k)} \right) + \frac{4.71(A/k)}{R_w f_w^{0.5}} \right] \right\}^2 \quad (16)$$

where $R_w = U_w A / \nu$ is the wave Reynolds number and $A = U_w T / (2\pi)$ is the amplitude of the wave orbital excursion distance. Like Eq. (14), Eq. (16) has the advantage of representing hydraulically smooth and rough turbulence as well as the transitional range between them (Demir & García, 2007). In the absence of currents, $KC = U_m T / D = U_w T / D$, because $U_m = U_w$ when $U_c = 0$.

4.1.3 Self-burial of Objects Under Waves Plus Mean Currents: For the case of waves plus mean currents, where U_c is significantly less than U_w , Eqs. (15) and (16) can still be used to estimate τ_b , but with U_w supplemented by an appropriate contribution from U_c (Cataño et al., 2011). The maximum wave plus current velocity (U_m), which replaces U_w in the presence of waves plus currents, was calculated in the present study as

$$U_m = \sqrt{U_w^2 + U_c^2 + 2U_w U_c |\cos \beta|} \quad (17)$$

where β is the angle between U_w and U_c , and U_c is calculated as described in Section 2.1. Under waves plus currents, U_m is used in calculating A , R_w and f_w , as well as τ_b and KC . For collinear combined waves and currents in wave flume observations, $\beta = 0$.

For the field observations examined in this paper, U_w in Eq. (17) was estimated from observations following the guidance of Myrhaug & Ong (2009) for a natural oceanic random wave spectrum. The orbital velocity amplitude corresponding to the highest 1/3 among random waves ($U_{w1/3}$) in a stationary narrow-band sea state is used here, as it is reasonable to assume that it is mainly the highest waves that are responsible for the scour process (Myrhaug & Ong, 2009). Here $U_w = U_{w1/3}$ is calculated as $U_{w1/3} = 2\sigma_U$ (Dean & Dalrymple, 1991), where σ_U is the standard deviation of the instantaneous velocity time-series over the course a ~ 10 minute ‘‘burst’’. Following Friedrichs (2007), the most energetic burst preceding each observation of B/D is chosen to represent U_w . It is assumed that each high-energy wave event (each typically a day to several days in duration) lasted long enough for self-burial to reach its equilibrium value.

The field observations considered here were collected on the inner shelf, between 1 and 10 km offshore, and all at $h \approx 12$ m (Trembanis et al., 2007). During wave events large enough to induce significant seabed scour at these locations, U_w and U_c tend to be at a relatively large angle to each other, and here we let $\beta = 90^\circ$ in Eq. (17) for the field cases.

Finally, Eqs. (13) – (14) were used to adjust U_{obs} to a consistent mean current reference value, U_c , that could be used to compare current forcing across experiments. Here we define U_c to be the current speed that is predicted by Eqs. (13) – (14) at $z = D$.

4.2 Compilation and Analysis Methods for Initiation of Motion of Objects

Sufficiently complete data on the initiation of motion of objects under waves or currents with object diameters larger than the surrounding roughness were identified in 14 papers, reports, theses and dissertations (Table 4). A total of 406 data points for initiation of motion were compiled, including 182 measurements for gravel clasts, 28 for glass spheres, and 196 for cylinders of various densities. 132 of the gravel measurements were from natural streams; all other measurements were from lab experiments. 68 of the cylinder measurements were collected under waves; all other measurements were under unidirectional flow. For gravel and spheres, only cases for which $D > 0.5$ cm and for which D is larger than the bed grain size are reproduced here. The compiled data sets are provided in detailed tabular form in Appendix B of this report.

Compilation of the data summarized in Table 4 required definitions for bed roughness, k , and procedures for estimating U_{crit} at $z = D$. For observations over rough beds, k was taken to be the far-field effective bed roughness as defined by the Nikuradse equivalent roughness height. Following this convention, the effective roughness of gravel beds in the absence of bedforms is approximately $k = 2.5 d_{50}$ (Garcia, 2008) and that for a bed of close-packed uniform spheres is $k = 0.75 d_{bed}$ (Schlichting & Gersten, 2000). For steady flow over smooth beds, $z_0 = \nu/(9u^*)$, and k was set to a minimum value of $k = 30 \nu/(9u^*)$. For cases with a carpeted bed, following Rennie et al. (2017), k was set to 0.5 times the carpet’s fiber height. For cylinders on a smooth bed roughened with a coating of sand of diameter d_{coat} , a contribution of $k = 2.5 d_{coat}$ was utilized in the ratio D/k , but the far field k relevant to log-layer structure did not include d_{coat} . For sand-

roughened cylinders on a carpeted bed, $k = d_{coat} + 0.5$ times the carpet's fiber height (Rennie et al. 2017).

Table 4. Properties at initiation of motion of objects with $D > 0.5$ cm on beds composed of objects or roughness elements smaller than D . Objects include: gravel clasts on mobile beds in natural streams ($N = 1-4$) and in lab flumes (5-10); spheres on beds formed of fixed, close-packed spheres (11); cylinders on a smooth bed under waves (12) or under steady flow (13-14); and cylinders on a rough, fixed bed under steady flow (14). N = reference number, D = object diameter (vertical dimension for cylinders), ρ_o = object density, $\Theta_{U_{crit}}$ = object's critical mobility number, f_I = inertial force factor (see Eq. (12)), and T = wave period.

N	Reference	D cm	D/k g/cm ³	ρ_o/ρ	$\Theta_{U_{crit}}$
1	Hammond et al. (1984)*	0.8-3.5	0.42-1.9	2.7	1.5-2.3
2	Carling (1983)*	2.1-43	0.43-8.6	2.7	0.93-4.8
3	Milhous (1973)*	2.4-11	0.48-2.3	2.7	1.0-2.6
4	Mao & Surian (2010)	1.6-6.4	0.46-1.9	2.7	0.85-4.2
5	Kuhnle (1993)	0.7-1.0	2.8-8.1	2.7	0.92-1.8
6	Patel & Ranga Raju (1999)	0.5-1.4	0.59-2.0	2.7	1.4-2.3
7	Wilcock (1987)**	0.5-0.6	0.47-1.3	2.7	0.90-1.4
8	Day (1980)**	0.5-0.7	1.2-1.5	2.7	1.0-1.1
9	Misri et al. (1984)**	0.5-1.3	0.52-1.5	2.7	1.2-1.5
10	Dhamotharan et al. (1980)**	0.5-0.7	0.94-1.3	2.7	1.8-2.0
11	James (1993)	0.6-2.2	1.6-5.8	2.3-2.6	0.23-0.86
12	Williams (2001)	1.8-11	59-440	2.1-7.6	0.0093 ⁺ -0.11 ⁺
13	Davis et al. (1999)	4.8-12	74-360	1.6-3.2	0.016-0.035
14	Rennie et al. (2017)	2.5-11	10-460	1.2-7.9	0.020-0.41

*As reported by Komar (1996); **as reported by Wilcock & Southard (1988);

⁺ $f_I \Theta_{U_{crit}}$ values with $T = 1-9$ sec.

For steady flow cases where published values were of the critical Shields parameter (Θ_{crit}) rather than the critical flow velocity (U_{crit}), U_{crit} at a height $z = D$ above the bed was estimated based on a log-profile. If an observed U_{crit} under unidirectional flow was provided at a height other than $z = D$, a boundary layer log-profile was used to adjust U_{crit} to its expected value at $z = D$. For unidirectional flow over beds intermediate between smooth and fully rough turbulent, z_0 for use in the log adjustment was determined as a function of u_*k/ν following Yalin (1992) as presented by Garcia (2008) (see Eqs. (13) – (14) above).

For smooth beds under waves, the effective roughness for D/k was computed as $k = 30 \nu/(9u_*)$, with $u_* = (f_w/2)^{1/2}U_w$, such that U_w is the wave orbital velocity amplitude just above the wave boundary layer. The wave friction factor, f_w , for smooth beds was calculated iteratively from the below equation following Pedocchi & Garcia (2009):

$$f_w = \left(1.9 \log \left(0.7 f_w \frac{U_w^2}{\omega \nu} \right) \right)^{-2} \quad (18)$$

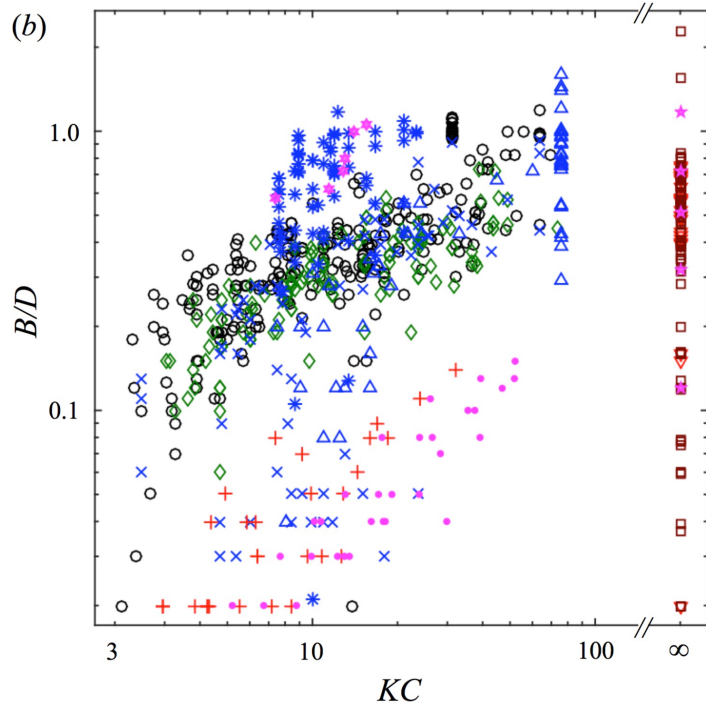
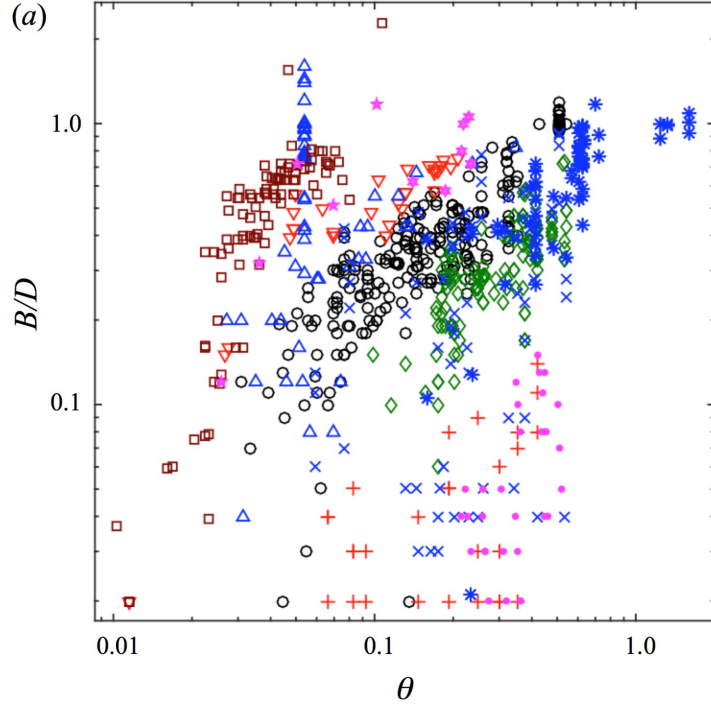


Figure 3. All observations of B/D plotted as a function of (a) θ and (b) KC . Cylinders with waves plus currents in the field = $*$ (all others are lab measurements); cylinders with $\alpha < 60^\circ$ = \times (all others have $\alpha \geq 60^\circ$); cylinders with $D < 2.6$ cm for waves only = \triangle and for currents only = \square (all other objects have $D \geq 3.0$ cm); other cylinders and spheres with currents only = ∇ ; cylinders with waves plus currents = \diamond ; cylinders and spheres with waves only = \circ ; conical frustums with waves only = $+$; conical frustums with waves plus currents = \bullet ; tapered cylinders with waves only = \star ; tapered cylinders with currents only = \star .

where $\omega = 2\pi/T$. At initiation of motion under waves, U_{crit} at the top of the object was taken to be equal to U_w , such that the top of the object was assumed to extend above the top of the wave boundary layer.

5 Results and Discussion

5.1 Results and Discussion for Self-Burial of Objects by Scour

All data for equilibrium burial depth of objects by scour (B/D) are plotted as a function of the Shields parameter (θ) in Fig. 3a and as a function of the Keulegan-Carpenter number (KC) in Fig. 3b. The distinct trends in equilibrium burial depth seen for different classes of objects under various forcing scenarios in Fig. 3a and Fig. 3b strongly suggest that neither θ alone nor KC alone can adequately predict B/D for all the available observations involving currents, waves, and combinations of both. For example, cylinders subject to currents alone systematically bury deeper at a given value of θ than similar objects subject to wave forcing (Fig. 3a). And the cylinders observed in the field buried significantly deeper for a given value of KC than cylinders observed in the lab (Fig. 3b).

These and other distinct trends in B/D as a function of θ , KC , and additional parameters can be better understood by considering current- versus wave-forced cases separately, and by systematically examining the influence of several of the possible governing factors for each case via an informal step-wise multiple regression.

5.1.1 Self-burial by Scour Under Mean Currents Only: Although $KC = U_m T/D$ is correlated to B/D under waves (Fig. 3b), KC cannot be used to predict different degrees of burial under mean currents because KC is effectively infinite for all mean flows. Authors such as Sumer & Fredsøe (2002) who predict B/D under mean flows based on KC alone have argued that under conditions of live-bed scour ($\theta > \theta_{cr}$), self-burying objects of the same shape will all eventually reach the same equilibrium burial depth (in the absence of bed liquefaction or other complicating effects as outlined in Section 3.1). For cylinders, Sumer et al. (2001) found the universal live-bed value of B/D under mean currents to be about 0.7, while for spheres, Truelsen et al. (2005) found the live-bed value of B/D to be about 0.5. These authors recognize that θ will still increase B/D under clear-water scour, and θ also decreases the time-scale needed to reach equilibrium B/D under live-bed conditions.

In contrast to KC , the Shields parameter, $\theta = \tau_b/[(\rho_s - \rho)gd_{50}]$, can effectively distinguish among mean current forcing scenarios as bottom stress and sand grain vary (Fig. 4). The data compiled for mean current forcing in Fig. 4 suggest that B/D increases as a function θ for live-bed scour, as well as for clear-water scour, although the exponents relating B/D to θ are of smaller magnitude for live-bed scour.

Relationships for clear-water and live-bed scour displayed in Fig. 4 were found by fitting relationships of the form $B/D = f\theta = a\theta^b$ for θ greater and less than 0.04, respectively. The intersection of the best-fit lines for clear-water and live-bed scour occurred near $\theta_{cr} = 0.04$ for

both smaller ($D < 2.6$ cm) and larger ($D \geq 8.6$ cm) cylinders. (No burial data were identified in the literature for cylinders with D between 2.6 and 8.6 cm under steady flow conditions.)

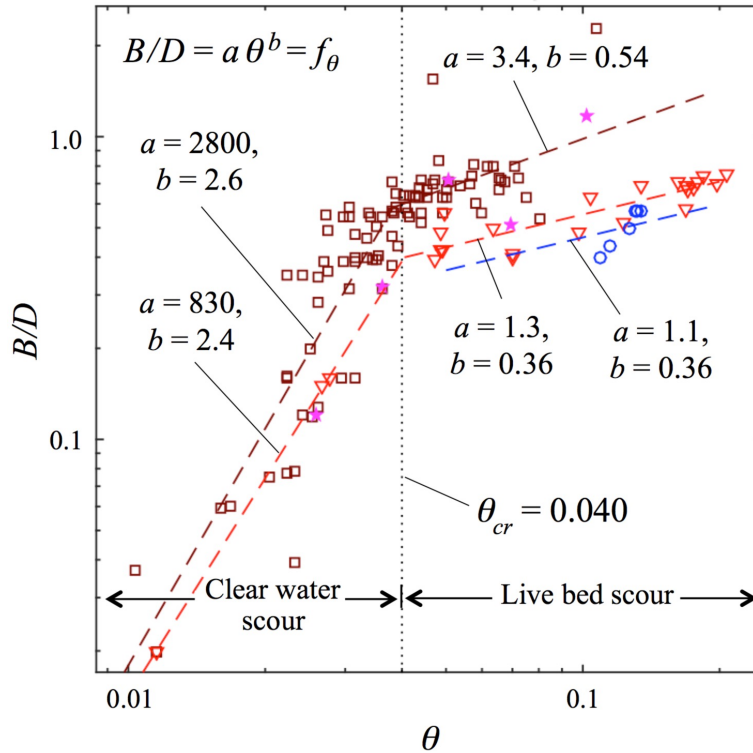


Figure 4. All observations of B/D under steady currents in the absence of waves plotted as a function of θ . Cylinders with $D < 2.6$ cm = \square ; other cylinders (all $D \geq 8.6$ cm) = ∇ ; tapered cylinders ($D = 8$ cm) = \star ; spheres (all $D \geq 3.0$ cm) = \circ . The coefficients a and b displayed above and associated with the dashed lines are utilized in $f\theta$ as part of the relations applied in Fig. 5 and Fig. 6. For $\theta < 0.04$, the power-law fit to ∇ is used for \star ; for $\theta > 0.04$, the power-law fit to \square is used for \star .

The dashed lines in Fig. 4 highlight different relationships between θ and B/D for larger and smaller cylinders, especially under conditions of live-bed scour, with a distinct behavior seen in the available observations with $D < 2.6$ cm. Small cylinders may bury deeper (in terms of B/D) because small cylinders are more likely to interact with sandy bedforms. A continuous relationship between B/D and d_{50}/D of the form $B/D = a(d_{50}/D)^b$ was also examined for steady currents across all D , but it was not found to be significant at 90% confidence (p -value > 0.1). Also, its use tended to degrade the overall predictive power of the individual relationships for B/D within the larger and smaller cylinder populations respectively.

There are not sufficient data available to resolve detailed relationships between B/D and θ under steady currents for shapes other than cylinders. The dashed line in Fig. 4 associated with spheres (all the spheres have $D \geq 3$ cm) is also a relationship of the form $B/D = f\theta = a\theta^b$, where b was set equal to the value of b found for larger cylinders, but with a reduced by a best-fit factor of 0.84. Based on available observations, one may reasonably infer that spheres tend to bury less under

mean currents than cylinders likely because their more rounded shape sheds eddies more weakly (c.f., Truelsen et al. 2005). However, more observations are needed before the best-fit exponential relation with θ can be confidently resolved for spheres.

In contrast to spheres, available data on tapered (i.e., bullet-shaped) cylinders suggest that they bury deeper than non-tapered cylinders of the same diameter. This may be associated with their tendency to rotate their blunt end toward the flow at an angle relatively close to 45° , enhancing the intensity of vortex shedding (Rennie et al., 2017). This is consistent with the finding of Sumer & Fredsøe (2002) that square pilings oriented at 45° toward flow scour more intensely than round pilings or than square pilings oriented at 90° .

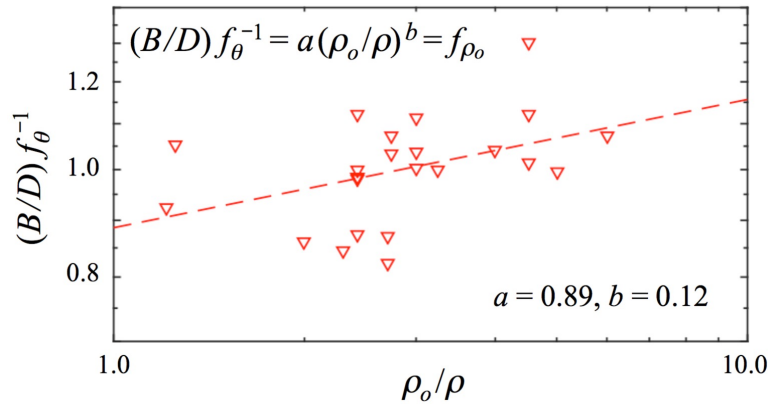


Figure 5. B/D for steady currents normalized by the power-law relations from Fig. 4 and plotted as a function of ρ_o/ρ for large cylinders. Coefficients a and b in the above figure are associated with the dashed line and are utilized in f_{ρ_o} as part of the relationship applied in Fig. 6. The above coefficient for f_{ρ_o} is used only for large cylinders, ∇ . $f_{\rho_o} = 1$ for the other object classes subject to steady currents in the absence of waves.

After normalizing by the relationships between θ and B/D displayed in Fig. 4, parameterizations of the form $f_{\rho_o} = a(\rho_o/\rho)^b$, where ρ_o is object density, were tested against $(B/D) (f_{\theta})^{-1}$, which represents the remaining unexplained variance in B/D . A statistically significant relationship was found between object density and residual variance for larger cylinders (p -value < 0.05), but not for small cylinders, tapered cylinders or spheres. For all available cylinders with $D > 2.6$ cm, significantly deeper burial was found under steady flow as ρ_o/ρ increased (Fig. 5). This trend is consistent with the findings of Cataño-Lopera & García (2006) for self-burying cylinders under waves and supports the conclusion that greater density of objects can favor deeper self-burial, even in the absence of bed fluidization.

After normalizing by the relationships between θ and B/D , parameterizations of the form $f_{L/D} = a(L/D)^b$ were also tested against $(B/D) (f_{\theta})^{-1}$, but no significant relationships were found.

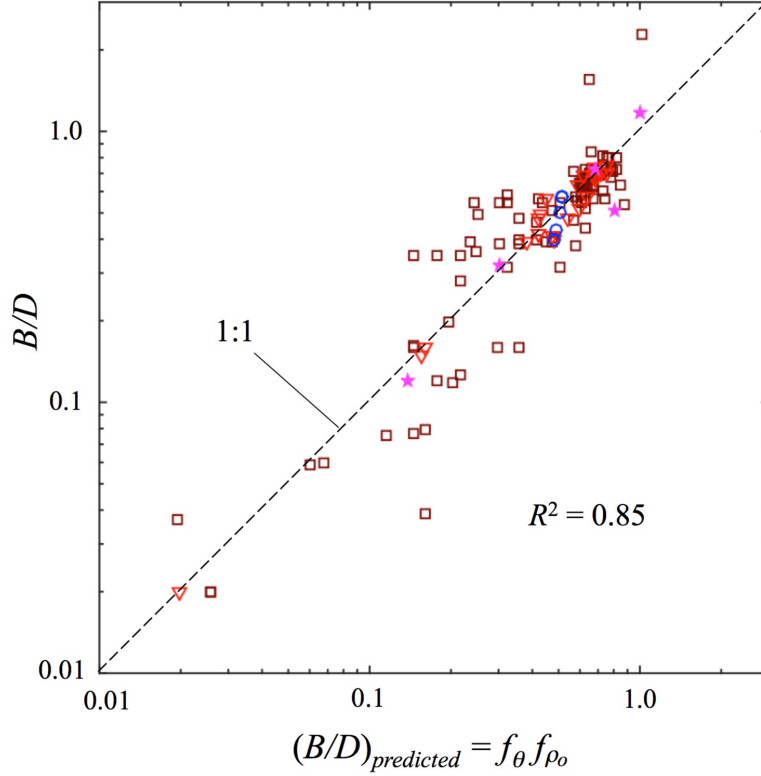


Figure 6. All available observations of B/D for currents in the absence of waves, plotted as a function the final parameterized model for B/D under steady flow, $(B/D)_{predicted} = f\theta f\rho_0$. Symbols are as in Fig. 4. The formulations and coefficients for $f\theta$ and $f\rho_0$ are provided in Fig. 4 and Fig. 5. To calculate $f\theta$ for \star , the coefficients for ∇ and \square were used for θ less than and greater than 0.04, respectively. (Cases with $U_w > 0$, e.g., the field cases in Tables 1 and 2, are not included in Figs. 4, 5 or 6.)

Combining the above results, the final parameterized model for predicted B/D for self-burying objects subject to currents in the absence of waves is

$$(B/D)_{predicted} = f\theta f\rho_0 \quad (20)$$

with the formulations and coefficients for $f\theta$ and $f\rho_0$ provided in Fig. 4 and Fig. 5. To calculate $f\theta$ for tapered cylinders, the coefficients for large and small cylinders were used for θ less than and greater than 0.04, respectively. For tapered cylinders, spheres and small cylinders, $f\rho_0 = 1$. Fig. 6 compares Eq. (20) to all 126 available observations of self-burial of objects in sandy beds under steady currents in the absence of waves. For these cases, Eq. (20) explains 85% of the observed variance in B/D .

5.1.2 Self-burial by Scour Under Waves and Under Waves Plus Currents: In contrast to steady currents, KC alone is better correlated to B/D in the presence of waves ($R^2 = 0.2$) than is θ alone ($R^2 = 0.07$), at least when all 635 available observations of object self-burial including waves from Fig. 3 are utilized. Thus the first parameter we consider in our step-wise multiple regression for B/D under wave-dominated conditions is KC .

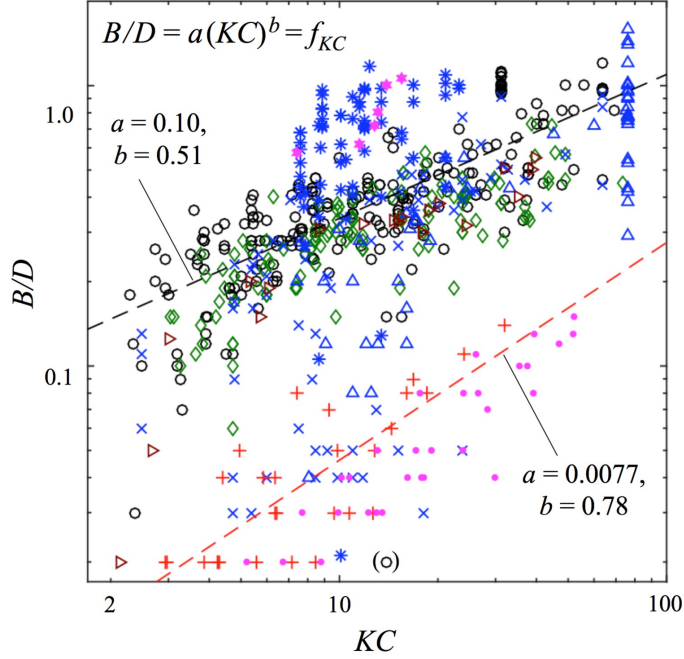


Figure 7. All observations of B/D that include waves, plotted as a function of KC . Symbols are as in Fig. 2 except that here \circ = cylinders with waves only and \triangleright = spheres with waves only. Best-fit relationships are shown above for \circ and for $+$ (conical frustums with waves only). The coefficients a and b displayed above are utilized in f_{KC} as part of the relations applied in Fig. 8 through Fig. 11. (o) = assumed outlier not included in analysis.

Among the various classes of objects, simultaneously strong and very distinct relationships between KC and B/D were seen (i) for conical frustums under waves only (pluses in Fig. 7) and (ii) for cylinders under waves only (circles in Fig. 7, specifically for $D \geq 3$ cm and $\alpha > 60^\circ$). Here we define $f_{KC} = a(KC)^b$ to be the form of the power law function that represents the contribution of KC to our final parameterized model for B/D for all objects. The best-fit values for a and b for conical frustums under waves were also applied to conical frustums under waves plus currents. The best-fit values for a and b for cylinders under waves were applied to all the other cases in Fig. 7. (The best-fit lines in Fig. 7 were constrained almost exclusive by live-bed data, since 97% of the o and $+$ points in Fig. 7 are cases for which $\theta > 0.05$.)

The results found here for B/D as a function of KC are consistent with those reported by previous authors. Cataño-Lopera et al. (2011), the original source of the conical frustum data, reported a similar value for b , namely $B/D \sim KC^{4/5}$ (here we found $B/D \sim KC^{0.79}$). However, they did not present a corresponding value for a . The best-fit power law relationship found here for the self-burial of cylinders, $B/D = 0.10 KC^{0.51}$, is nearly identical to that reported by Sumer & Fredsøe (1990) for the depth of scour (S) by waves under vertically fixed pipelines, $S/D = 0.10 KC^{0.50}$.

After normalizing by the relationship between KC and B/D that is displayed in Fig. 7, an equation of the form $f_{U_{c||}} = \exp[-c(U_{c||}/U_m)]$ was tested against the remaining unexplained variance in burial, $(B/D)f_{KC}^{-1}$. In the above exponential relation, $U_{c||}$ is the component of the mean current that is parallel to wave orbital velocity. In lab flumes we let $U_{c||} = U_c$, whereas for

field data during storms on the inner shelf we assume $U_{c\parallel}/U_m \approx 0$. (Note that in the field data, the effect of U_c on scour is still included through its enhancement of U_m in Eq. (17) and via the replacement of U_w by U_m in Eqs. (15) and (16).) The reason an exponential relation is used rather than a power law is that $f_{U_{c\parallel}} = \exp[-c(U_{c\parallel}/U_m)] = 1$ for $U_{c\parallel}/U_m = 0$. This allows a single value of c to be used for both cases with waves alone and also cases with waves plus currents. Consistent with previous findings (Cataño-Lopera & García, 2006, Cataño-Lopera et al., 2011), B/D was found to decrease as $U_{c\parallel}/U_m$ increased (Fig. 8a). Fig. 8a pools cases for $U_{c\parallel}/U_m > 0$ for both cylinders and conical frustums in order to derive a single value of $c = -1.1$ valid for all available observations.

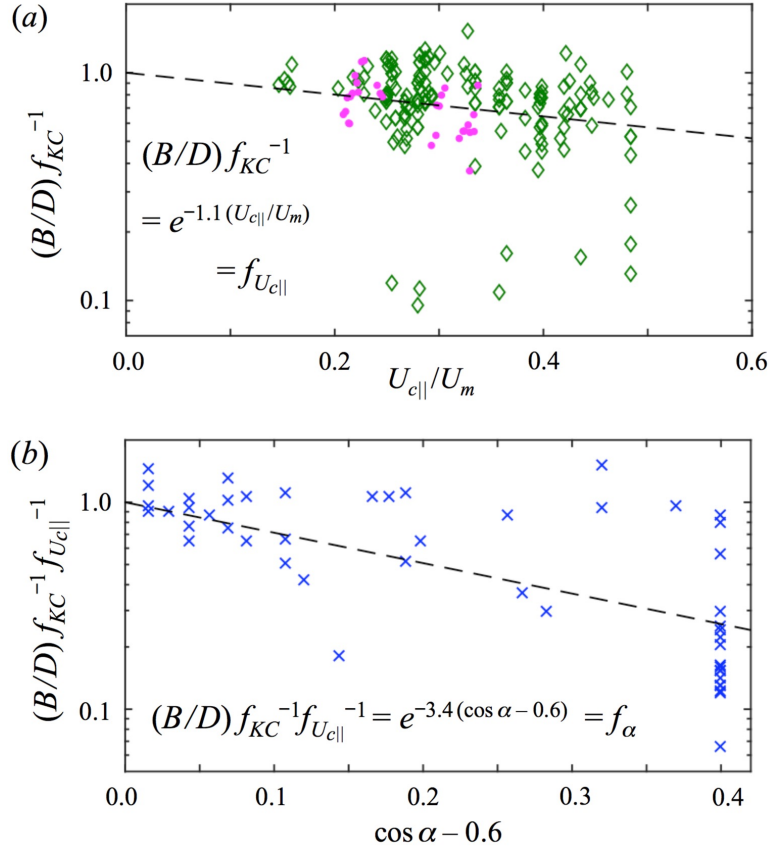


Figure 8. (a) B/D normalized by the power-law relations from Fig. 7 and plotted as a function of $U_{c\parallel}/U_m$ for all available data for which the mean current is parallel to the wave orbital velocity. Cylinders = \diamond ; conical frustums = \bullet . (b) B/D additionally normalized by the exponential relation from Fig. 8a and plotted as a function of $\cos \alpha$, for all available data with $\cos \alpha > 0.6$, where α is final the angle between a cylinder's long axis and wave orbital velocity. The exponential relations associated with the dashed lines (fit to all data in each plot) are utilized in $f_{U_{c\parallel}}$ and f_{α} as part of the relations applied in Fig. 9 through Fig. 11.

Next, after normalizing by $f_{U_{c\parallel}}$, a relationship of the form $f_{\alpha} = \exp[-c_1(\cos \alpha - c_2)]$ was tested against $(B/D)f_{KC}^{-1}f_{U_{c\parallel}}^{-1}$ (Fig. 8b), where α is the angle between wave orbital velocity and a cylinder's long axis. Consistent with the findings of Cataño-Lopera (2005), the original source of

the data, B/D was found to decrease as α decreases toward zero. However, the resulting analyses of Cataño-Lopera (2005) and Cataño-Lopera & García (2007) regarding the effects of a were graphical and did not provide a quantitative formulation its effects. The best-fit values of c_1 and c_2 found here, 3.4 and 0.6, provide an explicit method for accounting for α .

Once the effects of KC , $U_{c||}/U_m$ and a had been removed from B/D , a strong remaining relationship between scour-induced burial and the Shield's parameter of the form $f_{\theta W} = a\theta^b$ was evident for observations of cylinders that involved waves (Fig. 9), including small cylinders observed in the lab ($D < 2.6$ cm) and relatively large cylinders observed in the field ($D \approx 50$ cm). The best-fit values for a and for b for cylinders, displayed in Fig. 9, were well constrained by hundreds of observations of normalized B/D . The dozens of observations of normalized B/D for conical frustums were sufficient to confirm that no significant relationship exists between θ and B/D ($p = 0.86$), and for conical frustums we set $f_{\theta W} = 1$.

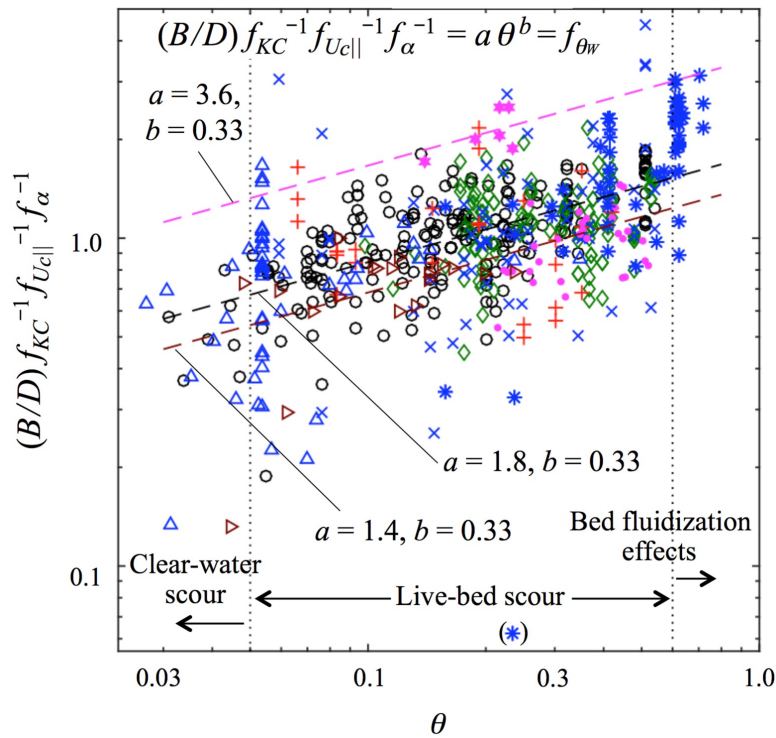


Figure 9. B/D normalized by the functional relationships from Fig. 7 and Fig. 8, and plotted as a function of θ for all cases that include waves. Symbols are as in Fig. 7. The coefficients a and b displayed above in association with the dashed lines are utilized in $f_{\theta W}$ as part of the relations applied in Fig. 10 and Fig. 11. From top to bottom, the dashed lines apply to tapered cylinders, cylinders, and spheres, respectively; $f_{\theta W} = 1$ for conical frustums. (*) = assumed outlier not included in analysis.

Trends for the exponent b were found to be similar to that for cylinders for the cases of tapered cylinders and spheres, but with a larger for tapered cylinders and smaller for spheres, respectively. A tendency for tapered cylinders to bury more and spheres less was likewise noted

for steady currents (see Section 5.1.1). Here the well-constrained value of b found for cylinders was also assigned to tapered cylinders and spheres, and a was then chosen to maximize the overall fit. It should be noted that the small number of observations available under waves for tapered cylinders (6) and for spheres (19) in comparison to cylinders (552) means that the trends for burial of tapered cylinders and spheres under waves are less well constrained than that for cylinders.

Normalized B/D as a function of θ in Fig. 9 suggests a transition occurs (i) from clear-water scour to classic live-bed scour under waves at $\theta \approx 0.05$ and (ii) from classic live-bed scour to fluidization of the upper bed via sheet flow at $\theta \approx 0.6$ (c.f., Dibajnia & Watanabe, 1992). These transition points are supported by the fact that the majority of values for normalized B/D for cylinders fall well below the trend line in Fig. 9 for $\theta < 0.05$ and fall well above the trend line for $B/D > 0.6$. Thus the best-fit values of a and b displayed on Fig. 9 were calculated based only on observations for $0.05 < \theta < 0.6$.

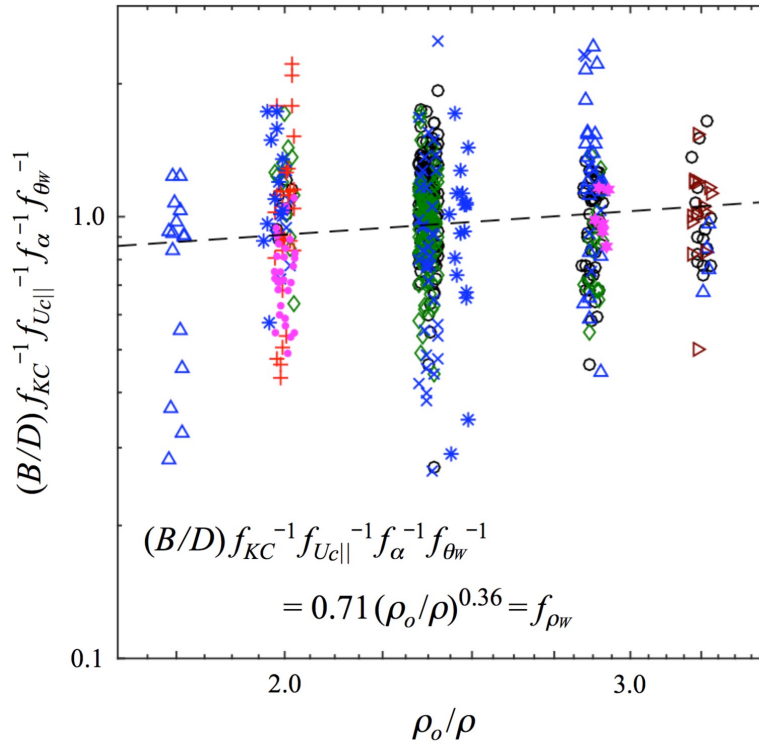


Figure 10. B/D normalized by the functional relationships from Fig. 7 through Fig. 9, for all non-fluidized live-bed data from Fig. 9 available within the range $1.7 < \rho_o/\rho < 3.3$. Symbols are as in Fig. 7 with minor random noise added to r_o/r to prevent complete visual overlap of symbols. Because it performed poorly outside of $1.7 < \rho_o/\rho < 3.3$, the power law relation displayed above was not utilized as part of the final parameterized model.

The sudden transition to relatively complete burial for the field data, indicated by * symbols at high θ in Fig. 9, provides evidence to support the use of $U_{w1/3}$ to estimate U_w under random

waves as suggested by Myhraug & Ong (2009). If a less energetic value of U_w were used for the field data in Fig. 9, such as $U_w = 2^{1/2}\sigma_U$ instead of $U_w = 2\sigma_U$, then the transition to an influence of sheet flow/fluidization on burial for the most energetic field data would not be nearly as clear.

Parameterizations of the form $f_{\rho_{oW}} = a(\rho_o/\rho)^b$, where ρ_o is object density, were also tested against the remaining unexplained variance in B/D under waves (Fig. 10). A statistically significant relationship was found for non-fluidized live-bed data from Fig. 9 within the range $1.7 < \rho_o/\rho < 3.3$, but not outside this range of ρ_o/ρ . Because $f_{\rho_{oW}} = a(\rho_o/\rho)^b$ performed poorly outside of $1.7 < \rho_o/\rho < 3.3$, $f_{\rho_{oW}}$ was not utilized as part of the final parameterized model. Other parameters tested for importance to B/D under waves included L/D and d_{50}/D . However, neither of these ratios was found to have statistically significant effects on normalized B/D , either within specific classes of objects or across multiple classes of objects.

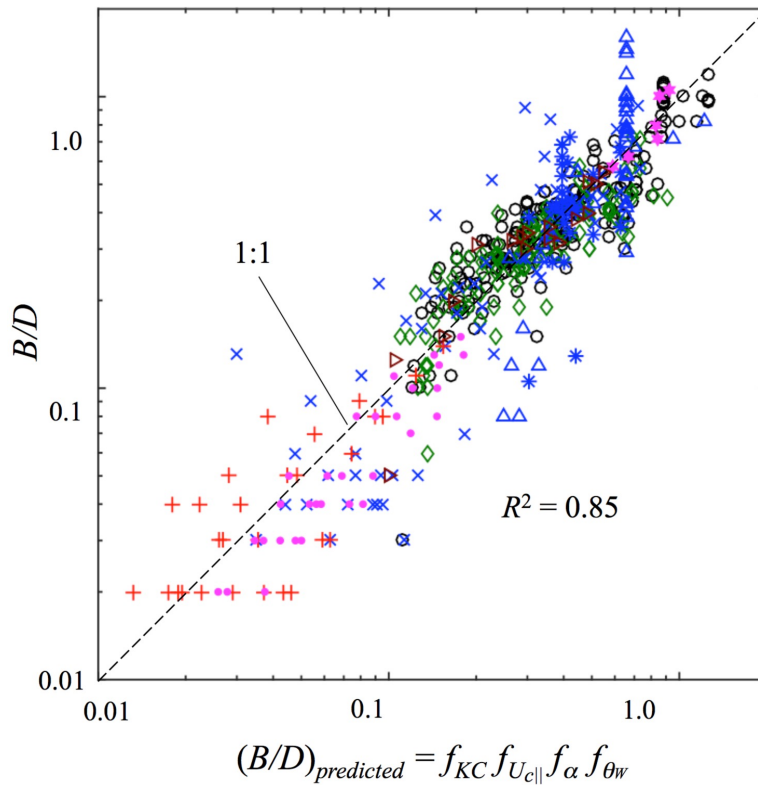


Figure 11. All available, non-fluidized, live-bed observations of B/D under waves (including cases with waves plus currents), plotted as a function of the final parameterized model for B/D under waves, $(B/D)_{predicted} = f_{KC} f_{Uc||} f_{\alpha} f_{\theta_w}$. Symbols are as in Fig. 7. The formulations and coefficients for f_{KC} , $f_{Uc||}$, f_{α} and f_{θ_w} are provided in Fig. 7, Fig. 8 and Fig. 9. (Cases with $U_w = 0$ in Table 3 are not included in Figs. 7 to 11.)

Combining the above results, the final parameterized model for predicted B/D for self-burying objects subject either to waves alone or to waves in combination with mean currents is

$$(B/D)_{predicted} = f_{KC} f_{Uc|} f_{\alpha} f_{\theta W} \quad (19)$$

with the formulations and coefficients for f_{KC} , $f_{Uc|}$, f_{α} and $f_{\theta W}$ provided in Fig. 7, Fig. 8 and Fig. 9. For f_{KC} , the a and b values for lower dashed line in Fig. 7 were applied to conical frustums, while the values for the upper dashed line were applied to all other cases. The relationships in Fig. 8 apply to all observations under waves. In Fig. 9, the lines from top to bottom apply to tapered cylinders, cylinders and spheres, while $f_{\theta W} = 1$ for conical frustums. Fig. 11 compares Eq. (19) to all 578 available observations of self-burial of objects in sand under non-fluidized, live-bed conditions under waves. For these cases, Eq. (19) explains 85% of the observed variance in B/D .

5.2 Results and Discussion for Initiation of Motion of Objects

Fig. 12a displays the critical mobility criteria ($f_I \Theta_{Ucrit}$) determined for 406 cases as a function of object diameter (D) divided by effective bed roughness (k). Θ_{Ucrit} is determined from observations according to Eq. (9), with the values of (i) U at $z = D$ needed for Θ_{Ucrit} and (ii) bed roughness, k , each determined as described in Section 4.2. (See Appendix B, Tables B1 to B3 for additional explanation.) Data covering the higher end of the D/k range in the lower-right corner of Fig. 12 (pink triangles and black squares) are for smooth cylinders placed on smooth beds (Davis et al., 1999; Williams, 2001; Rennie et al., 2017), leading to very small values of effective bed roughness and large values for D/k . The roughened cylinder and carpeted bed results of Rennie et al. (2017) (red stars) fill the previously existing gap in D/k space that is relevant to the initiation of motion of UXO-like objects. Overall, the observed values of Θ_{Ucrit} exhibit a clear decrease with D/k . Overlaid on Fig. 12 (blue dashed line) is the theoretical equation for the mobility of spheres (Eq. 11) derived in Section 3.2, for which the optimal value of the turbulent fluctuation parameter was found to be $\alpha_t = 0.86$.

Without accounting for F_I , observed values for Θ_{Ucrit} for the wave-driven data points (from Williams, 2001) fall well below the trend observed for unidirectional flow (Fig. 12b). It was determined that mobility in the lab data from Williams (2001) was forced by short period waves having a significant contribution from the inertial force, F_I , associated with time-varying horizontal pressure gradients. To account for this component, in Fig. 12a the mobility number was multiplied by f_I as given by Eq. (12), using $C_I/C_D = 2$. This correction factor can easily be applied to all the data in Fig. 12b, not only to Williams (2001), because all the other data have $KC = \infty$, which means $f_I = 1$. Note that for object sizes of interest, the low KC regime that produces $f_I \gg 1$ typically corresponds to short period waves ($T < 3$ s), which tend to have limited bottom orbital velocities. For the cases of cylinders under waves from Williams (2001), f_I varied from $f_I = 1.04$ for $T = 9$ sec, to $f_I = 32.0$ for $T = 1$ sec, with a median value of $f_I = 1.87$ for $T = 5$ sec. Plotting $f_I \Theta_{Ucrit}$ on the y -axis in Fig. 12a rather Θ_{Ucrit} causes the data from Williams (2001) to align better with the other data collected under unidirectional flow.

A power-law fit for all observations most relevant to object mobility ($D > 1$ cm) was made to determine the coefficients for the relationship $f_I \Theta_{Ucrit} = a_1(D/k)^{b_1}$, as suggested by the asymptotic

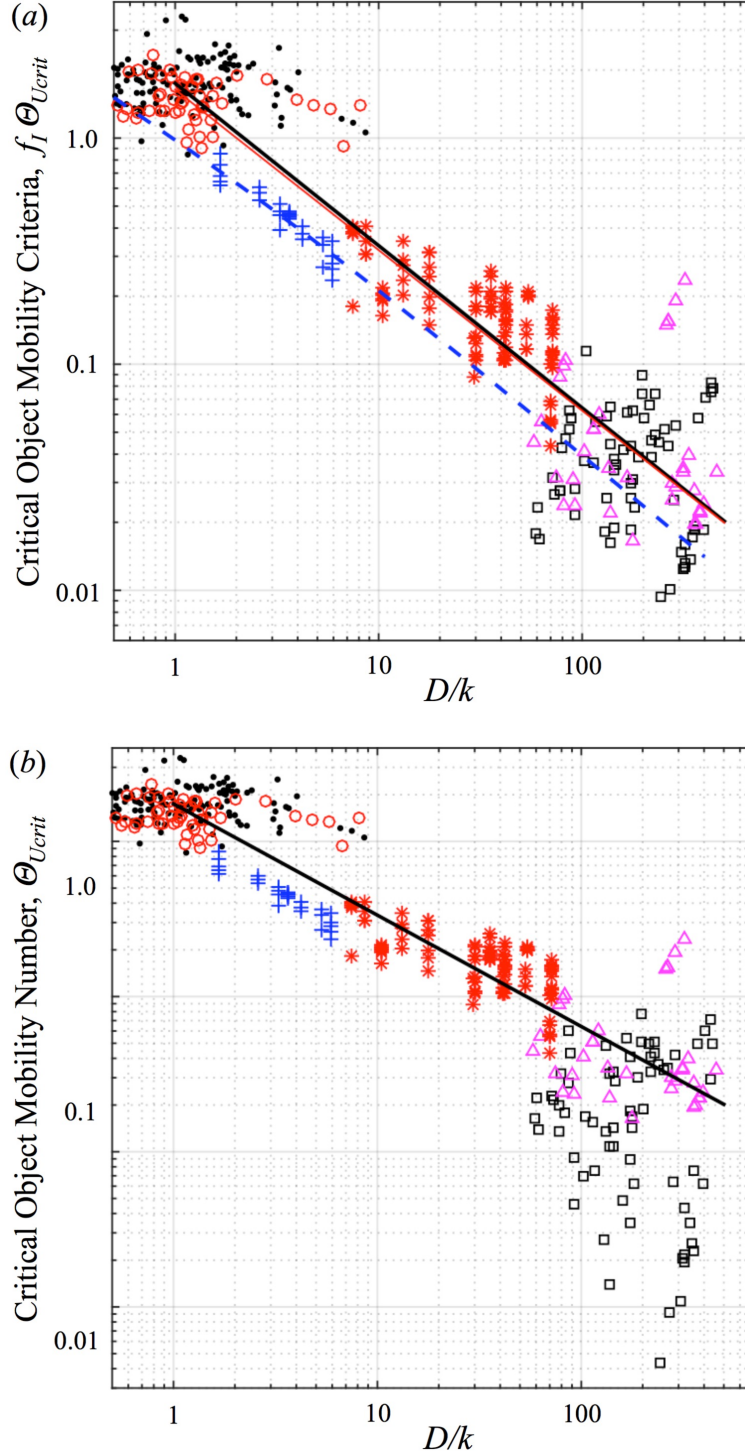


Figure 12. Threshold for the initiation of motion of underwater objects, (a) accounting for and (b) neglecting time-varying pressure gradients. Gravel in streams (\bullet) or flumes (\circ); rough cylinders and/or rough bed ($*$); smooth cylinders on smooth bed (Δ) with waves (\square). The dashed blue line in (a) shows the theoretical relationship for derived for spheres (Eq. (11)). The black solid line is the best-fit power law $f_I \Theta_{Ucrit} = a_1 (D/k)^{b_1}$ for all objects with $D > 1$ cm ($a_1 = 1.75$, $b_1 = -0.72$). The thin red line in (a) (almost indistinguishable from the black solid line) is the slightly different best-fit relationship published by Rennie et al. (2017) ($a_1 = 1.64$, $b_1 = -0.71$).

theoretical relationship for spheres derived in Section 3.2. Using all the data in Fig. 12a with $D > 1$ cm, the best-fit power-law coefficients at 95% confidence were determined to be $a_1 = 1.746 \pm 0.158$ and $b_1 = -0.718 \pm 0.027$, with a log-space coefficient of determination of $R^2 = 0.89$. This equation, $f_1 \Theta_{U_{crit}} = 1.75(D/k)^{-0.72}$, shown as the solid black line, has a power-law dependence close to that of Eq. (11), as derived from theory for spheres. The above best-fit power law relationship provides a method to estimate the threshold of mobility for use in the UnMES. Note that these values of a_1 and b_1 are slightly different from the best-fit values of $a_1 = 1.64$ and $b_1 = -0.71$ reported by Rennie et al. (2017). This is because Rennie et al. (2017) adjusted some of their far-field velocity observations by adding an expected local increase in velocity at the site of cylinder to account for the fraction of the vertical water column blocked by the seabed cylinder. For consistency with critical velocity observations reported by others, such a velocity adjustment was not applied here. Due to the relatively large scatter in the data, however, the best-fit values for $a_1 = 1.64$ and $b_1 =$ presented here and those in Rennie et al. (2017) are not significantly different statistically. The thin red line on Fig. 12a displays the best-fit line published by Rennie et al. (2017), which is almost indistinguishable from the black solid line.

6 Conclusions and Implications for Future Research

A compilation and analysis of 761 observations of equilibrium self-burial depth associated with scour on sandy beds is presented. Observed object burial-to-diameter ratios (B/D) vary by a factor of 100, D by a factor of 50, length-to-diameter ratios (L/D) by a factor of 30, object densities (ρ_o) by a factor of 9, and median sand size (d_{50}) by a factor of 5. Object shapes include cylinders, tapered cylinders, spheres and conical frustums. Nonetheless, simple parameterized models for B/D are identified via an informal, step-wise least-squares regression approach that account for 85% of observed variance.

The main factor which increases scour-induced B/D under steady currents (U_c) in the absence of waves is found to be an increasing Shields parameter, $\theta = \tau_b/[(\rho_s - \rho)gd_{50}]$, with distinctly different power law relations applicable to B/D as a function of θ for clear-water and live-bed scour. Greater B/D is observed as a function of θ for small cylinders ($D < 3$ cm), while smaller B/D is observed for spheres. After accounting for the effects of θ , normalized B/D for larger cylinders is observed to increase with greater ρ_o .

The main factor which increases scour-induced B/D under wave-dominated conditions is an increasing Keulegan-Carpenter number, $KC = U_m T/D$, with distinct power-law relations for conical frustums versus other object shapes, such that conical frustums bury less. After accounting for effects of KC , normalized B/D is shown to decrease as the strength of the component of U_c parallel to wave orbital velocity increases and as the angle between orbital velocity amplitude, U_w , and a cylinder's long axis decreases. Normalized B/D under waves is also shown to generally increase as a function of θ , with larger B/D at a given q for tapered cylinders relative to cylinders, and smaller B/D at a given θ for spheres relative to cylinders. Observations of B/D in the field suggest that the highest 1/3 of U_w may better represent scour in random waves, and they highlight the likely importance of burial by bed fluidization associated with sheet flow at high θ .

A total of 406 data points for initiation of motion were compiled for objects with $0.5 < D < 45$ cm on beds composed of objects or roughness elements smaller than D . The observations included 182 measurements for gravel clasts, 28 for glass spheres, and 196 for cylinders of various densities. 132 of the gravel measurements were from natural streams; all other measurements were from lab experiments. 68 of the cylinder measurements were collected under waves; all other measurements were under unidirectional flow. Density of the objects varied by a factor of 6.6 and the ratio of the object size to the effective roughness of the bed (D/k) ranged by a factor of 1000.

The force balance for onset of motion is parameterized by the mobility criteria, $f_I \Theta_{Ucrit}$ where Θ_{Ucrit} is the critical object mobility parameter, and f_I accounts for the possible effect of a time-varying horizontal pressure gradient. The threshold mobility parameter for an object on a rigid seabed is observed to systematically decrease D/k increases. Theory combined with observations suggested a power law relationship of the form $f_I \Theta_{Ucrit} = a_1(D/k)^{b_1}$. Using all compiled data with $D > 1$ cm, the best-fit power-law coefficients at 95% confidence were determined to be $a_1 = 1.75 \pm 0.16$ and $b_1 = -0.72 \pm 0.03$ with $R^2 = 0.89$. It should be noted however, that a range of coefficients is compatible with the relationships previously published in sediment entrainment literature due to the large scatter of the data available. The effect of inertia, as parameterized by f_I , is found to be occasionally significant, but only in the presence of rapidly varying horizontal pressure gradients (e.g., under short period waves) in combination with large D/k or small ρ_o .

Although the collaborative results between VIMS and JHU/APL described in this report has been highly effective with regards to advancing the practical prediction of near-field processes affecting UXO, less progress has been made to date with regards to predicting UXO re-exposure and migration in response to far field processes. As stated in the 2014 SERDP Program Review for Burial and Mobility Modeling of Munitions in the Underwater Environment (SERDP, 2014), “[To date there has been] little work performed to understand long-term migration patterns. Of particular interest may be the relationship between long-term migration patterns for UXO and far field effects... Far field phenomenology affects excavation, migration and burial independent of the UXO (e.g., sand ripple or large bedform migration).” Thus a follow-on collaborative project to further support UnMES is now underway by Friedrichs to investigate and parameterize transformation of the seabed at scales larger than UXO, including the effects of bedform migration and bed liquefaction. The title of this follow-on project is MR-2467, “Parameterized Process Models for Underwater Munitions Expert System”.

7 Literature Cited

- Bower, G.R., Richardson, M.D., Briggs, K.B., Elmore, P.A., Braithwaite, E.F., Bradley, J., Griffin, S., Wever, T.F. & Lühder, R. 2007. Measured and predicted burial of cylinders during the Indian Rocks Beach experiment. *IEEE Journal of Oceanic Engineering* 32(1): 91-102.
- Bradley, J., Griffin, S., Thiele, M., Richardson, M.D. & Thorne, P.D. 2007. An acoustic-instrumented mine for studying subsequent burial. *IEEE Journal of Oceanic Engineering* 32(1): 91-102.
- Brandt, A. & Rennie, S.E. 2013. Initial laboratory tests examining mobility of UXO due to bottom currents. KTF-13-072, Technical Memorandum. The Johns Hopkins University Applied Physical Laboratory.
- Carling, P.A. 1983. Threshold of coarse sediment transport in broad and narrow natural streams. *Earth Surface Processes and Landforms*, 8(1): 1-18.
- Carstens, M.R. & Martin, C.S. 1963. Settlement of cylindrical mines into the seabed under gravity waves. Final Report, US Navy Mine Defense Laboratory, Project No. A-628.
- Cataño-Lopera, Y.A. 2005. Burial of short cylinders induced by local scour and bedform migration under waves plus currents. PhD Thesis, College of Engineering, University of Illinois at Urbana-Champaign.
- Cataño-Lopera, Y.A., Demir, S.T. & García, M.H. 2007. Self-burial of short cylinders under oscillatory flows and combined waves plus currents. *IEEE Journal of Oceanic Engineering* 32(1): 191-203.
- Cataño-Lopera, Y.A. & García, M.H. 2006. Burial of short cylinders induced by scour under combined waves and currents. *ASCE Journal of Waterway Port Coastal and Ocean Engineering* 132(6): 439-449.
- Cataño-Lopera, Y.A. & García, M.H. 2007. Geometry of scour hole around, and the influence of the angle of attack on the burial of finite cylinders under combined flows. *Ocean Engineering* 34(5): 856-869.
- Cataño-Lopera, Y.A., Landry, B.J. & García, M.H. 2011. Scour and burial mechanics of conical frustums on a sandy bed under combined flow conditions. *Ocean Engineering* 38(10): 1256-1268.
- Davis, J.E., Fenical, S.W., Zhang, J. & Edge, B. 1999. Terminal velocity of cylinders rolling in uniform flows. *Journal of Hydraulic Engineering*, 125(9): 943-952.
- Davis, J.E., Edge, B.L. & Chen, H.C. 2007. Investigation of unrestrained cylinders rolling in steady uniform flows. *Ocean Engineering*, 34(10): 1431-1448.
- Day, T.J. 1980. A study of the transport of graded sediments. Report IT 190, Hydraulic Research Station, Wallingford, UK.
- Dean, R.G. & Dalrymple, R.A. 1991. *Water wave mechanics for engineers and scientists*. Singapore: World Scientific.
- Demir, S.T. & García, M.H. 2007. Experimental studies on burial of finite-length cylinders under oscillatory flow. *ASCE Journal of Waterway Port Coastal and Ocean Engineering* 133(2): 117-124.
- Dhamotharan, S., Wood, A., Parker, G. & Stefan, H. 1980. Bedload transport in a model gravel stream. Project Report 190. St. Anthony Falls Hydraulic Laboratory, University of Minnesota.

- Dibajnia, M. & Watanabe, A. 1992. Sheet flow under nonlinear waves and currents. *Coastal Engineering Proceedings* 23: 2015–2028.
- Friedrichs, C.T. 2007. Reformulation of mine scour equations using observations from MBP field sites. Final Report. US Office of Naval Research Coastal Geosciences Program, Grant N00014-05-1-0112.
- Friedrichs, C.T., Rennie, S.E. & Brandt, A. 2016. Self-burial of objects on sandy beds by scour: A synthesis of observations. In: Harris, J.M., Whitehouse, R.J.S. & Moxon, S. (eds.), *Scour and erosion*. CRC Press, 179-189.
- García, M.H. 2008. Sediment transport and morphodynamics. In: García, M.H. (ed.), *Sedimentation engineering: processes, measurements, modeling and practice*. American Society of Civil Engineers, 21-163.
- Goff, J.A., Mayer, L.A., Traykovski, P., Buynevich, I., Wilkens, R., Raymond, R., Glang, G., Evans, R.L., Olson, H. & Jenkins, C. 2005. Detailed investigation of sorted bedforms, or ‘rippled scour depressions’, within the Martha's Vineyard Coastal Observatory, Massachusetts. *Continental Shelf Research*, 25(4): 461-484.
- Hammond, F.D.C., Heathershaw, A.D. & Langhorne, D.N. 1984. A comparison between Shields' threshold criterion and the movement of loosely packed gravel in a tidal channel. *Sedimentology*, 31(1): 51-62.
- James, C.S. 1993. Entrainment of spheres: an experimental study of relative size and clustering effects. In: Marzo, M. & Puigdefàbragas, C. (eds.), *Alluvial sedimentation*. Blackwell, 3-10.
- Jenkins, S.A., Inman, D.L., Richardson, M.D., Wever, T.F. & Wasyl, J. 2007. Scour and burial mechanics of objects in the nearshore. *IEEE Journal of Oceanic Engineering* 32(1): 78-90.
- Kirchner, J.W., Dietrich, W.E., Iseya, F. & Ikeda, H. 1990. The variability of critical shear stress, friction angle, and grain protrusion in water-worked sediments. *Sedimentology* 37(4): 647-672.
- Komar, P.D. 1996. Entrainment of sediments from deposits of mixed grain sizes and densities. In: Carling, P.A. & Dawson, M.R. (eds.), *Advances in fluvial dynamics and stratigraphy*, John Wiley & Sons, 127-181.
- Komar, P.D. & Li, Z. 1988. Applications of grain-pivoting and sliding analyses to selective entrainment of gravel and to flow-competence evaluations. *Sedimentology* 35(4): 681-695.
- Kuhnle, R.A. 1993. Incipient motion of sand-gravel sediment mixtures. *Journal of Hydraulic Engineering*, 119(12): 1400-1415.
- Li, Z. & Komar, P.D. 1986. Laboratory measurements of pivoting angles for applications to selective entrainment of gravel in a current. *Sedimentology* 33(3): 413–423.
- Mao, L., & Surian, N. 2010. Observations on sediment mobility in a large gravel-bed river. *Geomorphology*, 114(3): 326-337.
- Mayer, L.A., Raymond, R., Glang, G., Richardson, M.D., Traykovski, P. & Trembanis, A.C. 2007. High-resolution mapping of mines and ripples at the Martha's Vineyard Coastal Observatory. *IEEE Journal of Oceanic Engineering* 32(1): 133-149.
- Miller, R.L. & Byrne, R.J. 1966. The angle of repose for a single grain on a fixed rough bed. *Sedimentology*, 6(4): 303–314
- Milhous, R.T. 1973. Sediment transport in a gravel-bottomed stream. PhD Thesis. Oregon State University, Corvallis.

- Misri, R.L., Garde, R.J. & Ranga Raju, K.G. 1984. Bed load transport of coarse nonuniform sediment. *Journal of Hydraulic Engineering*, 110(3): 312-328.
- Myrhaug, D. & Slaattelid, O.H. 1990. A rational approach to wave-current friction coefficients for rough, smooth, and transitional turbulent flow. *Coastal Engineering* 14(3): 265–293.
- Myrhaug, D. & Ong, M.C. 2009. Burial and scour of short cylinders under combined random waves and currents including effects of second order wave asymmetry. *Coastal Engineering* 56(1): 73-81.
- McNinch, J.E., Wells, J.T. & Trembanis, A.C. 2006. Predicting the fate of artefacts in energetic, shallow marine environments: an approach to site management. *International Journal of Nautical Archaeology* 35(2): 290-309.
- Nielsen, P. 1992. *Coastal bottom boundary layers and sediment transport*. World Scientific.
- Pang, C. & Liu, L. 2014. Variability of sand mobility surrounding cylinder object freely resting on the seabed under the action of typhoon. *International Journal of Geosciences* 5(7): 690-699.
- Pedocchi, F. & Garcia, M.H. 2009. Friction coefficient for oscillatory flow: the rough-smooth turbulent transition. *Journal of Hydraulic Engineering and Research*, 47(4): 438-444.
- Patel, P.L. & Ranga Raju, K.G. 1999. Critical tractive stress of nonuniform sediments. *Journal of Hydraulic Research*, 37(1): 39-58.
- Rennie, S.E., Brandt, A. & Friedrichs, C.T. 2017. Initiation of motion and scour burial of objects underwater. *Ocean Engineering* 131: 282-294.
- Schlichting, H. & Gersten, K. 2000. *Boundary layer theory* 8th edition. Springer.
- SERDP 2010. *Munitions in the underwater environment: state of the science and knowledge gaps*. Strategic Environmental Research and Development Program White Paper. US Department of Defense.
- SERDP 2011. *Improvements in the detection, classification, and remediation of military munitions underwater*. Munitions Response Area FY 2013 Statement of Need. Strategic Environmental Research and Development Program. US Department of Defense.
- SERDP 2014. *Program review for burial and mobility modeling of munitions in the underwater environment*. Strategic Environmental Research and Development Program White Paper. US Department of Defense.
- Soulsby, R. 1997. *Dynamics of marine sands*. HRWallingford/Thomas Telford.
- Stansby, P.K. & Starr, P. 1992. On a horizontal cylinder resting on a sand bed under waves and currents. *International Journal of Offshore and Polar Engineering* 2(4): 262-266.
- Starr, P. 1989. *Mobile bed interaction with a cylinder under currents and waves*. PhD Thesis, University of Manchester.
- Sumer, B.M. 2014. *Liquefaction around marine structures*. World Scientific.
- Sumer, B.M. & Fredsøe, J. 1990. Scour below pipelines in waves. *ASCE Journal of Waterway Port Coastal and Ocean Engineering* 116(3): 307-323.
- Sumer, B.M. & Fredsøe, J. 1994. Self-burial of pipelines at span shoulders. *International Journal of Offshore and Polar Engineering* 4(1): 189-194.
- Sumer, B.M. & Fredsøe, J. 2002. *The mechanics of scour in the marine environment*. World Scientific.
- Sumer, B.M. & Fredsøe, J. 2006. *Hydrodynamics around cylindrical structures*. World Scientific.
- Sumer, B.M., Truelsen, C., Sichmann, T. & Fredsøe, J. 2001. Onset of scour below pipelines and self-burial. *Coastal Engineering* 42(4): 313-335.

- Traykovski, P., Richardson, M.D., Mayer, L.A. & Irish, J.D. 2007. Mine burial experiments at the Martha's Vineyard Coastal Observatory. *IEEE Journal of Oceanic Engineering* 32(1): 150-166.
- Trembanis, A.C., Friedrichs, C.T., Richardson, M.D., Traykovski, P., Howd, P.A., Elmore, P.A. & Wever, T.F. 2007. Predicting seabed burial of cylinders by wave-induced scour: application to the sandy inner shelf off Florida and Massachusetts. *IEEE Journal of Oceanic Engineering* 32(1): 167-183.
- Truelsen, C., Sumer, B.M. & Fredsøe, J. 2005. Scour around spherical bodies and self-burial. *ASCE Journal of Waterway Port Coastal and Ocean Engineering* 131(1): 1-13.
- Voropayev, S.I., McEachern, G.B., Boyer, D.L. & Fernando, H.J.S. 1999. Dynamics of sand ripples and burial/scouring of cobbles in oscillatory flow. *Applied Ocean Research* 21(5): 249-261.
- Voropayev, S.I., Testik, F.Y., Fernando, H.J.S. & Boyer, D.L. 2003. Burial and scour around short cylinder under progressive shoaling waves. *Ocean Engineering* 30: 1647-1667.
- Whitehouse, R. 1998. Scour at marine structures. London: Thomas Telford.
- Wiberg, P.L. & Smith, J.D. 1987. Calculations of the critical shear stress for motion of uniform and heterogeneous sediments. *Water resources research*, 23(8): 1471-1480.
- Wilcock, P.R. 1987. Bed-load transport of mixed size sediment. PhD Thesis, Massachusetts Institute of Technology.
- Wilcock, P.R. & Southard, J.B. 1988. Experimental study of incipient motion in mixed-size sediment. *Water Resources Research*, 24(7): 1137-1151.
- Williams, L.W. 2001. Movement of submerged unexploded ordnance due to ocean waves. PhD Thesis, Texas A&M University.
- Wolfson, M.L. 2005. Multibeam observations of mine scour and burial near Clearwater, Florida, including a test of the VIMS 2D mine burial model. MS Thesis, College of Marine Science, University of South Florida.
- Wolfson, M.L., Naar, D.F., Howd, P.A., Locker, S.D., Donahue, B.D., Friedrichs, C.T., Trembanis, A.C., Richardson, M.D. & Wever, T.F. 2007. Multibeam observations of mine burial near Clearwater, Florida, including comparisons to predictions of wave-induced burial. *IEEE Journal of Oceanic Engineering* 32(1): 103-118.
- Yalin, M.S. 1992. River mechanics, New York: Pergamon.

Appendices

Appendix A. Data Compilation for Equilibrium Self-Burial of Objects by Scour

Table A1. Individual observations of self-burial of objects by scour, including object and environmental properties: *No.* = reference number (see text Tables 1 and 2), *Obs.* = observation number, *D* = object diameter (vertical dimension in cm), *L* = object length (maximum horizontal dimension in cm), ρ_o/ρ = object density in (kg/m³) / (1000 kg/m³), *d*₅₀ = median sand size in mm, *U*_w = far-field near-bed wave orbital velocity amplitude in m/s, *T* = wave period in sec, α = final angle in deg of object's long-axis relative to *U*_w (or *U*_c if *U*_w = 0), *U*_c(*z*_{obs}) = far-field current velocity in m/s at height *z*_{obs}, *z*_{obs} = observation height (m) above bed for *U*_w and/or *U*_c (important only for *U*_c), *B/D* = burial depth/object diameter, *KC* = Keulegan-Carpenter number (see main text Eq. (2)), and θ = Shields number (see text Eq. (1)). Additional notes regarding sources of individual parameters in Table A1 and their calculation are provided in Table A2.

<i>No.</i>	<i>Obs.</i>	<i>D</i>	<i>L</i>	ρ_o/ρ	<i>d</i> ₅₀	<i>U</i> _w	<i>T</i>	α	<i>U</i> _c (<i>z</i> _{obs})	<i>z</i> _{obs}	<i>B/D</i>	<i>KC</i>	θ
1	1	4.32	17.3	2.70	0.297	0.764	3.60	90	0.000	0.152	0.970	63.7	0.512
1	2	4.32	17.3	2.70	0.297	0.764	3.60	90	0.000	0.152	0.975	63.7	0.512
1	3	4.32	17.3	2.70	0.297	0.764	3.60	90	0.000	0.152	0.954	63.7	0.512
1	4	4.32	17.3	2.70	0.297	0.764	3.60	90	0.000	0.152	1.197	63.7	0.512
1	5	8.76	35.1	2.70	0.297	0.764	3.60	90	0.000	0.152	0.955	31.4	0.512
1	6	8.76	35.1	2.70	0.297	0.764	3.60	90	0.000	0.152	1.120	31.4	0.512
1	7	8.76	35.1	2.70	0.297	0.764	3.60	90	0.000	0.152	0.940	31.4	0.512
1	8	8.76	35.1	2.70	0.297	0.764	3.60	90	0.000	0.152	1.000	31.4	0.512
1	9	8.76	35.1	2.70	0.297	0.764	3.60	90	0.000	0.152	1.007	31.4	0.512
1	10	8.76	35.1	2.70	0.297	0.764	3.60	0	0.000	0.152	0.520	31.4	0.512
1	11	8.76	35.1	2.70	0.297	0.764	3.60	83	0.000	0.152	0.962	31.4	0.512
1	12	8.76	35.1	2.70	0.297	0.764	3.60	23	0.000	0.152	0.917	31.4	0.512
1	13	4.32	17.3	2.70	0.297	0.764	3.60	40	0.000	0.152	0.931	63.7	0.512
1	14	4.32	17.3	2.70	0.297	0.764	3.60	14	0.000	0.152	0.837	63.7	0.512
1	15	1.27	5.1	2.70	0.585	0.268	3.60	90	0.000	0.152	1.000	76.0	0.053
1	16	1.27	5.1	2.70	0.585	0.268	3.60	90	0.000	0.152	0.894	76.0	0.053
1	17	1.27	5.1	2.70	0.585	0.268	3.60	90	0.000	0.152	0.953	76.0	0.053
1	18	1.27	5.1	2.70	0.585	0.268	3.60	90	0.000	0.152	1.449	76.0	0.053
1	19	1.27	5.1	2.70	0.585	0.268	3.60	90	0.000	0.152	1.590	76.0	0.053
1	20	1.27	5.1	2.70	0.585	0.268	3.60	90	0.000	0.152	1.201	76.0	0.053
1	21	1.27	5.1	2.70	0.585	0.268	3.60	90	0.000	0.152	1.405	76.0	0.053
1	22	1.27	5.1	2.70	0.585	0.268	3.60	90	0.000	0.152	1.016	76.0	0.053
1	23	1.27	5.1	2.70	0.585	0.268	3.60	90	0.000	0.152	0.752	76.0	0.053
1	24	1.27	5.1	2.70	0.585	0.268	3.60	90	0.000	0.152	0.385	76.0	0.053
1	25	1.27	5.1	2.70	0.585	0.268	3.60	90	0.000	0.152	0.768	76.0	0.053
1	26	1.27	5.1	2.70	0.585	0.268	3.60	90	0.000	0.152	0.913	76.0	0.053
1	27	1.27	5.1	2.70	0.585	0.268	3.60	90	0.000	0.152	1.000	76.0	0.053
1	28	8.76	35.1	2.70	0.297	0.764	3.60	90	0.000	0.152	1.072	31.4	0.512

Table A1. Individual observations of self-burial of objects by scour (cont.)

<i>No.</i>	<i>Obs.</i>	<i>D</i>	<i>L</i>	ρ_o/ρ	d_{50}	U_w	<i>T</i>	α	$U_c(z_{obs})$	z_{obs}	<i>B/D</i>	<i>KC</i>	θ
1	29	8.76	35.1	2.70	0.297	0.764	3.60	90	0.000	0.152	1.079	31.4	0.512
1	30	8.76	35.1	2.70	0.297	0.764	3.60	90	0.000	0.152	0.963	31.4	0.512
1	31	8.76	35.1	2.70	0.297	0.764	3.60	90	0.000	0.152	0.993	31.4	0.512
1	32	8.76	35.1	2.70	0.297	0.764	3.60	90	0.000	0.152	1.023	31.4	0.512
1	33	8.76	35.1	2.70	0.297	0.764	3.60	90	0.000	0.152	0.951	31.4	0.512
1	34	8.76	35.1	2.70	0.297	0.764	3.60	90	0.000	0.152	0.984	31.4	0.512
1	35	4.32	17.3	2.70	0.297	0.764	3.60	90	0.000	0.152	0.977	63.7	0.512
1	36	1.27	5.1	2.70	0.585	0.268	3.60	90	0.000	0.152	0.417	76.0	0.053
1	37	1.27	5.1	2.70	0.585	0.268	3.60	90	0.000	0.152	0.429	76.0	0.053
1	38	1.27	5.1	2.70	0.585	0.268	3.60	90	0.000	0.152	0.776	76.0	0.053
1	39	1.27	5.1	2.70	0.585	0.268	3.60	90	0.000	0.152	0.839	76.0	0.053
1	40	1.27	5.1	2.70	0.585	0.268	3.60	90	0.000	0.152	0.748	76.0	0.053
1	41	1.27	5.1	2.70	0.585	0.268	3.60	90	0.000	0.152	0.961	76.0	0.053
1	42	1.27	5.1	2.70	0.585	0.268	3.60	90	0.000	0.152	0.543	76.0	0.053
1	43	1.27	5.1	2.70	0.585	0.268	3.60	90	0.000	0.152	0.787	76.0	0.053
1	44	1.27	5.1	2.70	0.585	0.268	3.60	90	0.000	0.152	0.292	76.0	0.053
1	45	1.27	5.1	2.70	0.585	0.268	3.60	90	0.000	0.152	0.532	76.0	0.053
1	46	1.27	5.1	2.70	0.585	0.268	3.60	90	0.000	0.152	0.788	76.0	0.053
1	47	1.27	5.1	2.70	0.585	0.268	3.60	90	0.000	0.152	0.732	76.0	0.053
1	48	8.76	35.1	2.70	0.297	0.764	3.60	90	0.000	0.152	1.103	31.4	0.512
1	49	8.76	35.1	2.70	0.297	0.764	3.60	90	0.000	0.152	1.107	31.4	0.512
2	50	2.54	50.8	1.80	0.220	0.112	1.69	90	0.000	0.092	0.200	7.5	0.031
2	51	2.54	50.8	1.80	0.220	0.115	1.77	90	0.000	0.092	0.040	8.0	0.031
2	52	2.54	50.8	1.80	0.220	0.108	2.12	90	0.000	0.092	0.200	9.0	0.027
2	53	2.54	50.8	1.80	0.220	0.125	1.84	90	0.000	0.092	0.120	9.1	0.035
2	54	2.54	50.8	1.80	0.220	0.153	1.66	90	0.000	0.092	0.310	10.0	0.050
2	55	2.54	50.8	1.80	0.220	0.145	1.93	90	0.000	0.092	0.200	11.0	0.044
2	56	2.54	50.8	1.80	0.220	0.167	1.67	90	0.000	0.092	0.080	11.0	0.057
2	57	2.54	50.8	1.80	0.220	0.175	1.67	90	0.000	0.092	0.280	11.5	0.061
2	58	2.54	50.8	1.80	0.220	0.152	2.02	90	0.000	0.092	0.120	12.1	0.046
2	59	2.54	50.8	1.80	0.220	0.190	1.67	90	0.000	0.092	0.080	12.5	0.070
2	60	2.54	50.8	1.80	0.220	0.165	2.01	90	0.000	0.092	0.120	13.1	0.053
2	61	2.54	50.8	1.80	0.220	0.147	2.60	90	0.000	0.092	0.200	15.1	0.041
2	62	2.54	50.8	1.80	0.220	0.168	2.42	90	0.000	0.092	0.160	16.0	0.051
2	63	2.54	50.8	1.80	0.220	0.157	2.59	90	0.000	0.092	0.350	16.0	0.045
2	64	2.54	50.8	1.80	0.220	0.204	1.99	90	0.000	0.092	0.120	16.0	0.074
2	65	2.54	50.8	1.80	0.220	0.213	1.96	90	0.000	0.092	0.310	16.4	0.080
2	66	2.54	50.8	1.80	0.220	0.232	1.87	90	0.000	0.092	0.330	17.1	0.093
2	67	2.54	50.8	1.80	0.220	0.224	1.95	90	0.000	0.092	0.330	17.2	0.087
2	68	2.54	50.8	1.80	0.220	0.277	1.61	90	0.000	0.092	0.430	17.6	0.131
2	69	2.54	50.8	1.80	0.220	0.188	2.57	90	0.000	0.092	0.280	19.0	0.060

Table A1. Individual observations of self-burial of objects by scour (cont.)

<i>No.</i>	<i>Obs.</i>	<i>D</i>	<i>L</i>	ρ_o/ρ	d_{50}	U_w	<i>T</i>	α	$U_c(z_{obs})$	z_{obs}	<i>B/D</i>	<i>KC</i>	θ
2	70	2.54	50.8	1.80	0.220	0.277	1.93	90	0.000	0.092	0.550	21.1	0.124
2	71	2.54	50.8	1.80	0.220	0.290	1.89	90	0.000	0.092	0.430	21.6	0.135
2	72	2.54	50.8	1.80	0.220	0.253	2.42	90	0.000	0.092	0.550	24.1	0.100
2	73	2.54	50.8	1.80	0.220	0.247	2.52	90	0.000	0.092	0.430	24.5	0.094
2	74	2.54	50.8	1.80	0.220	0.000	Inf	90	0.165	0.092	0.060	Inf	0.017
2	75	2.54	50.8	1.80	0.220	0.000	Inf	90	0.197	0.092	0.079	Inf	0.023
2	76	2.54	50.8	1.80	0.220	0.000	Inf	90	0.206	0.092	0.118	Inf	0.025
2	77	2.54	50.8	1.80	0.220	0.000	Inf	90	0.193	0.092	0.161	Inf	0.022
2	78	2.54	50.8	1.80	0.220	0.000	Inf	90	0.215	0.092	0.358	Inf	0.028
2	79	2.54	50.8	1.80	0.220	0.000	Inf	90	0.231	0.092	0.398	Inf	0.032
2	80	2.54	50.8	1.80	0.220	0.000	Inf	90	0.238	0.092	0.399	Inf	0.033
2	81	2.54	50.8	1.80	0.220	0.000	Inf	90	0.256	0.092	0.557	Inf	0.038
2	82	2.54	50.8	1.80	0.220	0.000	Inf	90	0.265	0.092	0.558	Inf	0.041
2	83	2.54	50.8	1.80	0.220	0.000	Inf	90	0.304	0.092	0.685	Inf	0.054
2	84	2.54	50.8	1.80	0.220	0.000	Inf	90	0.354	0.092	0.726	Inf	0.073
2	85	1.27	25.4	2.40	0.220	0.000	Inf	90	0.231	0.092	0.159	Inf	0.032
2	86	1.27	25.4	2.40	0.220	0.000	Inf	90	0.248	0.092	0.315	Inf	0.036
2	87	1.27	25.4	2.40	0.220	0.000	Inf	90	0.242	0.092	0.392	Inf	0.034
2	88	1.27	25.4	2.40	0.220	0.000	Inf	90	0.263	0.092	0.640	Inf	0.040
2	89	1.27	25.4	2.40	0.220	0.000	Inf	90	0.271	0.092	0.640	Inf	0.043
2	90	1.27	25.4	2.40	0.220	0.000	Inf	90	0.275	0.092	0.722	Inf	0.044
2	91	1.27	25.4	2.40	0.220	0.000	Inf	90	0.338	0.092	0.722	Inf	0.066
2	92	1.27	25.4	2.40	0.220	0.000	Inf	90	0.315	0.092	0.809	Inf	0.058
2	93	2.54	50.8	8.70	0.220	0.000	Inf	90	0.209	0.092	0.127	Inf	0.026
2	94	2.54	50.8	8.70	0.220	0.000	Inf	90	0.227	0.092	0.315	Inf	0.031
2	95	2.54	50.8	8.70	0.220	0.000	Inf	90	0.255	0.092	0.377	Inf	0.038
2	96	2.54	50.8	8.70	0.220	0.000	Inf	90	0.246	0.092	0.403	Inf	0.036
2	97	2.54	50.8	8.70	0.220	0.000	Inf	90	0.259	0.092	0.438	Inf	0.039
2	98	2.54	50.8	8.70	0.220	0.000	Inf	90	0.275	0.092	0.518	Inf	0.044
2	99	2.54	50.8	8.70	0.220	0.000	Inf	90	0.373	0.092	0.539	Inf	0.080
2	100	2.54	50.8	8.70	0.220	0.000	Inf	90	0.275	0.092	0.558	Inf	0.044
2	101	2.54	50.8	8.70	0.220	0.000	Inf	90	0.291	0.092	0.561	Inf	0.049
2	102	2.54	50.8	8.70	0.220	0.000	Inf	90	0.322	0.092	0.561	Inf	0.060
2	103	2.54	50.8	8.70	0.220	0.000	Inf	90	0.317	0.092	0.600	Inf	0.058
2	104	1.27	25.4	10.60	0.220	0.000	Inf	90	0.223	0.092	0.159	Inf	0.029
2	105	1.27	25.4	10.60	0.220	0.000	Inf	90	0.231	0.092	0.479	Inf	0.032
2	106	1.27	25.4	10.60	0.220	0.000	Inf	90	0.239	0.092	0.561	Inf	0.034
2	107	1.27	25.4	10.60	0.220	0.000	Inf	90	0.255	0.092	0.571	Inf	0.038
2	108	1.27	25.4	10.60	0.220	0.000	Inf	90	0.267	0.092	0.640	Inf	0.042
2	109	1.27	25.4	10.60	0.220	0.000	Inf	90	0.274	0.092	0.682	Inf	0.044
2	110	1.27	25.4	10.60	0.220	0.000	Inf	90	0.285	0.092	0.721	Inf	0.047

Table A1. Individual observations of self-burial of objects by scour (cont.)

<i>No.</i>	<i>Obs.</i>	<i>D</i>	<i>L</i>	ρ_o/ρ	d_{50}	U_w	<i>T</i>	α	$U_c(z_{obs})$	z_{obs}	<i>B/D</i>	<i>KC</i>	θ
2	111	1.27	25.4	10.60	0.220	0.000	Inf	90	0.331	0.092	0.800	Inf	0.063
2	112	1.27	25.4	10.60	0.220	0.000	Inf	90	0.326	0.092	0.801	Inf	0.062
2	113	1.27	25.4	10.60	0.220	0.000	Inf	90	0.350	0.092	0.802	Inf	0.071
2	114	2.54	45.0	2.40	0.220	0.000	Inf	90	0.127	0.092	0.037	Inf	0.010
2	115	2.54	45.0	2.40	0.220	0.000	Inf	90	0.197	0.092	0.039	Inf	0.023
2	116	2.54	45.0	2.40	0.220	0.000	Inf	90	0.161	0.092	0.059	Inf	0.016
2	117	2.54	45.0	2.40	0.220	0.000	Inf	90	0.184	0.092	0.075	Inf	0.021
2	118	2.54	45.0	2.40	0.220	0.000	Inf	90	0.193	0.092	0.077	Inf	0.022
2	119	2.54	45.0	2.40	0.220	0.000	Inf	90	0.201	0.092	0.120	Inf	0.024
2	120	2.54	45.0	2.40	0.220	0.000	Inf	90	0.193	0.092	0.160	Inf	0.022
2	121	2.54	45.0	2.40	0.220	0.000	Inf	90	0.205	0.092	0.198	Inf	0.025
2	122	2.54	45.0	2.40	0.220	0.000	Inf	90	0.209	0.092	0.282	Inf	0.026
2	123	2.54	45.0	2.40	0.220	0.000	Inf	90	0.209	0.092	0.346	Inf	0.026
2	124	2.54	45.0	2.40	0.220	0.000	Inf	90	0.193	0.092	0.348	Inf	0.022
2	125	2.54	45.0	2.40	0.220	0.000	Inf	90	0.201	0.092	0.348	Inf	0.024
2	126	2.54	45.0	2.40	0.220	0.000	Inf	90	0.224	0.092	0.385	Inf	0.030
2	127	2.54	45.0	2.40	0.220	0.000	Inf	90	0.231	0.092	0.386	Inf	0.032
2	128	2.54	45.0	2.40	0.220	0.000	Inf	90	0.213	0.092	0.388	Inf	0.027
2	129	2.54	45.0	2.40	0.220	0.000	Inf	90	0.245	0.092	0.390	Inf	0.035
2	130	2.54	45.0	2.40	0.220	0.000	Inf	90	0.238	0.092	0.464	Inf	0.033
2	131	2.54	45.0	2.40	0.220	0.000	Inf	90	0.254	0.092	0.466	Inf	0.038
2	132	2.54	45.0	2.40	0.220	0.000	Inf	90	0.245	0.092	0.507	Inf	0.035
2	133	2.54	45.0	2.40	0.220	0.000	Inf	90	0.224	0.092	0.546	Inf	0.030
2	134	2.54	45.0	2.40	0.220	0.000	Inf	90	0.227	0.092	0.546	Inf	0.031
2	135	2.54	45.0	2.40	0.220	0.000	Inf	90	0.227	0.092	0.586	Inf	0.031
2	136	2.54	45.0	2.40	0.220	0.000	Inf	90	0.248	0.092	0.546	Inf	0.036
2	137	2.54	45.0	2.40	0.220	0.000	Inf	90	0.267	0.092	0.546	Inf	0.042
2	138	2.54	45.0	2.40	0.220	0.000	Inf	90	0.241	0.092	0.547	Inf	0.034
2	139	2.54	45.0	2.40	0.220	0.000	Inf	90	0.257	0.092	0.586	Inf	0.039
2	140	2.54	45.0	2.40	0.220	0.000	Inf	90	0.264	0.092	0.588	Inf	0.041
2	141	2.54	45.0	2.40	0.220	0.000	Inf	90	0.279	0.092	0.626	Inf	0.045
2	142	2.54	45.0	2.40	0.220	0.000	Inf	90	0.270	0.092	0.628	Inf	0.043
2	143	2.54	45.0	2.40	0.220	0.000	Inf	90	0.293	0.092	0.628	Inf	0.050
2	144	2.54	45.0	2.40	0.220	0.000	Inf	90	0.273	0.092	0.629	Inf	0.044
2	145	2.54	45.0	2.40	0.220	0.000	Inf	90	0.290	0.092	0.629	Inf	0.049
2	146	2.54	45.0	2.40	0.220	0.000	Inf	90	0.360	0.092	0.632	Inf	0.075
2	147	2.54	45.0	2.40	0.220	0.000	Inf	90	0.257	0.092	0.649	Inf	0.039
2	148	2.54	45.0	2.40	0.220	0.000	Inf	90	0.293	0.092	0.666	Inf	0.050
2	149	2.54	45.0	2.40	0.220	0.000	Inf	90	0.279	0.092	0.667	Inf	0.045
2	150	2.54	45.0	2.40	0.220	0.000	Inf	90	0.336	0.092	0.673	Inf	0.065
2	151	2.54	45.0	2.40	0.220	0.000	Inf	90	0.311	0.092	0.699	Inf	0.056

Table A1. Individual observations of self-burial of objects by scour (cont.)

<i>No.</i>	<i>Obs.</i>	<i>D</i>	<i>L</i>	ρ_o/ρ	d_{50}	U_w	<i>T</i>	α	$U_c(z_{obs})$	z_{obs}	<i>B/D</i>	<i>KC</i>	θ
2	152	2.54	45.0	2.40	0.220	0.000	Inf	90	0.284	0.092	0.702	Inf	0.047
2	153	2.54	45.0	2.40	0.220	0.000	Inf	90	0.254	0.092	0.707	Inf	0.038
2	154	2.54	45.0	2.40	0.220	0.000	Inf	90	0.341	0.092	0.708	Inf	0.067
2	155	2.54	45.0	2.40	0.220	0.000	Inf	90	0.295	0.092	0.711	Inf	0.051
2	156	2.54	45.0	2.40	0.220	0.000	Inf	90	0.336	0.092	0.731	Inf	0.065
2	157	2.54	45.0	2.40	0.220	0.000	Inf	90	0.314	0.092	0.746	Inf	0.057
3	158	11.00	198.0	1.25	0.200	0.000	Inf	90	0.300	0.055	0.495	Inf	0.063
3	159	11.00	198.0	2.00	0.200	0.000	Inf	90	0.491	0.055	0.576	Inf	0.169
3	160	11.00	198.0	2.75	0.200	0.000	Inf	90	0.513	0.055	0.740	Inf	0.185
3	161	11.00	198.0	2.75	0.200	0.000	Inf	90	0.491	0.055	0.691	Inf	0.169
3	162	11.00	198.0	3.00	0.200	0.000	Inf	90	0.499	0.055	0.679	Inf	0.175
3	163	11.00	198.0	3.00	0.200	0.000	Inf	90	0.506	0.055	0.709	Inf	0.180
3	164	11.00	198.0	3.25	0.200	0.000	Inf	90	0.492	0.055	0.670	Inf	0.170
3	165	11.00	198.0	4.00	0.200	0.000	Inf	90	0.544	0.055	0.750	Inf	0.208
3	166	11.00	198.0	5.00	0.200	0.000	Inf	90	0.529	0.055	0.703	Inf	0.197
3	167	11.00	198.0	6.00	0.200	0.000	Inf	90	0.480	0.055	0.705	Inf	0.161
4	168	10.00	198.0	3.00	0.180	0.000	Inf	90	0.450	0.100	0.685	Inf	0.135
4	169	10.00	59.4	3.00	0.180	0.196	1.50	90	0.000	0.100	0.240	2.9	0.089
4	170	10.00	59.4	3.00	0.180	0.253	1.50	90	0.000	0.050	0.285	3.8	0.134
4	171	5.00	59.4	3.00	0.180	0.130	2.00	90	0.000	0.050	0.193	5.2	0.043
4	172	5.00	59.4	3.00	0.180	0.182	2.00	90	0.000	0.050	0.295	7.3	0.072
4	173	5.00	59.4	3.00	0.180	0.206	2.00	90	0.000	0.050	0.245	8.2	0.088
4	174	5.00	59.4	3.00	0.180	0.231	2.00	90	0.000	0.050	0.215	9.2	0.106
4	175	5.00	59.4	3.00	0.180	0.280	2.00	90	0.000	0.050	0.395	11.2	0.145
4	176	5.00	59.4	3.00	0.180	0.265	2.50	90	0.000	0.050	0.315	13.3	0.124
4	177	5.00	59.4	1.25	0.180	0.313	2.50	90	0.000	0.050	0.395	15.7	0.163
4	178	5.00	59.4	2.00	0.180	0.313	2.50	90	0.000	0.050	0.395	15.7	0.163
4	179	5.00	59.4	3.00	0.180	0.313	2.50	90	0.000	0.050	0.395	15.7	0.163
4	180	5.00	59.4	4.00	0.180	0.313	2.50	90	0.000	0.050	0.395	15.7	0.163
4	181	5.00	59.4	6.00	0.180	0.313	2.50	90	0.000	0.050	0.395	15.7	0.163
4	182	5.00	59.4	3.00	0.180	0.271	3.00	90	0.000	0.050	0.395	16.3	0.122
4	183	5.00	59.4	3.00	0.180	0.305	3.00	90	0.000	0.050	0.475	18.3	0.149
4	184	5.00	59.4	3.00	0.180	0.372	3.00	90	0.000	0.050	0.490	22.3	0.208
4	185	5.00	59.4	3.00	0.180	0.413	3.00	90	0.000	0.050	0.485	24.8	0.249
4	186	5.00	59.4	3.00	0.180	0.423	3.00	90	0.000	0.050	0.485	25.4	0.259
4	187	5.00	59.4	3.00	0.180	0.471	3.00	90	0.000	0.050	0.600	28.3	0.313
4	188	5.00	59.4	3.00	0.180	0.500	3.00	90	0.000	0.050	0.620	30.0	0.347
4	189	5.00	59.4	3.00	0.180	0.481	3.50	90	0.000	0.050	0.570	33.7	0.311
4	190	2.00	59.4	3.00	0.180	0.222	3.00	90	0.000	0.050	0.430	33.3	0.088
4	191	2.00	59.4	3.00	0.180	0.300	3.00	90	0.000	0.050	0.670	45.0	0.144
4	192	2.00	59.4	3.00	0.180	0.401	3.00	90	0.000	0.050	0.720	60.2	0.236

Table A1. Individual observations of self-burial of objects by scour (cont.)

<i>No.</i>	<i>Obs.</i>	<i>D</i>	<i>L</i>	ρ_o/ρ	d_{50}	U_w	<i>T</i>	α	$U_c(z_{obs})$	z_{obs}	<i>B/D</i>	<i>KC</i>	θ
4	193	2.00	59.4	3.00	0.180	0.502	3.00	90	0.000	0.050	0.820	75.3	0.350
5	194	15.20	30.5	2.30	0.250	0.199	1.90	90	0.000	0.206	0.100	2.5	0.066
5	195	15.20	30.5	2.30	0.250	0.209	1.70	90	0.000	0.206	0.120	2.3	0.074
5	196	15.20	30.5	2.30	0.250	0.147	3.40	90	0.000	0.206	0.070	3.3	0.034
5	197	15.20	30.5	2.30	0.250	0.172	2.90	90	0.000	0.206	0.090	3.3	0.045
5	198	15.20	30.5	2.30	0.250	0.187	2.60	90	0.000	0.206	0.100	3.2	0.054
5	199	15.20	30.5	2.30	0.250	0.210	2.30	90	0.000	0.206	0.110	3.2	0.068
5	200	15.20	30.5	2.30	0.250	0.224	2.00	90	0.000	0.206	0.190	3.0	0.079
5	201	15.20	30.5	2.30	0.250	0.240	1.90	90	0.000	0.206	0.180	3.0	0.090
5	202	15.20	30.5	2.30	0.250	0.244	1.70	90	0.000	0.206	0.200	2.7	0.096
5	203	15.20	30.5	2.30	0.250	0.145	4.10	90	0.000	0.206	0.120	3.9	0.031
5	204	15.20	30.5	2.30	0.250	0.175	3.40	90	0.000	0.206	0.130	3.9	0.044
5	205	15.20	30.5	2.30	0.250	0.205	2.90	90	0.000	0.206	0.150	3.9	0.060
5	206	15.20	30.5	2.30	0.250	0.232	2.60	90	0.000	0.206	0.150	4.0	0.077
5	207	15.20	30.5	2.30	0.250	0.256	2.30	90	0.000	0.206	0.220	3.9	0.094
5	208	15.20	30.5	2.30	0.250	0.278	2.00	90	0.000	0.206	0.240	3.7	0.113
5	209	15.20	30.5	2.30	0.250	0.294	1.90	90	0.000	0.206	0.230	3.7	0.127
5	210	15.20	30.5	2.30	0.250	0.312	1.70	90	0.000	0.206	0.250	3.5	0.146
5	211	15.20	30.5	2.30	0.250	0.167	4.10	90	0.000	0.206	0.110	4.5	0.039
5	212	15.20	30.5	2.30	0.250	0.210	3.40	90	0.000	0.206	0.110	4.7	0.060
5	213	15.20	30.5	2.30	0.250	0.243	2.90	90	0.000	0.206	0.190	4.6	0.080
5	214	15.20	30.5	2.30	0.250	0.268	2.60	90	0.000	0.206	0.190	4.6	0.098
5	215	15.20	30.5	2.30	0.250	0.310	2.30	90	0.000	0.206	0.180	4.7	0.131
5	216	15.20	30.5	2.30	0.250	0.337	2.00	90	0.000	0.206	0.270	4.4	0.158
5	217	15.20	30.5	2.30	0.250	0.355	1.90	90	0.000	0.206	0.260	4.4	0.176
5	218	15.20	30.5	2.30	0.250	0.378	1.70	90	0.000	0.206	0.310	4.2	0.203
5	219	15.20	30.5	2.30	0.250	0.207	4.10	90	0.000	0.206	0.200	5.6	0.055
5	220	15.20	30.5	2.30	0.250	0.251	3.40	90	0.000	0.206	0.160	5.6	0.081
5	221	15.20	30.5	2.30	0.250	0.293	2.90	90	0.000	0.206	0.220	5.6	0.110
5	222	15.20	30.5	2.30	0.250	0.344	2.60	90	0.000	0.206	0.280	5.9	0.151
5	223	15.20	30.5	2.30	0.250	0.379	2.30	90	0.000	0.206	0.280	5.7	0.186
5	224	15.20	30.5	2.30	0.250	0.414	2.00	90	0.000	0.206	0.320	5.5	0.226
5	225	15.20	30.5	2.30	0.250	0.454	1.90	90	0.000	0.206	0.340	5.7	0.271
5	226	15.20	30.5	2.30	0.250	0.237	4.10	90	0.000	0.206	0.210	6.4	0.069
5	227	15.20	30.5	2.30	0.250	0.288	3.40	90	0.000	0.206	0.200	6.4	0.102
5	228	15.20	30.5	2.30	0.250	0.338	2.90	90	0.000	0.206	0.270	6.5	0.142
5	229	15.20	30.5	2.30	0.250	0.388	2.60	90	0.000	0.206	0.280	6.6	0.186
5	230	15.20	30.5	2.30	0.250	0.431	2.30	90	0.000	0.206	0.280	6.5	0.233
5	231	15.20	30.5	2.30	0.250	0.457	2.00	90	0.000	0.206	0.330	6.0	0.270
5	232	15.20	30.5	2.30	0.250	0.263	4.10	90	0.000	0.206	0.280	7.1	0.083
5	233	15.20	30.5	2.30	0.250	0.321	3.40	90	0.000	0.206	0.270	7.2	0.123

Table A1. Individual observations of self-burial of objects by scour (cont.)

<i>No.</i>	<i>Obs.</i>	<i>D</i>	<i>L</i>	ρ_o/ρ	d_{50}	U_w	<i>T</i>	α	$U_c(z_{obs})$	z_{obs}	<i>B/D</i>	<i>KC</i>	θ
5	234	15.20	30.5	2.30	0.250	0.443	2.90	90	0.000	0.206	0.300	8.5	0.228
5	235	15.20	30.5	2.30	0.250	0.430	2.60	90	0.000	0.206	0.340	7.4	0.223
5	236	15.20	30.5	2.30	0.250	0.475	2.30	90	0.000	0.206	0.410	7.2	0.277
5	237	15.20	30.5	2.30	0.250	0.293	4.10	90	0.000	0.206	0.250	7.9	0.100
5	238	15.20	30.5	2.30	0.250	0.345	3.40	90	0.000	0.206	0.300	7.7	0.140
5	239	15.20	30.5	2.30	0.250	0.399	2.90	90	0.000	0.206	0.310	7.6	0.189
5	240	15.20	30.5	2.30	0.250	0.447	2.60	90	0.000	0.206	0.310	7.7	0.239
5	241	15.20	30.5	2.30	0.250	0.332	4.10	90	0.000	0.206	0.320	9.0	0.124
5	242	15.20	30.5	2.30	0.250	0.386	3.40	90	0.000	0.206	0.370	8.6	0.170
5	243	15.20	30.5	2.30	0.250	0.260	5.10	90	0.000	0.206	0.310	8.7	0.076
5	244	15.20	30.5	2.30	0.250	0.408	4.10	90	0.000	0.206	0.350	11.0	0.178
5	245	15.20	30.5	2.30	0.250	0.337	2.00	90	0.000	0.206	0.320	4.4	0.158
5	246	15.20	30.5	2.30	0.250	0.260	1.60	90	0.000	0.206	0.260	2.7	0.109
5	247	15.20	30.5	2.30	0.250	0.384	6.00	90	0.000	0.206	0.310	15.2	0.144
5	248	15.20	30.5	2.30	0.250	0.256	2.30	90	0.000	0.206	0.280	3.9	0.094
5	249	15.20	30.5	2.30	0.250	0.355	2.30	90	0.000	0.206	0.280	5.4	0.165
5	250	15.20	30.5	2.30	0.250	0.342	4.10	90	0.000	0.206	0.380	9.2	0.131
5	251	15.20	30.5	2.30	0.250	0.408	4.10	90	0.000	0.206	0.420	11.0	0.178
5	252	15.20	30.5	2.30	0.250	0.397	6.90	90	0.000	0.206	0.420	18.0	0.147
5	253	15.20	30.5	2.30	0.250	0.397	6.90	90	0.000	0.206	0.480	18.0	0.147
5	254	15.20	30.5	2.30	0.250	0.443	2.90	90	0.000	0.206	0.470	8.5	0.228
5	255	15.20	30.5	2.30	0.250	0.384	6.00	90	0.000	0.206	0.360	15.2	0.144
5	256	15.20	30.5	2.30	0.250	0.392	2.90	90	0.000	0.206	0.430	7.5	0.184
5	257	15.20	30.5	2.30	0.250	0.414	2.00	90	0.000	0.206	0.340	5.5	0.226
5	258	15.20	30.5	2.30	0.250	0.522	2.40	90	0.000	0.206	0.430	8.2	0.323
5	259	15.20	30.5	2.30	0.250	0.522	2.40	90	0.000	0.206	0.420	8.2	0.323
5	260	10.20	20.3	2.30	0.250	0.472	6.90	90	0.000	0.206	0.510	31.9	0.200
5	261	10.20	20.3	2.30	0.250	0.522	2.40	90	0.000	0.206	0.450	12.3	0.323
5	262	10.20	20.3	2.30	0.250	0.435	2.90	90	0.000	0.206	0.410	12.4	0.221
5	263	10.20	20.3	2.30	0.250	0.500	4.10	90	0.000	0.206	0.480	20.1	0.256
5	264	10.20	20.3	2.30	0.250	0.207	4.10	90	0.000	0.206	0.240	8.3	0.055
5	265	12.50	25.3	2.30	0.250	0.472	6.90	90	0.000	0.206	0.410	26.1	0.200
5	266	25.40	102.0	2.00	0.250	0.250	5.10	90	0.000	0.206	0.180	5.0	0.071
5	267	25.40	102.0	2.00	0.250	0.488	6.90	90	0.000	0.206	0.440	13.3	0.213
5	268	20.30	81.0	2.00	0.250	0.250	5.10	90	0.000	0.206	0.230	6.3	0.071
5	269	5.10	20.3	7.80	0.250	0.320	3.40	90	0.000	0.206	0.420	21.3	0.123
5	270	5.10	20.3	7.80	0.250	0.500	4.10	90	0.000	0.206	0.730	40.2	0.256
5	271	5.10	20.3	7.80	0.250	0.384	3.40	90	0.000	0.206	0.570	25.6	0.169
5	272	8.60	35.1	2.70	0.250	0.472	6.90	90	0.000	0.206	0.480	37.9	0.200
5	273	8.60	26.2	2.70	0.250	0.250	5.10	90	0.000	0.206	0.300	14.8	0.071
5	274	8.60	26.3	2.70	0.250	0.472	6.90	90	0.000	0.206	0.510	37.9	0.200

Table A1. Individual observations of self-burial of objects by scour (cont.)

<i>No.</i>	<i>Obs.</i>	<i>D</i>	<i>L</i>	ρ_o/ρ	d_{50}	U_w	<i>T</i>	α	$U_c(z_{obs})$	z_{obs}	<i>B/D</i>	<i>KC</i>	θ
5	275	8.60	26.2	2.70	0.250	0.207	4.10	90	0.000	0.206	0.260	9.9	0.055
5	276	15.20	30.5	2.30	0.250	0.207	1.80	90	0.072	0.206	0.100	3.3	0.116
5	277	15.20	30.5	2.30	0.250	0.195	2.40	90	0.072	0.206	0.150	4.2	0.098
5	278	15.20	30.5	2.30	0.250	0.232	1.90	90	0.072	0.206	0.140	3.8	0.132
5	279	15.20	30.5	2.30	0.250	0.286	1.90	90	0.072	0.206	0.190	4.4	0.176
5	280	15.20	30.5	2.30	0.250	0.386	1.60	90	0.072	0.206	0.250	4.8	0.288
5	281	15.20	30.5	2.30	0.250	0.422	1.90	90	0.072	0.206	0.230	6.1	0.312
5	282	15.20	30.5	2.30	0.250	0.387	2.70	90	0.072	0.206	0.260	8.1	0.246
5	283	15.20	30.5	2.30	0.250	0.407	2.70	90	0.072	0.206	0.290	8.5	0.265
5	284	15.20	30.5	2.30	0.250	0.394	3.20	90	0.072	0.206	0.300	9.8	0.240
5	285	15.20	30.5	2.30	0.250	0.213	1.70	90	0.117	0.206	0.110	3.7	0.157
5	286	15.20	30.5	2.30	0.250	0.237	1.90	90	0.117	0.206	0.220	4.4	0.172
5	287	15.20	30.5	2.30	0.250	0.291	1.90	90	0.117	0.206	0.280	5.1	0.221
5	288	15.20	30.5	2.30	0.250	0.391	1.60	90	0.117	0.206	0.260	5.3	0.345
5	289	15.20	30.5	2.30	0.250	0.306	2.70	90	0.117	0.206	0.190	7.5	0.211
5	290	15.20	30.5	2.30	0.250	0.427	1.90	90	0.117	0.206	0.260	6.8	0.369
5	291	15.20	30.5	2.30	0.250	0.401	2.30	90	0.117	0.206	0.280	7.8	0.319
5	292	15.20	30.5	2.30	0.250	0.413	2.70	90	0.117	0.206	0.300	9.4	0.317
5	293	15.20	30.5	2.30	0.250	0.400	3.10	90	0.117	0.206	0.280	10.5	0.291
5	294	15.20	30.5	2.30	0.250	0.218	1.70	90	0.173	0.206	0.170	4.3	0.210
5	295	15.20	30.5	2.30	0.250	0.206	2.30	90	0.173	0.206	0.190	5.7	0.181
5	296	15.20	30.5	2.30	0.250	0.243	1.40	90	0.173	0.206	0.250	3.8	0.250
5	297	15.20	30.5	2.30	0.250	0.407	2.30	90	0.173	0.206	0.380	8.7	0.389
5	298	15.20	30.5	2.30	0.250	0.418	2.60	90	0.173	0.206	0.370	10.0	0.388
5	299	15.20	30.5	2.30	0.250	0.421	5.80	90	0.173	0.206	0.400	22.5	0.312
5	300	15.20	30.5	2.30	0.250	0.511	2.20	90	0.173	0.206	0.330	9.8	0.531
5	301	15.20	30.5	2.30	0.250	0.452	5.80	90	0.173	0.206	0.300	23.6	0.343
5	302	15.20	30.5	2.30	0.250	0.452	5.80	90	0.173	0.206	0.470	23.6	0.343
5	303	15.20	30.5	2.30	0.250	0.452	5.80	90	0.173	0.206	0.400	23.6	0.343
5	304	15.20	30.5	2.30	0.250	0.190	2.00	90	0.173	0.206	0.120	4.7	0.175
5	305	15.20	30.5	2.30	0.250	0.230	2.30	90	0.173	0.206	0.180	6.0	0.202
5	306	15.20	30.5	2.30	0.250	0.316	3.70	90	0.173	0.206	0.260	11.8	0.248
5	307	15.20	30.5	2.30	0.250	0.449	2.70	90	0.173	0.206	0.390	11.0	0.421
5	308	15.20	30.5	2.30	0.250	0.449	2.70	90	0.173	0.206	0.330	11.0	0.421
5	309	15.20	30.5	2.30	0.250	0.306	2.70	90	0.173	0.206	0.230	8.4	0.262
5	310	15.20	30.5	2.30	0.250	0.350	1.40	90	0.173	0.206	0.170	4.8	0.377
5	311	15.20	30.5	2.30	0.250	0.350	1.40	90	0.173	0.206	0.210	4.8	0.377
5	312	25.40	102.0	2.00	0.250	0.235	3.60	90	0.173	0.206	0.220	5.8	0.188
5	313	25.40	102.0	2.00	0.250	0.275	4.40	90	0.173	0.206	0.250	7.8	0.209
5	314	25.40	102.0	2.00	0.250	0.257	5.10	90	0.173	0.206	0.270	8.7	0.187
5	315	25.40	102.0	2.00	0.250	0.211	2.00	90	0.173	0.206	0.150	3.1	0.202

Table A1. Individual observations of self-burial of objects by scour (cont.)

<i>No.</i>	<i>Obs.</i>	<i>D</i>	<i>L</i>	ρ_o/ρ	d_{50}	U_w	<i>T</i>	α	$U_c(z_{obs})$	z_{obs}	<i>B/D</i>	<i>KC</i>	θ
5	316	20.30	81.0	2.00	0.250	0.239	3.60	90	0.173	0.206	0.190	7.3	0.188
5	317	20.30	81.0	2.00	0.250	0.279	4.40	90	0.173	0.206	0.150	9.8	0.209
5	318	20.30	81.0	2.00	0.250	0.261	5.10	90	0.173	0.206	0.290	10.9	0.187
5	319	20.30	81.0	2.00	0.250	0.215	2.00	90	0.173	0.206	0.120	3.8	0.202
5	320	8.50	26.2	2.70	0.250	0.256	3.60	90	0.173	0.206	0.260	17.5	0.189
5	321	8.50	26.2	2.70	0.250	0.296	4.40	90	0.173	0.206	0.330	23.4	0.210
5	322	8.60	26.3	2.70	0.250	0.489	5.80	90	0.173	0.206	0.470	43.6	0.370
5	323	8.50	26.2	2.70	0.250	0.278	5.10	90	0.173	0.206	0.330	26.1	0.188
5	324	8.50	26.2	2.70	0.250	0.232	2.00	90	0.173	0.206	0.290	9.2	0.203
5	325	10.20	20.3	2.30	0.250	0.533	3.60	90	0.173	0.206	0.400	24.5	0.479
5	326	10.20	20.3	2.30	0.250	0.533	3.60	90	0.173	0.206	0.410	24.5	0.479
5	327	10.20	20.3	2.30	0.250	0.531	2.30	90	0.173	0.206	0.490	15.6	0.542
5	328	12.50	25.4	2.30	0.250	0.508	5.80	90	0.173	0.206	0.380	31.2	0.397
5	329	7.60	20.3	7.80	0.250	0.491	5.80	90	0.173	0.206	0.570	49.3	0.369
5	330	15.20	30.5	2.30	0.250	0.355	2.30	90	0.000	0.206	0.280	5.4	0.165
5	331	15.20	30.5	2.30	0.250	0.180	2.00	90	0.000	0.206	0.030	2.4	0.055
5	332	15.20	30.5	2.30	0.250	0.256	2.30	90	0.000	0.206	0.280	3.9	0.094
5	333	15.20	30.5	2.30	0.250	0.342	4.10	90	0.000	0.206	0.380	9.2	0.131
5	334	15.20	30.5	2.30	0.250	0.408	4.10	90	0.000	0.206	0.420	11.0	0.178
5	335	15.20	30.5	2.30	0.250	0.397	6.90	90	0.000	0.206	0.420	18.0	0.147
5	336	15.20	30.5	2.30	0.250	0.443	2.90	90	0.000	0.206	0.470	8.5	0.228
5	337	15.20	30.5	2.30	0.250	0.384	6.00	90	0.000	0.206	0.360	15.2	0.144
5	338	15.20	30.5	2.30	0.250	0.392	2.90	90	0.000	0.206	0.430	7.5	0.184
5	339	15.20	30.5	2.30	0.250	0.414	2.00	90	0.000	0.206	0.340	5.5	0.226
5	340	15.20	30.5	2.30	0.250	0.522	2.40	90	0.000	0.206	0.430	8.2	0.323
5	341	10.20	20.3	2.30	0.250	0.472	6.90	90	0.000	0.206	0.390	31.9	0.200
5	342	15.20	30.5	2.30	0.250	0.304	1.80	90	0.000	0.206	0.360	3.6	0.137
5	343	15.20	30.5	2.30	0.250	0.218	4.40	90	0.000	0.206	0.200	6.3	0.059
5	344	15.20	30.5	2.30	0.250	0.403	6.40	90	0.000	0.206	0.330	17.0	0.154
5	345	15.20	30.5	2.30	0.250	0.326	3.90	90	0.000	0.206	0.360	8.4	0.122
5	346	15.20	30.5	2.30	0.250	0.233	1.50	90	0.000	0.206	0.180	2.3	0.092
5	347	15.20	30.5	2.30	0.250	0.290	2.70	90	0.000	0.206	0.320	5.2	0.111
5	348	15.20	30.5	2.30	0.250	0.370	5.70	90	0.000	0.206	0.020	13.9	0.137
5	349	15.20	30.5	2.30	0.250	0.195	3.90	90	0.000	0.206	0.210	5.0	0.051
5	350	15.20	30.5	2.30	0.250	0.296	3.90	90	0.000	0.206	0.270	7.6	0.103
5	351	20.30	81.0	2.00	0.250	0.244	4.80	90	0.000	0.206	0.230	5.8	0.070
5	352	25.40	102.0	2.00	0.250	0.244	4.80	90	0.000	0.206	0.190	4.6	0.070
5	353	8.60	26.3	2.70	0.250	0.244	4.80	90	0.000	0.206	0.300	13.6	0.070
5	354	10.20	20.3	2.30	0.250	0.500	4.10	89	0.000	0.206	0.480	20.1	0.256
5	355	8.60	35.1	2.70	0.250	0.472	6.90	88	0.000	0.206	0.480	37.9	0.200
5	356	10.20	20.3	2.30	0.250	0.472	6.90	88	0.000	0.206	0.510	31.9	0.200

Table A1. Individual observations of self-burial of objects by scour (cont.)

<i>No.</i>	<i>Obs.</i>	<i>D</i>	<i>L</i>	ρ_o/ρ	d_{50}	U_w	<i>T</i>	α	$U_c(z_{obs})$	z_{obs}	<i>B/D</i>	<i>KC</i>	θ
5	357	10.20	20.3	2.30	0.250	0.472	6.90	87	0.000	0.206	0.300	31.9	0.200
5	358	10.20	20.3	2.30	0.250	0.522	2.40	87	0.000	0.206	0.450	12.3	0.323
5	359	12.50	25.3	2.30	0.250	0.472	6.90	86	0.000	0.206	0.410	26.1	0.200
5	360	15.20	30.5	2.30	0.250	0.397	6.90	85	0.000	0.206	0.480	18.0	0.147
5	361	10.20	20.3	2.30	0.250	0.435	2.90	85	0.000	0.206	0.410	12.4	0.221
5	362	10.20	20.3	2.30	0.250	0.500	4.10	84	0.000	0.206	0.370	20.1	0.256
5	363	15.20	30.5	2.30	0.250	0.522	2.40	81	0.000	0.206	0.420	8.2	0.323
5	364	25.40	102.0	2.00	0.250	0.488	6.90	80	0.000	0.206	0.440	13.3	0.213
5	365	8.60	35.1	2.70	0.250	0.522	2.40	77	0.000	0.206	0.600	14.6	0.323
5	366	15.20	30.5	2.30	0.250	0.392	2.90	76	0.000	0.206	0.290	7.5	0.184
5	367	10.20	20.3	2.30	0.250	0.554	2.60	76	0.000	0.206	0.650	14.1	0.351
5	368	15.20	30.5	2.30	0.250	0.397	6.90	75	0.000	0.206	0.310	18.0	0.147
5	369	20.30	81.0	2.00	0.250	0.488	6.90	75	0.000	0.206	0.420	16.6	0.213
5	370	10.20	20.3	2.30	0.250	0.488	6.90	75	0.000	0.206	0.370	33.0	0.213
5	371	12.50	25.4	2.30	0.250	0.488	6.90	75	0.000	0.206	0.440	26.9	0.213
5	372	15.20	30.5	2.30	0.250	0.408	4.10	74	0.000	0.206	0.390	11.0	0.178
5	373	15.20	30.5	2.30	0.250	0.384	6.00	74	0.000	0.206	0.350	15.2	0.144
5	374	15.20	30.5	2.30	0.250	0.414	2.00	74	0.000	0.206	0.410	5.5	0.226
5	375	12.50	25.4	2.30	0.250	0.554	2.60	74	0.000	0.206	0.400	11.5	0.351
5	376	15.20	30.5	2.30	0.250	0.392	2.90	73	0.000	0.206	0.440	7.5	0.184
5	377	15.20	30.5	2.30	0.250	0.443	2.90	72	0.000	0.206	0.330	8.5	0.228
5	378	15.20	30.5	2.30	0.250	0.522	2.40	72	0.000	0.206	0.360	8.2	0.323
5	379	8.60	35.1	2.70	0.250	0.435	2.90	72	0.000	0.206	0.390	14.7	0.221
5	380	10.20	20.3	2.30	0.250	0.500	4.10	72	0.000	0.206	0.550	20.1	0.256
5	381	12.50	25.4	2.30	0.250	0.267	5.10	72	0.000	0.206	0.340	10.9	0.080
5	382	15.20	30.5	2.30	0.250	0.342	4.10	71	0.000	0.206	0.380	9.2	0.131
5	383	15.20	30.5	2.30	0.250	0.384	6.00	71	0.000	0.206	0.330	15.2	0.144
5	384	12.50	25.3	2.30	0.250	0.522	2.40	71	0.000	0.206	0.550	10.0	0.323
5	385	10.20	20.3	2.30	0.250	0.522	2.40	70	0.000	0.206	0.430	12.3	0.323
5	386	15.20	30.5	2.30	0.250	0.342	4.10	70	0.000	0.206	0.370	9.2	0.131
5	387	15.20	30.5	2.30	0.250	0.443	2.90	70	0.000	0.206	0.420	8.5	0.228
5	388	8.60	26.3	2.70	0.250	0.472	6.90	70	0.000	0.206	0.510	37.9	0.200
5	389	10.20	20.3	2.30	0.250	0.435	2.90	70	0.000	0.206	0.340	12.4	0.221
5	390	15.20	30.5	2.30	0.250	0.355	2.30	70	0.000	0.206	0.270	5.4	0.165
5	391	8.60	26.3	2.70	0.250	0.435	2.90	69	0.000	0.206	0.440	14.7	0.221
5	392	15.20	30.5	2.30	0.250	0.256	2.30	68	0.000	0.206	0.250	3.9	0.094
5	393	8.60	35.1	2.70	0.250	0.260	5.10	68	0.000	0.206	0.410	15.4	0.076
5	394	10.20	20.3	2.30	0.250	0.260	5.10	68	0.000	0.206	0.390	13.0	0.076
5	395	8.60	26.3	2.70	0.250	0.260	5.10	67	0.000	0.206	0.150	15.4	0.076
5	396	15.20	30.5	2.30	0.250	0.355	2.30	66	0.000	0.206	0.390	5.4	0.165
5	397	5.10	20.3	7.80	0.250	0.522	2.40	66	0.000	0.206	0.620	24.6	0.323

Table A1. Individual observations of self-burial of objects by scour (cont.)

<i>No.</i>	<i>Obs.</i>	<i>D</i>	<i>L</i>	ρ_o/ρ	d_{50}	U_w	<i>T</i>	α	$U_c(z_{obs})$	z_{obs}	<i>B/D</i>	<i>KC</i>	θ
5	398	10.20	20.3	2.30	0.250	0.522	2.40	66	0.000	0.206	0.470	12.3	0.323
5	399	15.20	30.5	2.30	0.250	0.408	4.10	65	0.000	0.206	0.380	11.0	0.178
5	400	15.20	30.5	2.30	0.250	0.414	2.00	65	0.000	0.206	0.250	5.5	0.226
5	401	10.20	20.3	2.30	0.250	0.260	5.10	65	0.000	0.206	0.330	13.0	0.076
5	402	12.50	25.3	2.30	0.250	0.260	5.10	65	0.000	0.206	0.300	10.6	0.076
5	403	12.50	25.3	2.30	0.250	0.435	2.90	65	0.000	0.206	0.280	10.1	0.221
5	404	8.60	26.3	2.70	0.250	0.522	2.40	65	0.000	0.206	0.680	14.6	0.323
5	405	15.20	30.5	2.30	0.250	0.355	2.30	64	0.000	0.206	0.360	5.4	0.165
5	406	5.10	20.3	7.80	0.250	0.435	2.90	64	0.000	0.206	0.370	24.7	0.221
5	407	15.20	30.5	2.30	0.250	0.522	2.40	63	0.000	0.206	0.380	8.2	0.323
5	408	10.20	20.3	2.30	0.250	0.267	5.10	63	0.000	0.206	0.260	13.4	0.080
5	409	15.20	30.5	2.30	0.250	0.256	2.30	62	0.000	0.206	0.300	3.9	0.094
5	410	15.20	30.5	2.30	0.250	0.408	4.10	62	0.000	0.206	0.350	11.0	0.178
5	411	15.20	30.5	2.30	0.250	0.188	2.00	60	0.000	0.206	0.120	2.5	0.059
5	412	12.50	25.3	2.30	0.250	0.500	4.10	60	0.000	0.206	0.400	16.4	0.256
5	413	10.20	20.3	2.30	0.250	0.435	2.90	58	0.000	0.206	0.390	12.4	0.221
5	414	20.30	81.0	2.00	0.250	0.554	2.60	56	0.000	0.206	0.390	7.1	0.351
5	415	8.60	35.1	2.70	0.250	0.500	4.10	55	0.000	0.206	0.770	23.8	0.256
5	416	7.60	20.3	7.80	0.250	0.522	2.40	54	0.000	0.206	0.540	16.5	0.323
5	417	20.30	81.0	2.00	0.250	0.267	5.10	54	0.000	0.206	0.270	6.7	0.080
5	418	25.40	102.0	2.00	0.250	0.554	2.60	54	0.000	0.206	0.250	5.7	0.351
5	419	15.20	30.5	2.30	0.250	0.392	2.90	52	0.000	0.206	0.280	7.5	0.184
5	420	25.40	102.0	2.00	0.250	0.267	5.10	51	0.000	0.206	0.220	5.4	0.080
5	421	15.20	30.5	2.30	0.250	0.397	6.90	50	0.000	0.206	0.480	18.0	0.147
5	422	15.20	30.5	2.30	0.250	0.384	6.00	50	0.000	0.206	0.270	15.2	0.144
5	423	5.10	20.3	7.80	0.250	0.260	5.10	50	0.000	0.206	0.420	26.0	0.076
5	424	8.60	26.3	2.70	0.250	0.500	4.10	49	0.000	0.206	0.460	23.8	0.256
5	425	15.20	30.5	2.30	0.250	0.414	2.00	47	0.000	0.206	0.160	5.5	0.226
5	426	15.20	30.5	2.30	0.250	0.188	2.00	45	0.000	0.206	0.110	2.5	0.059
5	427	5.10	20.3	7.80	0.250	0.472	6.90	45	0.000	0.206	0.440	63.9	0.200
5	428	7.60	20.3	7.80	0.250	0.435	2.90	45	0.000	0.206	0.480	16.6	0.221
5	429	15.20	30.5	2.30	0.250	0.443	2.90	44	0.000	0.206	0.130	8.5	0.228
5	430	10.20	20.3	2.30	0.250	0.260	5.10	42	0.000	0.206	0.070	13.0	0.076
5	431	7.60	20.3	7.80	0.250	0.500	4.10	38	0.000	0.206	0.620	27.0	0.256
5	432	7.60	20.3	7.80	0.250	0.472	6.90	38	0.000	0.206	0.370	42.9	0.200
5	433	15.20	30.5	2.30	0.250	0.342	4.10	37	0.000	0.206	0.210	9.2	0.131
5	434	7.60	20.3	7.80	0.250	0.260	5.10	31	0.000	0.206	0.390	17.5	0.076
5	435	15.20	30.5	2.30	0.250	0.188	2.00	30	0.000	0.206	0.060	2.5	0.059
5	436	15.20	30.5	2.30	0.250	0.414	2.00	23	0.000	0.206	0.230	5.5	0.226
5	437	15.20	30.5	2.30	0.250	0.355	2.30	0	0.000	0.206	0.030	5.4	0.165
5	438	15.20	30.5	2.30	0.250	0.188	2.00	0	0.000	0.206	0.130	2.5	0.059

Table A1. Individual observations of self-burial of objects by scour (cont.)

<i>No.</i>	<i>Obs.</i>	<i>D</i>	<i>L</i>	ρ_o/ρ	d_{50}	U_w	<i>T</i>	α	$U_c(z_{obs})$	z_{obs}	<i>B/D</i>	<i>KC</i>	θ
5	439	15.20	30.5	2.30	0.250	0.342	4.10	0	0.000	0.206	0.050	9.2	0.131
5	440	15.20	30.5	2.30	0.250	0.408	4.10	0	0.000	0.206	0.050	11.0	0.178
5	441	15.20	30.5	2.30	0.250	0.397	6.90	0	0.000	0.206	0.030	18.0	0.147
5	442	15.20	30.5	2.30	0.250	0.443	2.90	0	0.000	0.206	0.040	8.5	0.228
5	443	15.20	30.5	2.30	0.250	0.384	6.00	0	0.000	0.206	0.050	15.2	0.144
5	444	15.20	30.5	2.30	0.250	0.392	2.90	0	0.000	0.206	0.060	7.5	0.184
5	445	15.20	30.5	2.30	0.250	0.522	2.40	0	0.000	0.206	0.090	8.2	0.323
5	446	10.20	20.3	2.30	0.250	0.533	3.60	93	0.173	0.206	0.410	24.5	0.479
5	447	15.20	30.5	2.30	0.250	0.511	2.20	90	0.173	0.206	0.330	9.8	0.531
5	448	15.20	30.5	2.30	0.250	0.452	5.80	90	0.173	0.206	0.300	23.6	0.343
5	449	15.20	30.5	2.30	0.250	0.190	2.00	90	0.173	0.206	0.120	4.7	0.175
5	450	15.20	30.5	2.30	0.250	0.230	2.30	90	0.173	0.206	0.180	6.0	0.202
5	451	15.20	30.5	2.30	0.250	0.316	3.70	90	0.173	0.206	0.260	11.8	0.248
5	452	15.20	30.5	2.30	0.250	0.449	2.70	90	0.173	0.206	0.390	11.0	0.421
5	453	15.20	30.5	2.30	0.250	0.306	2.70	90	0.173	0.206	0.230	8.4	0.262
5	454	15.20	30.5	2.30	0.250	0.350	1.40	90	0.173	0.206	0.170	4.8	0.377
5	455	15.20	30.5	2.30	0.250	0.362	1.80	90	0.173	0.206	0.400	6.3	0.362
5	456	15.20	30.5	2.30	0.250	0.362	5.90	90	0.173	0.206	0.420	20.6	0.257
5	457	15.20	30.5	2.30	0.250	0.393	3.90	90	0.173	0.206	0.400	14.4	0.319
5	458	20.30	81.0	2.00	0.250	0.234	3.80	90	0.173	0.206	0.210	7.6	0.181
5	459	25.40	102.0	2.00	0.250	0.230	3.80	90	0.173	0.206	0.240	6.1	0.181
5	460	8.60	26.3	2.70	0.250	0.251	3.80	90	0.173	0.206	0.300	18.0	0.182
5	461	25.40	102.0	2.00	0.250	0.183	2.20	90	0.173	0.206	0.150	3.1	0.172
5	462	20.30	81.0	2.00	0.250	0.187	2.20	90	0.173	0.206	0.210	3.9	0.172
5	463	10.20	20.3	2.30	0.250	0.533	3.60	88	0.173	0.206	0.400	24.5	0.479
5	464	12.50	25.4	2.30	0.250	0.508	5.80	87	0.173	0.206	0.380	31.2	0.397
5	465	8.60	26.3	2.70	0.250	0.489	5.80	86	0.173	0.206	0.470	43.6	0.370
5	466	10.20	20.3	2.30	0.250	0.485	5.80	86	0.173	0.206	0.340	36.7	0.369
5	467	15.20	30.5	2.30	0.250	0.449	2.70	86	0.173	0.206	0.330	11.0	0.421
5	468	10.20	20.3	2.30	0.250	0.485	5.80	85	0.173	0.206	0.370	36.7	0.369
5	469	10.20	20.3	2.30	0.250	0.512	5.80	85	0.173	0.206	0.330	38.2	0.397
5	470	15.20	30.5	2.30	0.250	0.452	5.80	84	0.173	0.206	0.400	23.6	0.343
5	471	15.20	30.5	2.30	0.250	0.452	5.80	81	0.173	0.206	0.470	23.6	0.343
5	472	10.20	20.3	2.30	0.250	0.531	2.30	81	0.173	0.206	0.490	15.6	0.542
5	473	15.20	30.5	2.30	0.250	0.350	1.40	80	0.173	0.206	0.210	4.8	0.377
5	474	15.20	30.5	2.30	0.250	0.316	3.70	78	0.173	0.206	0.280	11.8	0.248
5	475	15.20	30.5	2.30	0.250	0.306	2.70	77	0.173	0.206	0.280	8.4	0.262
5	476	10.20	20.3	2.30	0.250	0.444	2.60	76	0.173	0.206	0.420	15.4	0.410
5	477	15.20	30.5	2.30	0.250	0.230	2.30	76	0.173	0.206	0.180	6.0	0.202
5	478	15.20	30.5	2.30	0.250	0.306	2.70	76	0.173	0.206	0.290	8.4	0.262
5	479	15.20	30.5	2.30	0.250	0.452	5.80	75	0.173	0.206	0.380	23.6	0.343

Table A1. Individual observations of self-burial of objects by scour (cont.)

<i>No.</i>	<i>Obs.</i>	<i>D</i>	<i>L</i>	ρ_o/ρ	d_{50}	U_w	<i>T</i>	α	$U_c(z_{obs})$	z_{obs}	<i>B/D</i>	<i>KC</i>	θ
5	480	15.20	30.5	2.30	0.250	0.190	2.00	75	0.173	0.206	0.060	4.7	0.175
5	481	15.20	30.5	2.30	0.250	0.316	3.70	75	0.173	0.206	0.290	11.8	0.248
5	482	8.60	35.1	2.70	0.250	0.489	5.80	73	0.173	0.206	0.450	43.6	0.370
5	483	15.20	30.5	2.30	0.250	0.449	2.70	73	0.173	0.206	0.300	11.0	0.421
5	484	15.20	30.5	2.30	0.250	0.316	3.70	72	0.173	0.206	0.260	11.8	0.248
5	485	20.30	81.0	2.00	0.250	0.499	5.80	72	0.173	0.206	0.400	19.2	0.397
5	486	5.10	20.3	7.80	0.250	0.546	3.60	71	0.173	0.206	0.460	49.0	0.479
5	487	8.60	35.1	2.70	0.250	0.448	2.60	71	0.173	0.206	0.580	18.3	0.411
5	488	12.50	25.4	2.30	0.250	0.527	2.30	71	0.173	0.206	0.430	12.7	0.542
5	489	15.20	30.5	2.30	0.250	0.511	2.20	70	0.173	0.206	0.360	9.8	0.531
5	490	10.20	20.3	2.30	0.250	0.276	4.40	70	0.173	0.206	0.340	18.8	0.197
5	491	10.20	20.3	2.30	0.250	0.276	4.40	70	0.173	0.206	0.360	18.8	0.197
5	492	5.10	20.3	7.80	0.250	0.498	5.80	69	0.173	0.206	0.450	73.4	0.369
5	493	10.20	20.3	2.30	0.250	0.276	4.40	69	0.173	0.206	0.270	18.8	0.197
5	494	15.20	30.5	2.30	0.250	0.230	2.30	69	0.173	0.206	0.280	6.0	0.202
5	495	15.20	30.5	2.30	0.250	0.449	2.70	69	0.173	0.206	0.420	11.0	0.421
5	496	15.20	30.5	2.30	0.250	0.350	2.40	69	0.173	0.206	0.260	8.2	0.318
5	497	8.60	26.3	2.70	0.250	0.448	2.60	68	0.173	0.206	0.520	18.3	0.411
5	498	10.20	20.3	2.30	0.250	0.444	2.60	68	0.173	0.206	0.330	15.4	0.410
5	499	15.20	30.5	2.30	0.250	0.449	2.70	68	0.173	0.206	0.340	11.0	0.421
5	500	10.20	20.3	2.30	0.250	0.533	3.60	67	0.173	0.206	0.420	24.5	0.479
5	501	7.60	20.3	7.80	0.250	0.450	2.60	67	0.173	0.206	0.440	20.7	0.411
5	502	15.20	30.5	2.30	0.250	0.306	2.70	67	0.173	0.206	0.280	8.4	0.262
5	503	15.20	30.5	2.30	0.250	0.511	2.20	66	0.173	0.206	0.380	9.8	0.531
5	504	10.20	20.3	2.30	0.250	0.274	4.40	66	0.173	0.206	0.360	18.7	0.195
5	505	8.60	35.1	2.70	0.250	0.280	4.40	65	0.173	0.206	0.190	22.4	0.197
5	506	12.50	25.3	2.30	0.250	0.272	4.40	65	0.173	0.206	0.340	15.3	0.196
5	507	5.10	20.3	7.80	0.250	0.457	2.60	65	0.173	0.206	0.450	30.8	0.411
5	508	15.20	30.5	2.30	0.250	0.190	2.00	64	0.173	0.206	0.100	4.7	0.175
5	509	15.20	30.5	2.30	0.250	0.306	2.70	63	0.173	0.206	0.310	8.4	0.262
5	510	12.50	25.3	2.30	0.250	0.481	5.80	62	0.173	0.206	0.470	29.9	0.369
5	511	12.50	25.4	2.30	0.250	0.270	4.40	62	0.173	0.206	0.190	15.3	0.195
5	512	8.60	26.3	2.70	0.250	0.537	3.60	61	0.173	0.206	0.450	29.1	0.480
5	513	5.10	20.3	7.80	0.250	0.289	4.40	61	0.173	0.206	0.340	37.7	0.197
5	514	15.20	30.5	2.30	0.250	0.511	2.20	60	0.173	0.206	0.300	9.8	0.531
5	515	15.20	30.5	2.30	0.250	0.316	3.70	60	0.173	0.206	0.310	11.8	0.248
5	516	12.50	25.3	2.30	0.250	0.529	3.60	58	0.173	0.206	0.370	20.0	0.478
5	517	8.60	26.3	2.70	0.250	0.280	4.40	58	0.173	0.206	0.360	22.4	0.197
5	518	7.60	20.3	7.80	0.250	0.491	5.80	57	0.173	0.206	0.570	49.3	0.369
5	519	8.60	35.1	2.70	0.250	0.537	3.60	56	0.173	0.206	0.470	29.1	0.480
5	520	15.20	30.5	2.30	0.250	0.452	5.80	56	0.173	0.206	0.390	23.6	0.343

Table A1. Individual observations of self-burial of objects by scour (cont.)

<i>No.</i>	<i>Obs.</i>	<i>D</i>	<i>L</i>	ρ_o/ρ	d_{50}	U_w	<i>T</i>	α	$U_c(z_{obs})$	z_{obs}	<i>B/D</i>	<i>KC</i>	θ
5	521	25.40	102.0	2.00	0.250	0.495	5.80	56	0.173	0.206	0.420	15.3	0.397
5	522	7.60	20.3	7.80	0.250	0.282	4.40	55	0.173	0.206	0.420	25.3	0.197
5	523	10.20	20.3	2.30	0.250	0.444	2.60	55	0.173	0.206	0.480	15.4	0.410
5	524	15.20	30.5	2.30	0.250	0.230	2.30	55	0.173	0.206	0.180	6.0	0.202
5	525	20.30	81.0	2.00	0.250	0.518	2.30	54	0.173	0.206	0.240	7.8	0.541
5	526	25.40	102.0	2.00	0.250	0.514	2.30	54	0.173	0.206	0.280	6.3	0.542
5	527	15.20	30.5	2.30	0.250	0.190	2.00	52	0.173	0.206	0.160	4.7	0.175
5	528	15.20	30.5	2.30	0.250	0.350	1.40	52	0.173	0.206	0.230	4.8	0.377
5	529	20.30	81.0	2.00	0.250	0.261	4.40	52	0.173	0.206	0.190	9.4	0.195
5	530	10.20	20.3	2.30	0.250	0.485	5.80	50	0.173	0.206	0.460	36.7	0.369
5	531	12.50	25.3	2.30	0.250	0.440	2.60	48	0.173	0.206	0.280	12.6	0.410
5	532	15.20	30.5	2.30	0.250	0.230	2.30	48	0.173	0.206	0.210	6.0	0.202
5	533	25.40	102.0	2.00	0.250	0.257	4.40	48	0.173	0.206	0.140	7.5	0.195
5	534	7.60	20.3	7.80	0.250	0.539	3.60	47	0.173	0.206	0.500	32.9	0.480
5	535	15.20	30.5	2.30	0.250	0.350	1.40	39	0.173	0.206	0.170	4.8	0.377
5	536	15.20	30.5	2.30	0.250	0.190	2.00	28	0.173	0.206	0.040	4.7	0.175
5	537	15.20	30.5	2.30	0.250	0.511	2.20	0	0.173	0.206	0.040	9.8	0.531
5	538	15.20	30.5	2.30	0.250	0.452	5.80	0	0.173	0.206	0.050	23.6	0.343
5	539	15.20	30.5	2.30	0.250	0.190	2.00	0	0.173	0.206	0.030	4.7	0.175
5	540	15.20	30.5	2.30	0.250	0.230	2.30	0	0.173	0.206	0.040	6.0	0.202
5	541	15.20	30.5	2.30	0.250	0.316	3.70	0	0.173	0.206	0.040	11.8	0.248
5	542	15.20	30.5	2.30	0.250	0.449	2.70	0	0.173	0.206	0.040	11.0	0.421
5	543	15.20	30.5	2.30	0.250	0.306	2.70	0	0.173	0.206	0.050	8.4	0.262
5	544	15.20	30.5	2.30	0.250	0.350	1.40	0	0.173	0.206	0.090	4.8	0.377
6	545	8.60	34.4	2.70	0.250	0.200	6.00	90	0.000	0.043	0.150	14.0	0.047
6	546	8.60	34.4	2.70	0.250	0.300	6.00	90	0.000	0.043	0.260	20.9	0.093
6	547	8.60	34.4	2.70	0.250	0.400	6.00	90	0.000	0.043	0.410	27.9	0.155
6	548	8.60	34.4	2.70	0.250	0.500	6.00	90	0.000	0.043	0.650	34.9	0.230
6	549	8.60	34.4	2.70	0.250	0.600	6.00	90	0.000	0.043	0.780	41.9	0.320
6	550	8.60	34.4	2.70	0.250	0.700	6.00	90	0.000	0.043	1.000	48.8	0.424
6	551	8.60	34.4	2.70	0.250	0.800	6.00	90	0.000	0.043	1.000	55.8	0.541
6	552	8.60	34.4	2.70	0.250	0.400	9.00	90	0.000	0.043	0.450	41.9	0.139
6	553	8.60	34.4	2.70	0.250	0.250	4.00	90	0.000	0.043	0.270	11.6	0.077
6	554	8.60	34.4	2.70	0.250	0.600	6.00	90	0.000	0.043	0.730	41.9	0.320
6	555	8.60	34.4	2.70	0.250	0.350	9.00	90	0.000	0.043	0.330	36.6	0.110
6	556	8.60	34.4	2.70	0.250	0.500	9.00	90	0.000	0.043	0.500	52.3	0.207
6	557	8.60	34.4	2.70	0.250	0.600	6.00	90	0.000	0.043	0.730	41.9	0.320
6	558	8.60	34.4	2.70	0.250	0.400	4.00	90	0.000	0.043	0.530	18.6	0.173
6	559	8.60	34.4	2.70	0.250	0.500	4.00	90	0.000	0.043	0.700	23.3	0.258
6	560	7.50	20.3	7.80	0.250	0.400	4.00	90	0.000	0.038	0.510	21.3	0.173
6	561	7.50	20.3	7.80	0.250	0.250	5.00	90	0.000	0.038	0.220	16.7	0.072

Table A1. Individual observations of self-burial of objects by scour (cont.)

<i>No.</i>	<i>Obs.</i>	<i>D</i>	<i>L</i>	ρ_o/ρ	d_{50}	U_w	<i>T</i>	α	$U_c(z_{obs})$	z_{obs}	<i>B/D</i>	<i>KC</i>	θ
6	562	7.50	20.3	7.80	0.250	0.400	12.0	90	0.000	0.038	0.460	64.0	0.129
6	563	7.50	20.3	7.80	0.250	0.650	8.00	90	0.000	0.038	0.820	69.3	0.344
6	564	7.50	20.3	7.80	0.250	0.300	4.00	90	0.000	0.038	0.380	16.0	0.105
6	565	7.50	20.3	7.80	0.250	0.400	7.00	90	0.000	0.038	0.390	37.3	0.148
6	566	7.50	20.3	7.80	0.250	0.600	5.00	90	0.000	0.038	0.860	40.0	0.337
6	567	10.00	20.0	2.30	0.250	0.300	6.00	90	0.000	0.050	0.290	18.0	0.093
6	568	10.00	20.0	2.30	0.250	0.600	6.00	90	0.000	0.050	0.790	36.0	0.320
6	569	10.00	20.0	2.30	0.250	0.250	5.00	90	0.000	0.050	0.240	12.5	0.072
6	570	10.00	20.0	2.30	0.250	0.400	12.0	90	0.000	0.050	0.440	48.0	0.129
6	571	10.00	20.0	2.30	0.250	0.650	8.00	90	0.000	0.050	0.820	52.0	0.344
6	572	12.50	25.0	2.30	0.250	0.200	3.00	90	0.000	0.063	0.190	4.8	0.057
6	573	12.50	25.0	2.30	0.250	0.350	6.00	90	0.000	0.063	0.320	16.8	0.122
6	574	12.50	25.0	2.30	0.250	0.600	10.0	90	0.000	0.063	0.820	48.0	0.281
7	575	8.60	34.4	2.70	0.250	0.250	6.00	90	0.190	0.050	0.280	31.6	0.193
7	576	10.00	20.0	2.30	0.250	0.250	6.00	90	0.190	0.050	0.290	27.4	0.195
7	577	8.60	34.4	2.70	0.250	0.450	6.00	90	0.190	0.050	0.580	45.5	0.373
7	578	10.00	20.0	2.30	0.250	0.450	6.00	90	0.190	0.050	0.560	39.4	0.377
7	579	8.60	34.4	2.70	0.250	0.500	5.00	90	0.250	0.050	0.720	44.6	0.525
7	580	10.00	20.0	2.30	0.250	0.500	5.00	90	0.250	0.050	0.730	38.6	0.530
7	581	8.60	34.4	2.70	0.250	0.000	Inf	90	0.340	0.050	0.400	Inf	0.070
7	582	10.00	20.0	2.30	0.250	0.000	Inf	90	0.340	0.050	0.410	Inf	0.070
7	583	8.60	34.4	2.70	0.250	0.000	Inf	90	0.450	0.050	0.520	Inf	0.123
8-14	584	47.00	150.0	2.37	0.171	0.505	7.00	90	0.180	4.000	0.269	7.8	0.317
8-14	585	47.00	150.0	2.37	0.171	0.505	7.00	90	0.180	4.000	0.414	7.8	0.317
8-14	586	47.00	150.0	2.37	0.171	0.549	6.10	90	0.291	4.000	0.269	7.8	0.413
8-14	587	47.00	150.0	2.37	0.171	0.549	6.10	90	0.291	4.000	0.368	7.8	0.413
8-14	588	47.00	150.0	2.37	0.171	0.668	6.90	90	0.299	4.000	0.544	10.5	0.547
8-14	589	47.00	150.0	2.37	0.171	0.668	6.90	90	0.299	4.000	0.335	10.5	0.547
8-14	590	47.00	150.0	2.37	0.171	1.186	9.10	90	0.229	4.000	1.000	23.3	1.329
8-14	591	47.00	150.0	2.37	0.171	1.186	9.10	90	0.229	4.000	0.975	23.3	1.329
8-14	592	47.00	150.0	2.37	0.171	0.571	6.90	90	0.200	4.000	0.597	8.7	0.395
8-14	593	47.00	150.0	2.37	0.171	0.571	6.90	90	0.200	4.000	0.444	8.7	0.395
8-14	594	47.00	150.0	2.37	0.171	0.728	9.60	90	0.268	4.000	0.677	15.5	0.569
8-14	595	47.00	150.0	2.37	0.171	0.728	9.60	90	0.268	4.000	0.642	15.5	0.569
8-14	596	47.00	150.0	2.37	0.171	0.740	7.00	90	0.281	4.000	0.873	11.6	0.636
8-14	597	47.00	150.0	2.37	0.171	0.740	7.00	90	0.281	4.000	0.842	11.6	0.636
8-14	598	53.30	203.0	1.98	0.135	0.534	7.30	90	0.164	1.100	0.679	7.6	0.414
8-14	599	53.30	203.0	1.98	0.135	0.534	7.30	90	0.164	1.100	0.534	7.6	0.414
8-14	600	53.30	203.0	1.98	0.135	0.534	7.30	90	0.164	1.100	0.590	7.6	0.414
8-14	601	53.30	203.0	1.98	0.135	0.534	7.30	90	0.164	1.100	0.399	7.6	0.414
8-14	602	53.30	203.0	1.98	0.135	0.534	7.30	90	0.164	1.100	0.679	7.6	0.414

Table A1. Individual observations of self-burial of objects by scour (cont.)

<i>No.</i>	<i>Obs.</i>	<i>D</i>	<i>L</i>	ρ_o/ρ	d_{50}	U_w	<i>T</i>	α	$U_c(z_{obs})$	z_{obs}	<i>B/D</i>	<i>KC</i>	θ
8-14	603	53.30	203.0	1.98	0.135	0.534	7.30	90	0.164	1.100	0.434	7.6	0.414
8-14	604	53.30	203.0	1.98	0.135	0.534	7.30	90	0.164	1.100	0.623	7.6	0.414
8-14	605	53.30	203.0	1.98	0.135	0.534	7.30	90	0.164	1.100	0.472	7.6	0.414
8-14	606	47.00	150.0	2.37	0.135	0.534	7.30	90	0.164	1.100	0.340	8.6	0.413
8-14	607	47.00	150.0	2.37	0.135	0.534	7.30	90	0.164	1.100	0.723	8.6	0.413
8-14	608	47.00	150.0	2.37	0.559	0.534	7.30	90	0.164	1.100	0.106	8.6	0.158
8-14	609	47.00	150.0	2.37	0.559	0.534	7.30	90	0.164	1.100	0.388	8.6	0.158
8-14	610	53.30	203.0	1.98	0.135	0.650	6.90	90	0.239	1.100	0.759	8.9	0.610
8-14	611	53.30	203.0	1.98	0.135	0.650	6.90	90	0.239	1.100	0.822	8.9	0.610
8-14	612	53.30	203.0	1.98	0.135	0.650	6.90	90	0.239	1.100	0.707	8.9	0.610
8-14	613	53.30	203.0	1.98	0.135	0.650	6.90	90	0.239	1.100	0.716	8.9	0.610
8-14	614	53.30	203.0	1.98	0.135	0.650	6.90	90	0.239	1.100	0.962	8.9	0.610
8-14	615	53.30	203.0	1.98	0.135	0.650	6.90	90	0.239	1.100	0.925	8.9	0.610
8-14	616	53.30	203.0	1.98	0.135	0.650	6.90	90	0.239	1.100	0.830	8.9	0.610
8-14	617	53.30	203.0	1.98	0.135	0.650	6.90	90	0.239	1.100	0.830	8.9	0.610
8-14	618	47.00	150.0	2.37	0.135	0.650	6.90	90	0.239	1.100	0.787	10.1	0.608
8-14	619	47.00	150.0	2.37	0.135	0.650	6.90	90	0.239	1.100	0.617	10.1	0.608
8-14	620	47.00	150.0	2.37	0.135	0.650	6.90	90	0.239	1.100	0.532	10.1	0.608
8-14	621	47.00	150.0	2.37	0.135	0.650	6.90	90	0.239	1.100	0.787	10.1	0.608
8-14	622	47.00	150.0	2.37	0.559	0.650	6.90	90	0.239	1.100	0.021	10.1	0.234
8-14	623	47.00	150.0	2.37	0.559	0.650	6.90	90	0.239	1.100	0.426	10.1	0.234
8-14	624	53.30	203.0	1.98	0.135	0.714	8.80	90	0.101	1.100	0.713	11.9	0.625
8-14	625	53.30	203.0	1.98	0.135	0.714	8.80	90	0.101	1.100	0.703	11.9	0.625
8-14	626	53.30	203.0	1.98	0.135	0.714	8.80	90	0.101	1.100	0.720	11.9	0.625
8-14	627	53.30	203.0	1.98	0.135	0.714	8.80	90	0.101	1.100	0.585	11.9	0.625
8-14	628	53.30	203.0	1.98	0.135	0.714	8.80	90	0.101	1.100	0.981	11.9	0.625
8-14	629	53.30	203.0	1.98	0.135	0.714	8.80	90	0.101	1.100	0.962	11.9	0.625
8-14	630	53.30	203.0	1.98	0.135	0.714	8.80	90	0.101	1.100	0.962	11.9	0.625
8-14	631	53.30	203.0	1.98	0.135	0.714	8.80	90	0.101	1.100	0.755	11.9	0.625
8-14	632	47.00	150.0	2.37	0.135	0.714	8.80	90	0.101	1.100	0.979	13.5	0.625
8-14	633	47.00	150.0	2.37	0.135	0.714	8.80	90	0.101	1.100	0.745	13.5	0.625
8-14	634	47.00	150.0	2.37	0.135	0.714	8.80	90	0.101	1.100	0.872	13.5	0.625
8-14	635	47.00	150.0	2.37	0.559	0.714	8.80	90	0.101	1.100	0.128	13.5	0.237
8-14	636	47.00	150.0	2.37	0.559	0.714	8.80	90	0.101	1.100	0.404	13.5	0.237
8-14	637	53.30	203.0	1.98	0.650	0.807	7.00	90	0.252	4.000	0.438	10.9	0.295
8-14	638	53.30	203.0	1.98	0.650	0.807	7.00	90	0.252	4.000	0.409	10.9	0.295
8-14	639	53.30	203.0	1.98	0.171	0.807	7.00	90	0.252	4.000	0.760	11.0	0.724
8-14	640	53.30	203.0	1.98	0.171	0.807	7.00	90	0.252	4.000	0.910	11.0	0.724
8-14	641	53.30	203.0	1.98	0.171	0.807	7.90	90	0.252	4.000	1.170	12.4	0.704
8-14	642	53.30	203.0	1.98	0.650	1.087	7.90	90	0.384	4.000	0.551	16.8	0.487
8-14	643	53.30	203.0	1.98	0.650	1.087	7.90	90	0.384	4.000	0.360	16.8	0.487

Table A1. Individual observations of self-burial of objects by scour (cont.)

<i>No.</i>	<i>Obs.</i>	<i>D</i>	<i>L</i>	ρ_o/ρ	d_{50}	U_w	<i>T</i>	α	$U_c(z_{obs})$	z_{obs}	<i>B/D</i>	<i>KC</i>	θ
8-14	644	53.30	203.0	1.98	0.171	1.087	7.90	90	0.384	4.000	0.879	16.8	1.237
8-14	645	53.30	203.0	1.98	0.171	1.087	7.90	90	0.384	4.000	1.003	16.8	1.237
8-14	646	53.30	203.0	1.98	0.650	1.279	8.50	90	0.398	4.000	0.551	21.1	0.624
8-14	647	53.30	203.0	1.98	0.650	1.279	8.50	90	0.398	4.000	0.436	21.1	0.624
8-14	648	53.30	203.0	1.98	0.171	1.279	8.50	90	0.398	4.000	0.928	21.1	1.613
8-14	649	53.30	203.0	1.98	0.171	1.279	8.50	90	0.398	4.000	1.015	21.1	1.613
8-14	650	53.30	203.0	1.98	0.171	1.279	8.50	90	0.398	4.000	1.094	21.1	1.613
15	651	2.54	9.9	2.72	0.420	0.000	Inf	90	0.200	0.220	0.020	Inf	0.012
15	652	10.50	32.0	2.42	0.420	0.000	Inf	90	0.200	0.220	0.020	Inf	0.012
15	653	2.50	10.0	7.90	0.420	0.000	Inf	90	0.200	0.220	0.020	Inf	0.012
15	654	2.54	9.9	2.72	0.420	0.000	Inf	90	0.308	0.220	0.490	Inf	0.028
15	655	10.50	32.0	2.42	0.420	0.000	Inf	90	0.309	0.220	0.160	Inf	0.028
15	656	2.50	10.0	7.90	0.420	0.000	Inf	90	0.306	0.220	0.550	Inf	0.027
15	657	10.30	31.9	4.52	0.420	0.000	Inf	90	0.303	0.220	0.150	Inf	0.027
15	658	2.54	9.9	2.72	0.420	0.000	Inf	90	0.405	0.220	0.840	Inf	0.048
15	659	10.50	32.0	1.21	0.420	0.000	Inf	90	0.401	0.220	0.390	Inf	0.047
15	660	10.50	32.0	2.42	0.420	0.000	Inf	90	0.408	0.220	0.420	Inf	0.049
15	661	10.50	32.0	2.42	0.420	0.000	Inf	90	0.406	0.220	0.420	Inf	0.049
15	662	10.50	32.0	2.42	0.420	0.000	Inf	90	0.407	0.220	0.480	Inf	0.049
15	663	2.50	10.0	7.90	0.420	0.000	Inf	90	0.399	0.220	1.550	Inf	0.047
15	664	10.30	31.9	4.52	0.420	0.000	Inf	90	0.410	0.220	0.560	Inf	0.050
15	665	2.54	9.9	2.72	0.420	0.000	Inf	90	0.595	0.220	2.270	Inf	0.107
15	666	10.50	32.0	2.42	0.420	0.000	Inf	90	0.570	0.220	0.480	Inf	0.098
15	667	10.30	31.9	4.52	0.420	0.000	Inf	90	0.588	0.220	0.630	Inf	0.104
16	668	6.20	6.2	2.00	0.180	0.000	Inf	90	0.398	0.031	0.570	Inf	0.140
16	669	6.20	6.2	3.00	0.180	0.000	Inf	90	0.398	0.031	0.570	Inf	0.138
16	670	6.20	6.2	4.00	0.180	0.000	Inf	90	0.398	0.031	0.570	Inf	0.136
16	671	7.30	7.3	3.60	0.180	0.000	Inf	90	0.398	0.037	0.500	Inf	0.132
16	672	6.20	6.2	3.00	0.180	0.120	1.10	90	0.000	0.031	0.020	2.1	0.047
16	673	6.20	6.2	3.00	0.180	0.150	1.10	90	0.000	0.031	0.050	2.7	0.065
16	674	6.20	6.2	3.00	0.180	0.150	1.25	90	0.000	0.031	0.125	3.0	0.062
16	675	6.20	6.2	3.00	0.180	0.220	1.50	90	0.000	0.031	0.200	5.3	0.107
16	676	6.20	6.2	3.00	0.180	0.150	2.50	90	0.000	0.031	0.190	6.1	0.050
16	677	6.20	6.2	3.00	0.180	0.215	2.50	90	0.000	0.031	0.310	8.7	0.088
16	678	6.20	6.2	3.00	0.180	0.270	2.70	90	0.000	0.031	0.320	11.8	0.125
16	679	6.20	6.2	3.00	0.180	0.260	3.50	90	0.000	0.031	0.330	14.7	0.109
16	680	6.20	6.2	3.00	0.180	0.275	3.50	90	0.000	0.031	0.340	15.5	0.120
16	681	6.20	6.2	3.00	0.180	0.315	3.70	90	0.000	0.031	0.360	18.8	0.148
16	682	3.00	3.0	3.00	0.180	0.215	2.50	90	0.000	0.015	0.300	17.9	0.088
16	683	3.00	3.0	3.00	0.180	0.270	2.70	90	0.000	0.015	0.317	24.3	0.125
16	684	3.00	3.0	3.00	0.180	0.320	3.00	90	0.000	0.015	0.510	32.0	0.161

Table A1. Individual observations of self-burial of objects by scour (cont.)

<i>No.</i>	<i>Obs.</i>	<i>D</i>	<i>L</i>	ρ_o/ρ	d_{50}	U_w	<i>T</i>	α	$U_c(z_{obs})$	z_{obs}	<i>B/D</i>	<i>KC</i>	θ
16	685	3.00	3.0	3.00	0.180	0.300	3.50	90	0.000	0.015	0.400	35.0	0.138
16	686	3.00	3.0	3.00	0.180	0.315	3.70	90	0.000	0.015	0.504	38.9	0.148
16	687	3.00	3.0	3.00	0.180	0.340	3.50	90	0.000	0.015	0.550	39.7	0.171
16	688	6.20	6.2	3.00	0.180	0.000	480	90	0.370	0.031	0.435	Inf	0.119
16	689	7.30	7.3	3.60	0.180	0.190	2.20	90	0.000	0.037	0.150	5.7	0.075
16	690	7.30	7.3	3.60	0.180	0.370	3.00	90	0.000	0.037	0.325	15.2	0.206
16	691	7.30	7.3	3.60	0.180	0.420	3.50	90	0.000	0.037	0.382	20.1	0.246
16	692	7.30	7.3	3.60	0.180	0.000	480	90	0.370	0.037	0.400	Inf	0.114
17	693	25.00	50.0	2.00	0.250	0.550	2.52	90	0.000	0.050	0.020	5.5	0.350
17	694	25.00	50.0	2.00	0.250	0.259	3.72	90	0.000	0.050	0.020	3.9	0.083
17	695	25.00	50.0	2.00	0.250	0.377	1.97	90	0.000	0.050	0.020	3.0	0.193
17	696	25.00	50.0	2.00	0.250	0.494	2.18	90	0.000	0.050	0.020	4.3	0.302
17	697	15.00	30.0	2.00	0.250	0.204	2.16	90	0.000	0.050	0.020	2.9	0.066
17	698	15.00	30.0	2.00	0.250	0.257	2.48	90	0.000	0.050	0.020	4.3	0.093
17	699	15.00	30.0	2.00	0.250	0.322	1.97	90	0.000	0.050	0.020	4.2	0.147
17	700	15.00	30.0	2.00	0.250	0.647	3.72	90	0.000	0.050	0.080	16.1	0.419
17	701	15.00	30.0	2.00	0.250	0.550	2.52	90	0.000	0.050	0.070	9.2	0.350
17	702	15.00	30.0	2.00	0.250	0.462	2.73	90	0.000	0.050	0.020	8.4	0.250
17	703	15.00	30.0	2.00	0.250	0.259	3.72	90	0.000	0.050	0.030	6.4	0.083
17	704	15.00	30.0	2.00	0.250	0.377	1.97	90	0.000	0.050	0.050	5.0	0.193
17	705	15.00	30.0	2.00	0.250	0.494	2.18	90	0.000	0.050	0.020	7.2	0.302
17	706	10.00	20.0	2.00	0.250	0.204	2.16	90	0.000	0.050	0.040	4.4	0.066
17	707	10.00	20.0	2.00	0.250	0.257	2.48	90	0.000	0.050	0.030	6.4	0.093
17	708	10.00	20.0	2.00	0.250	0.322	1.97	90	0.000	0.050	0.040	6.3	0.147
17	709	10.00	20.0	2.00	0.250	0.647	3.72	90	0.000	0.050	0.110	24.1	0.419
17	710	10.00	20.0	2.00	0.250	0.462	2.73	90	0.000	0.050	0.030	12.6	0.250
17	711	10.00	20.0	2.00	0.250	0.259	3.72	90	0.000	0.050	0.030	9.6	0.083
17	712	10.00	20.0	2.00	0.250	0.377	1.97	90	0.000	0.050	0.080	7.4	0.193
17	713	10.00	20.0	2.00	0.250	0.494	2.18	90	0.000	0.050	0.030	10.8	0.302
17	714	7.50	15.0	2.00	0.250	0.204	2.16	90	0.000	0.050	0.040	5.9	0.066
17	715	7.50	15.0	2.00	0.250	0.647	3.72	90	0.000	0.050	0.140	32.1	0.419
17	716	7.50	15.0	2.00	0.250	0.550	2.52	90	0.000	0.050	0.080	18.5	0.350
17	717	7.50	15.0	2.00	0.250	0.462	2.73	90	0.000	0.050	0.090	16.8	0.250
17	718	7.50	15.0	2.00	0.250	0.259	3.72	90	0.000	0.050	0.050	12.9	0.083
17	719	7.50	15.0	2.00	0.250	0.377	1.97	90	0.000	0.050	0.050	9.9	0.193
17	720	7.50	15.0	2.00	0.250	0.494	2.18	90	0.000	0.050	0.060	14.4	0.302
17	721	25.00	50.0	2.00	0.250	0.504	3.90	90	0.153	0.050	0.040	10.7	0.461
17	722	25.00	50.0	2.00	0.250	0.531	5.65	90	0.153	0.050	0.040	16.1	0.447
17	723	15.00	30.0	2.00	0.250	0.293	2.16	90	0.153	0.050	0.020	6.7	0.273
17	724	15.00	30.0	2.00	0.250	0.349	2.52	90	0.153	0.050	0.020	8.8	0.319
17	725	15.00	30.0	2.00	0.250	0.340	1.52	90	0.153	0.050	0.020	5.2	0.362

Table A1. Individual observations of self-burial of objects by scour (cont.)

<i>No.</i>	<i>Obs.</i>	<i>D</i>	<i>L</i>	ρ_o/ρ	d_{50}	U_w	<i>T</i>	α	$U_c(z_{obs})$	z_{obs}	<i>B/D</i>	<i>KC</i>	θ
17	726	15.00	30.0	2.00	0.250	0.561	3.90	90	0.153	0.050	0.050	19.1	0.520
17	727	15.00	30.0	2.00	0.250	0.298	3.90	90	0.153	0.050	0.030	12.3	0.234
17	728	15.00	30.0	2.00	0.250	0.504	3.90	90	0.153	0.050	0.080	17.6	0.449
17	729	15.00	30.0	2.00	0.250	0.462	5.65	90	0.153	0.050	0.080	24.0	0.362
17	730	15.00	30.0	2.00	0.250	0.531	5.65	90	0.153	0.050	0.080	26.5	0.436
17	731	10.00	20.0	2.00	0.250	0.293	2.16	90	0.153	0.050	0.030	9.9	0.266
17	732	10.00	20.0	2.00	0.250	0.349	2.52	90	0.153	0.050	0.030	13.0	0.311
17	733	10.00	20.0	2.00	0.250	0.313	2.82	90	0.153	0.050	0.030	13.5	0.264
17	734	10.00	20.0	2.00	0.250	0.551	5.46	90	0.153	0.050	0.080	39.2	0.454
17	735	10.00	20.0	2.00	0.250	0.340	1.52	90	0.153	0.050	0.030	7.7	0.353
17	736	10.00	20.0	2.00	0.250	0.561	3.90	90	0.153	0.050	0.070	28.4	0.510
17	737	10.00	20.0	2.00	0.250	0.298	3.90	90	0.153	0.050	0.040	18.1	0.227
17	738	10.00	20.0	2.00	0.250	0.504	3.90	90	0.153	0.050	0.110	26.1	0.440
17	739	10.00	20.0	2.00	0.250	0.462	5.65	90	0.153	0.050	0.100	35.5	0.354
17	740	10.00	20.0	2.00	0.250	0.531	5.65	90	0.153	0.050	0.130	39.4	0.427
17	741	7.50	15.0	2.00	0.250	0.293	2.16	90	0.153	0.050	0.050	13.1	0.260
17	742	7.50	15.0	2.00	0.250	0.349	2.52	90	0.153	0.050	0.050	17.1	0.305
17	743	7.50	15.0	2.00	0.250	0.313	2.82	90	0.153	0.050	0.040	17.8	0.259
17	744	7.50	15.0	2.00	0.250	0.304	4.82	90	0.153	0.050	0.040	29.9	0.215
17	745	7.50	15.0	2.00	0.250	0.551	5.46	90	0.153	0.050	0.130	51.8	0.448
17	746	7.50	15.0	2.00	0.250	0.340	1.52	90	0.153	0.050	0.040	10.2	0.346
17	747	7.50	15.0	2.00	0.250	0.561	3.90	90	0.153	0.050	0.100	37.5	0.504
17	748	7.50	15.0	2.00	0.250	0.298	3.90	90	0.153	0.050	0.050	23.9	0.222
17	749	7.50	15.0	2.00	0.250	0.462	5.65	90	0.153	0.050	0.120	46.9	0.348
17	750	7.50	15.0	2.00	0.250	0.531	5.65	90	0.153	0.050	0.150	52.1	0.421
18	751	5.00	22.0	2.72	0.200	0.287	2.00	90	0.000	0.200	0.620	11.5	0.139
18	752	5.00	22.0	2.72	0.130	0.321	2.00	90	0.000	0.200	0.720	12.8	0.234
18	753	5.00	22.0	2.72	0.150	0.328	2.00	90	0.000	0.200	0.800	13.1	0.216
18	754	5.00	22.0	2.72	0.171	0.349	2.00	90	0.000	0.200	1.000	14.0	0.217
18	755	5.00	22.0	2.72	0.205	0.387	2.00	90	0.000	0.200	1.060	15.5	0.228
18	756	5.00	22.0	2.72	0.115	0.248	1.50	90	0.000	0.200	0.580	7.4	0.187
19	757	7.90	31.8	2.43	0.420	0.000	Inf	90	0.299	0.220	0.120	Inf	0.026
19	758	7.94	31.8	2.43	0.420	0.000	Inf	90	0.351	0.220	0.320	Inf	0.036
19	759	7.94	31.8	2.43	0.420	0.000	Inf	90	0.414	0.220	0.720	Inf	0.051
19	760	7.94	31.8	2.43	0.420	0.000	Inf	90	0.482	0.220	0.510	Inf	0.069
19	761	7.94	31.8	2.43	0.420	0.000	Inf	90	0.583	0.220	1.170	Inf	0.102

Table A2. Notes regarding sources of individual parameters in Table A1. See Table A1 and report text for additional definitions of variables.

<i>No.</i>	<i>Obs.</i>	<i>Notes</i>
1	1-49	Source: Carstens & Martin (1963). T (p.vi); z_{obs} is assumed to equal $1/2 h$, where h (p.4) is the height of the U-tube (note, z_{obs} is not needed for analysis of wave-only cases like No.1); D/L , d_{50} , ρ_o (p.9); B/D = final value of “Y/D South” from complete tests (p.13-48), except for Obs.23; D (p.13-48); U_w in Table A1 is based on reported Froude numbers (p.49), such that $F = U_w/[(s-1) g d_{50}]^{1/2}$ with $s = 2.6$; α (p.67).
	23	B/D = “Y/D South” at cycle 210 because a stable burial depth was established by cycle 210 and then maintained for next 120 wave cycles (p.36).
2	54-157	Sources: Starr (1989) [S89]; Stansby & Starr (1992) [SS92]. z_{obs} is assumed to equal $0.368 h$, where h (S89 p.41, SS92 p.262) is the total water depth, and $0.368 h$ is the height z above the bed where $U_c(z)$ from a log-profile is the same as depth-averaged U_c . d_{50} (S89 p.26, SS92 p.263); L (S89 p.29-30, SS92 p.263).
	50-73	Waves only. D (SS92 p.264); B/D , KC , Shields parameter (ψ) as reported by authors (S89 Fig.5.5 p.117, SS92 Fig.9 p.265). For waves, ψ was calculated by SS92 (p.263) using $\tau_b/\rho = U_w(\nu 2\pi/T)^{1/2}$, where $\nu = 10^{-6} \text{ m}^2/\text{s}$ is kinematic viscosity. It follows then that U_w can be recovered from $U_w^3 = D [\psi (s-1) g d_{50}]^2 KC/(\nu 2\pi)$. T is then calculated from KC .
	74-113	Currents only. B/D (S89 Fig.4.3 p.85, SS92 Fig.2 p.264); D , ρ_o (S89 p.86, SS92 p.264); $U_c(z_{obs})$ in Table A1 is derived from the reported Shields parameter values (S89 Fig.4.3 p.85, SS92 Fig.2 p.264). SS92 states (p.263) that “In a current the bed shear stress is determined from the standard Nikuradse friction factor curves and the mean current magnitude.” A best-fit friction factor was derived for use here by comparing the distribution of observed $U_c(z_{obs})$ (S89 Fig.4.6. p.90, SS92 Fig.4 p.264) to the reported Shields parameters.
	114-157	Currents only. D , ρ_o , B/D , and reported Shields parameter (ψ) are given by S89 (Fig.4.4 p.88). Observed U_c cases were not available, so U_c in Table A1 is estimated as $U_c(z_{obs}) = 2.5 u^* \log(z_{obs}/z_0)$, where $z_0 = 2.5d_{50}/30$, and $u^* = [\psi (s-1) g d_{50}]^{1/2}$.
3	158-167	Source: Sumer & Fredsoe (1994). D , L , d_{50} , U_c , ρ_o , z_{obs} , h (p.31); B/D (Fig.10 p.34).
4	168-193	Source: Sumer et al. (2001). h , L (p.315); d_{50} , D , U_c , U_w , T , ρ_o (p.318); z_{obs} (p.319); B/D (Fig.15 p.331) (but there is no burial data available for Test S13).
5	194-544	Source: Cataño-Lopera (2005) [CL05]. d_{50} (p.10); h (p.11); $z_{obs} = 0.368 h$ is assumed for the mean current (called U by CL05), since their U is defined as depth-averaged (p.14); L , D , T , B/D , α , $U_c(z_{obs}) = U$ (p.196-210). U_w in Table A1 is calculated as follows: CL05 reports their $U_m = U_w + U_c(z = D/2)$ (p.25). If one assumes that their U_{wc} (p.56, 196-210) equals their U_m , it then follows that U_w can be derived from their U_{wc} (p.196-210) as $U_w = U_{wc} - U_c(z = D/2)$, where a log-profile with $z_0 = 2.5d_{50}/30$ is used to adjust their $U = U_c(z_{obs})$ down to $U_c(z = D/2)$.
6	545-574	Source: Demir & García (2007). h , d_{50} (p.118); U_w , T , D , ρ_o , L/D , B/D , z_{obs} (p.119), although z_{obs} is not used for analysis of wave-only cases such as No.6.
7	575-583	Source: Cataño-Lopera et al. (2007). h (p.192); U_w , U_c , T , D , ρ_o , L/D , B/D , z_{obs} , d_{50} (p.193).
8-14	584-650	Sources for wave and current observations: P. Howd pers. comm. [HPC]; P. Traykovski pers. comm. [TPC]. This group includes all the field observations in Table A1. U_w for Obs. 584-650 is calculated as $U_w = 2\sigma_U$ where σ_U is the standard deviation of the instantaneous velocity time-series observed over the course of a ~ 10 minute “burst”. (For

Table A2. Notes regarding sources of individual parameters in Table A1 (cont.)

<i>No.</i>	<i>Obs.</i>	<i>Notes</i>
		natural irregular waves, $2\sigma_U$ corresponds roughly to the highest 1/3 of waves. For irregular waves, the highest 1/3 of waves is assumed to represent the characteristic orbital velocity causing scour.) U_c is the magnitude of the mean velocity over each of the same bursts. U_c and wave statistics were provided for Obs. 584-597,637-650 by TPC and for Obs. 598-636 by HPC. Following the approach of Friedrichs (2007), the most energetic burst preceding each observation of B/D is chosen to represent U_w and U_c . It is assumed that each high-energy wave event (each typically a day to several days in duration) lasted long enough for self-burial to reach its equilibrium value. The field data associated with sources 8-14 are presented in Table A1 in order of their occurrence in time, from July 2001 to November 2003. Thus the additional sources described
584-597		Additional sources: Traykovski et al. (2007) [T07]; Trembanis et al. (2007) [TR07]; Goff et al. (2005) [G05]. h (T07 p.151); L , D , ρ_o (T07 p.152); z_{obs} (TPC); d_{50} is the geometric mean of sand size from bed sampling stations 19.5, 20.1, 20.2, 20.3, 21.12, and 22 in G05 (p.468). Percentage burial by area, PBA (T07 p.160; TR07 p.173-174) was estimated either from the blockage of the cylinder's optical sensors (Obs. 584 to 596, even Obs. numbers) or from the changing acoustic shadow length as measured by side-scan sonar (Obs. 585 to 597, odd). PBA was converted to B/D here according to $B/D = 0.5 \{1 - \sin[\pi(0.5 - PBA/100)]\}$ (TR07 p.169). Optical and acoustic measures of PBA were noisy at the times of the most energetic U_w , so equilibrium B/D corresponding to each U_w was taken as the median value of recorded B/D for a lower wave period following the wave event as indicated below (dd/mm/yy - dd/mm/yy), each following the time of maximum U_w (dd/mm/yy).
584-585	U_w	07/12/01; B/D 08/12/01 - 14/12/01
586-587	U_w	21/12/01; B/D 21/12/01 - 25/12/01
588-589	U_w	29/12/01; B/D 01/01/02 - 06/01/02
590-591	U_w	07/01/02; B/D 17/01/02 - 20/01/02
592-593	U_w	10/04/02; B/D 11/04/02 - 25/04/02
594-595	U_w	29/04/02; B/D 08/05/02 - 14/05/02
596-597	U_w	14/05/02; B/D 14/05/02 - 29/05/02
598-636		Additional sources: Bowers et al. (2007) [B07]; Wolfson (2005) [W05]. h (W05 p.xii); D , L , ρ_o (B07 p.92); d_{50} (B07 p.93); z_{obs} (HPC). B/D is determined for four cylinders based on settling derived from pressure sensors on cylinders (B07 p.97; TR07 p.172) for Obs. 598-601,610-613,624-627, averaged over periods after maximum U_w . B/D is determined by multibeam surveying of highest point on up to 10 cylinders relative to surrounding seabed on dates after maximum U_w (W05 p.31,46,65,78,91,103,115,128,138,148) for Obs. 602-609,614-623,628-636. Dates indicated below.
598-601	U_w	17/01/03; B/D 17/01/03 - 23/01/03)
602-609	U_w	17/01/03; B/D 20/01/03
610-613	U_w	23/01/03; B/D 24/01/03 - 22/02/03
614-623	U_w	23/01/03; B/D 06/02/03
624-627	U_w	23/02/03; B/D 23/02/03 - 15/03/03
628-636	U_w	23/02/03; B/D 13/03/03
637-650		Additional sources: Bradley et al. (2007) [BR07]; Mayer et al. (2007) [M07]. D , L , ρ_o (BR07 p.65); h (BR07 p.68); z_{obs} (TPC); d_{50} for coarse sand cases is the geometric mean from bed sampling stations 19.1, 19.2, 19.3, 19.41, 19.42, 21.11, 21.2, and 21.3 in G05 (p.468); d_{50} for fine sand cases is from G05 as described for Obs. 584-597. B/D is from (i) acoustic shadow (T07 p.164; TR07 p.177-179) for Obs. 637,642,646 as described above for Obs. 585-597; (ii) pressure sensors (BR07 p.70; TR07 p.177-179) for Obs.

Table A2. Notes regarding sources of individual parameters in Table A1 (cont.)

<i>No.</i>	<i>Obs.</i>	<i>Notes</i>
		638-640,643-645,647-649 as described above for Obs. 598-601; (iii) multibeam surveying (M07 p.145) for Obs.641,650 as described above for Obs. 602-609. Dates indicated below.
	637-640	U_w 05/10/03; B/D 05/10/03 - 15/10/03
	641	U_w 05/10/03; B/D 06/10/03
	642-645	U_w 15/10/03; B/D 15/10/03 - 28/11/03
	646-649	U_w 29/11/03; B/D 29/11/03 - 05/12/03
	650	U_w 29/11/03; B/D 04/12/03
15	651-667	Source: Rennie et al. (2017) [R17]. h , z_{obs} , D , L , ρ_o (p.285); d_{50} (p.286); U_c , B/D (p.289). Note: Obs. 651,652,653, which were reported as $B/D = 0$ by R17 were recorded as $B/D = 0.02$ here (equal to the lowest value reported by any other study) in order to allow analysis of $\log(B/D)$.
16	668-692	Source: Truelsen et al. (2005). d_{50} , h , D , L , U_c , U_w , ρ_o (p.5); B/D (p.10); z_{obs} (p.6, reported as “undisturbed flow velocity at center of sphere”) Note: In Friedrichs et al. (2016), d_{50} for this case was incorrectly reported as $d_{50} = 0.19$ mm rather than $d_{50} = 0.18$ mm. The corrected values increase θ for No.16 (as provided in Table A1) by 4% relative to the values of θ in Friedrichs et al. (2016).
17	693-750	Source: Cataño-Lopera et al. (2011). ρ_o (p.1257); d_{50} (p.1260) D , L , U_c , U_w , T , B/D (p.1261); h (p.1262); z_{obs} (p.1263).
18	751-756	Source: Pang & Liu (2014) [PL14]. Tests 3 to 8. d_{50} , h , D , L , T , B (p.695). Orbital velocity reported by PL14 appears much too low for observed burial. Thus U_w in Friedrichs et al. (2016) and in Table A1 is instead estimated from linear wave theory applied to the mean measured wave height (provided on p.695). Via personal communication, the lead author confirmed that “amplitude (cm)” in the paper refers to wave height and that the tapered cylinders were made of aluminum. It is possible the surprisingly high estimates of partial burial reported here are contaminated by ripple migration.
19	757-761	Source: Rennie et al. (2017). h , z_{obs} , D , L , ρ_o (p.285); d_{50} (p.286); U_c , B/D (p.289).

Appendix B. Data Compilation for Initiation of Motion of Objects

Table B1. Observations of initiation of motion of gravel clasts and spheres in steady flow: *No.* = reference number (see text Table 4), *Obs.* = observation number, *D* = diameter in cm of gravel clast or sphere beginning to move, *d_{bed}* = median diameter in cm of gravel or spheres forming the bed, *k* = effective roughness in cm of the far-field bed surface, θ_{crit} = Shields parameter characterizing the stress acting on the far-field bed at the time of initiation of motion of the object, ρ_o/ρ = object density in (kg/m^3) / (1000 kg/m^3), *U_{crit}* = far field current or wave orbital velocity in m/s at the height of the top of the object at initiation of object motion, and $\Theta_{U_{crit}}$ = mobility parameter observed at *U_{crit}* (see text Eq (9)). Additional notes regarding sources of individual parameters in Table B1 and their calculation are provided in Table B4.

<i>No.</i>	<i>Obs.</i>	<i>D</i>	<i>d_{bed}</i>	<i>k</i>	<i>D/k</i>	θ_{crit}	ρ_o/ρ	<i>U_{crit}</i>	$\Theta_{U_{crit}}$
1	1	0.79	0.75	1.87	0.42	0.0484	2.70	0.510	1.98
1	2	0.92	0.75	1.87	0.49	0.0505	2.70	0.595	2.31
1	3	0.98	0.75	1.87	0.52	0.0423	2.70	0.575	2.02
1	4	0.98	0.75	1.87	0.52	0.0399	2.70	0.559	1.91
1	5	0.98	0.75	1.87	0.52	0.0354	2.70	0.526	1.69
1	6	1.01	0.75	1.87	0.54	0.0329	2.70	0.520	1.61
1	7	1.10	0.75	1.87	0.59	0.0430	2.70	0.639	2.23
1	8	1.47	0.75	1.87	0.79	0.0326	2.70	0.707	2.04
1	9	1.46	0.75	1.87	0.78	0.0284	2.70	0.656	1.77
1	10	1.49	0.75	1.87	0.80	0.0262	2.70	0.641	1.65
1	11	1.50	0.75	1.87	0.80	0.0302	2.70	0.692	1.91
1	12	1.63	0.75	1.87	0.87	0.0289	2.70	0.723	1.92
1	13	1.72	0.75	1.87	0.92	0.0251	2.70	0.703	1.72
1	14	1.85	0.75	1.87	0.99	0.0267	2.70	0.769	1.91
1	15	1.95	0.75	1.87	1.04	0.0215	2.70	0.719	1.59
1	16	2.01	0.75	1.87	1.07	0.0194	2.70	0.699	1.46
1	17	2.05	0.75	1.87	1.10	0.0227	2.70	0.768	1.73
1	18	2.20	0.75	1.87	1.18	0.0219	2.70	0.797	1.73
1	19	2.36	0.75	1.87	1.26	0.0209	2.70	0.822	1.72
1	20	2.61	0.75	1.87	1.40	0.0194	2.70	0.855	1.68
1	21	2.82	0.75	1.87	1.51	0.0187	2.70	0.891	1.69
1	22	3.20	0.75	1.87	1.71	0.0174	2.70	0.945	1.67
1	23	3.54	0.75	1.87	1.89	0.0145	2.70	0.930	1.46
2	24	2.14	2.00	5.00	0.43	0.0421	2.70	0.788	1.74
2	25	2.54	2.00	5.00	0.51	0.0328	2.70	0.806	1.54
2	26	2.89	2.00	5.00	0.58	0.0351	2.70	0.932	1.80
2	27	3.14	2.00	5.00	0.63	0.0355	2.70	1.003	1.92
2	28	3.24	2.00	5.00	0.65	0.0286	2.70	0.925	1.58
2	29	3.34	2.00	5.00	0.67	0.0240	2.70	0.869	1.36
2	30	3.46	2.00	5.00	0.69	0.0274	2.70	0.955	1.58
2	31	3.46	2.00	5.00	0.69	0.0304	2.70	1.006	1.76

Table B1. Observations of initiation of motion of gravel clasts and spheres (cont.)

<i>No.</i>	<i>Obs.</i>	<i>D</i>	<i>d_{bed}</i>	<i>k</i>	<i>D/k</i>	θ_{crit}	ρ_o/ρ	<i>U_{crit}</i>	Θ_{Ucrit}
2	32	3.57	2.00	5.00	0.71	0.0366	2.70	1.135	2.16
2	33	3.79	2.00	5.00	0.76	0.0782	2.70	1.739	4.79
2	34	3.77	2.00	5.00	0.75	0.0263	2.70	1.004	1.60
2	35	3.80	2.00	5.00	0.76	0.0304	2.70	1.087	1.86
2	36	3.94	2.00	5.00	0.79	0.0339	2.70	1.181	2.13
2	37	4.04	2.00	5.00	0.81	0.0240	2.70	1.014	1.53
2	38	4.03	2.00	5.00	0.81	0.0224	2.70	0.978	1.42
2	39	4.18	2.00	5.00	0.84	0.0201	2.70	0.955	1.31
2	40	4.73	2.00	5.00	0.95	0.0217	2.70	1.094	1.52
2	41	4.79	2.00	5.00	0.96	0.0282	2.70	1.261	1.99
2	42	5.08	2.00	5.00	1.02	0.0281	2.70	1.318	2.05
2	43	5.12	2.00	5.00	1.02	0.0201	2.70	1.121	1.47
2	44	5.44	2.00	5.00	1.09	0.0204	2.70	1.185	1.55
2	45	5.54	2.00	5.00	1.11	0.0211	2.70	1.222	1.62
2	46	5.73	2.00	5.00	1.15	0.0202	2.70	1.227	1.58
2	47	6.11	2.00	5.00	1.22	0.0199	2.70	1.280	1.61
2	48	6.10	2.00	5.00	1.22	0.0155	2.70	1.129	1.25
2	49	6.68	2.00	5.00	1.34	0.0190	2.70	1.339	1.61
2	50	6.80	2.00	5.00	1.36	0.0202	2.70	1.400	1.73
2	51	7.85	2.00	5.00	1.57	0.0282	2.70	1.845	2.60
2	52	8.26	2.00	5.00	1.65	0.0181	2.70	1.535	1.71
2	53	8.63	2.00	5.00	1.73	0.0096	2.70	1.156	0.93
2	54	9.01	2.00	5.00	1.80	0.0203	2.70	1.735	2.00
2	55	9.17	2.00	5.00	1.83	0.0183	2.70	1.670	1.82
2	56	10.01	2.00	5.00	2.00	0.0189	2.70	1.810	1.96
2	57	10.00	2.00	5.00	2.00	0.0142	2.70	1.568	1.47
2	58	10.68	2.00	5.00	2.14	0.0119	2.70	1.507	1.28
2	59	11.44	2.00	5.00	2.29	0.0114	2.70	1.552	1.26
2	60	12.09	2.00	5.00	2.42	0.0188	2.70	2.074	2.13
2	61	15.43	2.00	5.00	3.09	0.0110	2.70	1.893	1.39
2	62	15.52	2.00	5.00	3.10	0.0139	2.70	2.137	1.76
2	63	15.80	2.00	5.00	3.16	0.0122	2.70	2.027	1.56
2	64	16.19	2.00	5.00	3.24	0.0194	2.70	2.601	2.51
2	65	16.53	2.00	5.00	3.31	0.0087	2.70	1.768	1.13
2	66	16.66	2.00	5.00	3.33	0.0094	2.70	1.848	1.23
2	67	17.82	2.00	5.00	3.56	0.0124	2.70	2.227	1.67
2	68	18.37	2.00	5.00	3.67	0.0120	2.70	2.239	1.64
2	69	20.15	2.00	5.00	4.03	0.0138	2.70	2.563	1.95
2	70	32.88	2.00	5.00	6.58	0.0071	2.70	2.583	1.22
2	71	37.45	2.00	5.00	7.49	0.0065	2.70	2.702	1.17
2	72	43.09	2.00	5.00	8.62	0.0056	2.70	2.759	1.06

Table B1. Observations of initiation of motion of gravel clasts and spheres (cont.)

<i>No.</i>	<i>Obs.</i>	<i>D</i>	<i>d_{bed}</i>	<i>k</i>	<i>D/k</i>	θ_{crit}	ρ_o/ρ	<i>U_{crit}</i>	Θ_{Ucrit}
3	73	2.41	2.00	5.00	0.48	0.0256	2.70	0.683	1.16
3	74	2.51	2.00	5.00	0.50	0.0441	2.70	0.925	2.05
3	75	2.59	2.00	5.00	0.52	0.0299	2.70	0.783	1.42
3	76	2.68	2.00	5.00	0.54	0.0287	2.70	0.791	1.40
3	77	2.88	2.00	5.00	0.58	0.0276	2.70	0.824	1.41
3	78	3.11	2.00	5.00	0.62	0.0372	2.70	1.021	2.01
3	79	3.15	2.00	5.00	0.63	0.0249	2.70	0.843	1.35
3	80	3.24	2.00	5.00	0.65	0.0328	2.70	0.991	1.82
3	81	3.34	2.00	5.00	0.67	0.0318	2.70	1.001	1.80
3	82	3.30	2.00	5.00	0.66	0.0228	2.70	0.838	1.28
3	83	3.42	2.00	5.00	0.68	0.0169	2.70	0.743	0.97
3	84	3.46	2.00	5.00	0.69	0.0222	2.70	0.861	1.28
3	85	3.48	2.00	5.00	0.70	0.0233	2.70	0.886	1.35
3	86	3.49	2.00	5.00	0.70	0.0245	2.70	0.910	1.42
3	87	3.55	2.00	5.00	0.71	0.0333	2.70	1.075	1.95
3	88	3.67	2.00	5.00	0.73	0.0313	2.70	1.071	1.88
3	89	4.16	2.00	5.00	0.83	0.0316	2.70	1.191	2.05
3	90	4.36	2.00	5.00	0.87	0.0267	2.70	1.138	1.78
3	91	4.33	2.00	5.00	0.87	0.0172	2.70	0.909	1.14
3	92	4.53	2.00	5.00	0.91	0.0188	2.70	0.984	1.28
3	93	5.23	2.00	5.00	1.05	0.0327	2.70	1.454	2.42
3	94	5.79	2.00	5.00	1.16	0.0290	2.70	1.483	2.28
3	95	5.94	2.00	5.00	1.19	0.0280	2.70	1.486	2.23
3	96	6.43	2.00	5.00	1.29	0.0274	2.70	1.563	2.28
3	97	6.55	2.00	5.00	1.31	0.0262	2.70	1.549	2.20
3	98	6.65	2.00	5.00	1.33	0.0253	2.70	1.540	2.14
3	99	6.86	2.00	5.00	1.37	0.0264	2.70	1.611	2.27
3	100	7.23	2.00	5.00	1.45	0.0246	2.70	1.620	2.17
3	101	7.38	2.00	5.00	1.48	0.0195	2.70	1.464	1.74
3	102	7.69	2.00	5.00	1.54	0.0248	2.70	1.704	2.26
3	103	7.41	2.00	5.00	1.48	0.0166	2.70	1.355	1.49
3	104	8.37	2.00	5.00	1.67	0.0247	2.70	1.812	2.35
3	105	8.43	2.00	5.00	1.69	0.0215	2.70	1.699	2.05
3	106	8.81	2.00	5.00	1.76	0.0246	2.70	1.879	2.40
3	107	9.16	2.00	5.00	1.83	0.0258	2.70	1.980	2.57
3	108	8.81	2.00	5.00	1.76	0.0219	2.70	1.772	2.14
3	109	8.78	2.00	5.00	1.76	0.0209	2.70	1.728	2.04
3	110	9.29	2.00	5.00	1.86	0.0225	2.70	1.870	2.26
3	111	9.25	2.00	5.00	1.85	0.0213	2.70	1.812	2.13
3	112	9.70	2.00	5.00	1.94	0.0205	2.70	1.843	2.10
3	113	9.78	2.00	5.00	1.96	0.0225	2.70	1.942	2.31

Table B1. Observations of initiation of motion of gravel clasts and spheres (cont.)

<i>No.</i>	<i>Obs.</i>	<i>D</i>	<i>d_{bed}</i>	<i>k</i>	<i>D/k</i>	θ_{crit}	ρ_o/ρ	<i>U_{crit}</i>	Θ_{Ucrit}
3	114	10.24	2.00	5.00	2.05	0.0200	2.70	1.894	2.10
3	115	10.36	2.00	5.00	2.07	0.0127	2.70	1.522	1.34
3	116	11.49	2.00	5.00	2.30	0.0186	2.70	1.987	2.06
4	117	1.56	1.36	3.41	0.46	0.0742	2.70	0.915	3.22
4	118	1.87	1.36	3.41	0.55	0.0427	2.70	0.810	2.11
4	119	1.99	1.36	3.41	0.58	0.0370	2.70	0.798	1.91
4	120	2.02	1.36	3.41	0.59	0.0365	2.70	0.802	1.91
4	121	2.48	1.36	3.41	0.73	0.0484	2.70	1.093	2.89
4	122	3.07	1.36	3.41	0.90	0.0488	2.70	1.304	3.32
4	123	3.15	1.36	3.41	0.92	0.0250	2.70	0.952	1.72
4	124	3.26	1.36	3.41	0.96	0.0600	2.70	1.515	4.22
4	125	3.68	1.36	3.41	1.08	0.0457	2.70	1.455	3.45
4	126	3.83	1.36	3.41	1.12	0.0433	2.70	1.462	3.34
4	127	3.94	1.36	3.41	1.15	0.0108	2.70	0.745	0.85
4	128	4.33	1.36	3.41	1.27	0.0224	2.70	1.154	1.85
4	129	4.62	1.36	3.41	1.35	0.0156	2.70	1.013	1.33
4	130	4.96	1.36	3.41	1.45	0.0167	2.70	1.105	1.48
4	131	5.31	1.36	3.41	1.56	0.0121	2.70	0.992	1.11
4	132	6.39	1.36	3.41	1.87	0.0153	2.70	1.281	1.54
5	133	0.97	0.05	0.12	8.07	0.0072	2.70	0.458	1.41
5	134	0.68	0.05	0.12	5.68	0.0078	2.70	0.377	1.36
5	135	0.95	0.06	0.14	6.78	0.0051	2.70	0.368	0.92
5	136	0.68	0.06	0.14	4.84	0.0088	2.70	0.381	1.40
5	137	0.96	0.10	0.24	4.00	0.0103	2.70	0.463	1.47
5	138	0.68	0.10	0.24	2.81	0.0148	2.70	0.430	1.82
6	139	0.55	0.34	0.84	0.65	0.0360	2.70	0.396	2.00
6	140	0.71	0.34	0.84	0.85	0.0290	2.70	0.443	1.90
6	141	0.89	0.34	0.84	1.06	0.0230	2.70	0.475	1.72
6	142	1.12	0.34	0.84	1.33	0.0180	2.70	0.502	1.53
6	143	1.41	0.34	0.84	1.68	0.0150	2.70	0.549	1.43
6	144	0.55	0.37	0.93	0.59	0.0380	2.70	0.393	1.98
6	145	0.71	0.37	0.93	0.76	0.0310	2.70	0.443	1.91
6	146	0.89	0.37	0.93	0.96	0.0260	2.70	0.490	1.84
6	147	1.12	0.37	0.93	1.20	0.0210	2.70	0.527	1.69
6	148	1.41	0.37	0.93	1.52	0.0170	2.70	0.569	1.55
6	149	0.55	0.26	0.65	0.84	0.0240	2.70	0.353	1.57
6	150	0.71	0.26	0.65	1.09	0.0190	2.70	0.388	1.45
6	151	0.89	0.26	0.65	1.38	0.0160	2.70	0.427	1.38
6	152	0.55	0.26	0.66	0.83	0.0240	2.70	0.351	1.55
6	153	0.71	0.26	0.66	1.08	0.0190	2.70	0.386	1.43
6	154	0.89	0.26	0.66	1.35	0.0160	2.70	0.424	1.36

Table B1. Observations of initiation of motion of gravel clasts and spheres (cont.)

<i>No.</i>	<i>Obs.</i>	<i>D</i>	<i>d_{bed}</i>	<i>k</i>	<i>D/k</i>	θ_{crit}	ρ_o/ρ	<i>U_{crit}</i>	Θ_{Ucrit}
6	155	0.55	0.28	0.70	0.78	0.0370	2.70	0.427	2.31
6	156	0.71	0.28	0.70	1.01	0.0230	2.70	0.417	1.68
6	157	0.89	0.28	0.70	1.28	0.0220	2.70	0.490	1.82
6	158	1.12	0.28	0.70	1.60	0.0190	2.70	0.542	1.77
6	159	1.41	0.28	0.70	2.02	0.0180	2.70	0.630	1.88
7	160	0.52	0.18	0.46	1.13	0.0123	2.70	0.270	0.96
7	161	0.62	0.18	0.46	1.34	0.0105	2.70	0.286	0.90
7	162	0.62	0.53	1.32	0.47	0.0316	2.70	0.348	1.40
8	163	0.53	0.18	0.45	1.18	0.0138	2.70	0.292	1.09
8	164	0.61	0.18	0.45	1.34	0.0120	2.70	0.302	1.02
8	165	0.70	0.18	0.45	1.54	0.0110	2.70	0.322	1.00
9	166	0.58	0.24	0.59	0.99	0.0204	2.70	0.353	1.47
9	167	0.53	0.38	0.95	0.56	0.0251	2.70	0.308	1.26
9	168	0.62	0.38	0.95	0.65	0.0219	2.70	0.329	1.22
9	169	0.84	0.38	0.95	0.89	0.0195	2.70	0.401	1.31
9	170	1.00	0.38	0.95	1.05	0.0178	2.70	0.440	1.32
9	171	1.19	0.38	0.95	1.25	0.0155	2.70	0.471	1.27
9	172	1.44	0.38	0.95	1.52	0.0132	2.70	0.505	1.19
9	173	0.52	0.40	1.00	0.52	0.0295	2.70	0.320	1.40
9	174	0.58	0.40	1.00	0.58	0.0263	2.70	0.335	1.35
9	175	0.65	0.40	1.00	0.65	0.0234	2.70	0.350	1.30
9	176	0.74	0.40	1.00	0.74	0.0219	2.70	0.376	1.32
9	177	0.85	0.40	1.00	0.85	0.0200	2.70	0.403	1.31
9	178	1.01	0.40	1.00	1.01	0.0178	2.70	0.437	1.29
9	179	1.27	0.40	1.00	1.27	0.0145	2.70	0.473	1.20
10	180	0.51	0.22	0.54	0.94	0.0288	2.70	0.385	2.01
10	181	0.60	0.22	0.54	1.12	0.0240	2.70	0.405	1.85
10	182	0.69	0.22	0.54	1.29	0.0219	2.70	0.432	1.82
11	183	0.63	0.50	0.38	1.66	0.00632	2.29	0.221	0.613
11	184	0.63	0.50	0.38	1.66	0.00667	2.29	0.227	0.646
11	185	0.63	0.50	0.38	1.66	0.00703	2.29	0.233	0.681
11	186	0.63	0.50	0.38	1.66	0.00791	2.29	0.247	0.764
11	187	0.63	0.50	0.38	1.66	0.00889	2.29	0.262	0.857
11	188	0.99	0.50	0.38	2.59	0.00445	2.56	0.283	0.530
11	189	0.99	0.50	0.38	2.59	0.00479	2.56	0.293	0.570
11	190	0.99	0.50	0.38	2.59	0.00511	2.56	0.303	0.608
11	191	1.22	0.50	0.38	3.21	0.00297	2.48	0.263	0.390
11	192	1.22	0.50	0.38	3.21	0.00348	2.48	0.284	0.456
11	193	1.22	0.50	0.38	3.21	0.00363	2.48	0.290	0.475
11	194	1.22	0.50	0.38	3.21	0.00389	2.48	0.300	0.509
11	195	1.38	0.50	0.38	3.63	0.00316	2.45	0.292	0.436

Table B1. Observations of initiation of motion of gravel clasts and spheres (cont.)

<i>No.</i>	<i>Obs.</i>	<i>D</i>	<i>d_{bed}</i>	<i>k</i>	<i>D/k</i>	θ_{crit}	ρ_o/ρ	<i>U_{crit}</i>	Θ_{Ucrit}
11	196	1.38	0.50	0.38	3.63	0.00323	2.45	0.296	0.445
11	197	1.38	0.50	0.38	3.63	0.00330	2.45	0.299	0.455
11	198	1.38	0.50	0.38	3.63	0.00337	2.45	0.302	0.464
11	199	1.38	0.50	0.38	3.63	0.00344	2.45	0.305	0.474
11	200	1.60	0.50	0.38	4.21	0.00242	2.41	0.281	0.355
11	201	1.60	0.50	0.38	4.21	0.00258	2.41	0.290	0.378
11	202	1.60	0.50	0.38	4.21	0.00278	2.41	0.300	0.407
11	203	2.00	0.50	0.38	5.27	0.00168	2.41	0.274	0.270
11	204	2.00	0.50	0.38	5.27	0.00210	2.41	0.305	0.336
11	205	2.00	0.50	0.38	5.27	0.00227	2.41	0.317	0.363
11	206	2.21	0.50	0.38	5.80	0.00141	2.48	0.274	0.235
11	207	2.21	0.50	0.38	5.80	0.00158	2.48	0.290	0.263
11	208	2.21	0.50	0.38	5.80	0.00169	2.48	0.300	0.281
11	209	2.21	0.50	0.38	5.80	0.00180	2.48	0.309	0.299
11	210	2.21	0.50	0.38	5.80	0.00209	2.48	0.333	0.347

Table B2. Laboratory observations from Williams (2001) of initiation of motion of cylinders on a smooth bed under waves: *No.* = reference number, *Obs.* = observation number; *D* = diameter of cylinder in cm, *k* = effective roughness in mm of the far-field bed surface, ρ_o/ρ = object density in (kg/m^3) / ($1000 \text{ kg}/\text{m}^3$), U_{w_crit} = far field near-bed wave orbital velocity at initiation of motion in m/s, *T* = wave period in sec, $f_I \Theta_{U_{crit}}$ = an inertial factor times the critical mobility parameter (see text Eqs. (9) and (12)), and *Runs* indicates the number of the runs from Williams (2001) immediately before and after initial motion that were averaged to determine U_{w_crit} . Additional notes regarding sources of individual parameters in Table B2 and their calculation are provided in Table B4.

<i>No.</i>	<i>Obs.</i>	<i>D</i>	<i>k</i>	<i>D/k</i>	ρ_o/ρ	U_{w_crit}	<i>T</i>	$f_I \Theta_{U_{crit}}$	<i>Runs</i>
12	211	10.50	0.432	243	4.76	0.041	3.0	0.0093	390, 391
12	212	10.50	0.297	354	4.76	0.094	3.5	0.0185	394, 395
12	213	10.50	0.298	352	4.76	0.100	4.0	0.0172	397, 398
12	214	10.50	0.330	319	4.76	0.087	4.5	0.0132	400, 401
12	215	10.50	0.333	316	4.76	0.090	5.0	0.0124	402, 403
12	216	10.50	0.306	343	4.76	0.116	6.0	0.0136	410, 411
12	217	10.50	0.343	306	4.76	0.065	3.0	0.0149	1, 2
12	218	10.50	0.386	272	4.76	0.059	4.0	0.0102	6, 10
12	219	10.50	0.328	320	4.76	0.092	5.0	0.0128	12, 13
12	220	10.50	0.265	396	4.76	0.155	6.0	0.0186	21, 22
12	221	7.50	0.267	281	4.27	0.124	4.0	0.0251	371, 372
12	222	7.50	0.232	323	8.28	0.154	3.5	0.0161	349, 350
12	223	7.50	0.210	357	8.28	0.201	4.0	0.0192	352, 354
12	224	4.76	0.344	138	3.16	0.037	1.0	0.0444	128, 129
12	225	4.76	0.298	159	3.16	0.070	2.0	0.0421	130, 131
12	226	4.76	0.236	202	3.16	0.138	3.0	0.0577	137, 138
12	227	4.76	0.209	227	3.16	0.226	5.0	0.0739	144, 145
12	228	4.76	0.221	215	3.16	0.222	6.0	0.0658	148, 149
12	229	4.76	0.165	289	7.08	0.347	4.5	0.0535	267, 268
12	230	4.76	0.178	267	7.08	0.312	5.0	0.0432	269, 270
12	231	4.76	0.468	102	1.63	0.045	5.0	0.0375	202, 203
12	232	4.76	0.348	137	1.63	0.097	7.0	0.0650	212, 213
12	233	6.03	0.141	429	6.87	0.317	2.0	0.0751	295, 296
12	234	6.03	0.136	444	6.87	0.417	3.0	0.0787	300, 301
12	235	6.03	0.141	427	6.87	0.498	5.0	0.0835	308, 309
12	236	6.03	0.162	373	6.87	0.414	6.0	0.0580	312, 313
12	237	6.03	0.150	401	6.87	0.459	5.5	0.0709	318, 319
12	238	3.18	0.342	92.9	3.29	0.057	2.3	0.0283	423, 424
12	239	3.18	0.281	113	3.29	0.105	3.5	0.0369	425, 426
12	240	3.18	0.343	92.7	3.29	0.081	4.6	0.0217	430, 431
12	241	3.18	0.243	131	3.29	0.185	6.0	0.0590	435, 436
12	242	3.18	0.272	117	3.29	0.073	1.5	0.0553	440, 441
12	243	2.86	0.276	104	2.09	0.071	1.5	0.1136	444, 445

Table B2. Laboratory observations of initiation of motion of cylinders under waves (cont.)

<i>No.</i>	<i>Obs.</i>	<i>D</i>	<i>k</i>	<i>D/k</i>	ρ_o/ρ	U_{w_crit}	<i>T</i>	$f_l\Theta_{Ucrit}$	<i>Runs</i>
12	244	2.86	0.348	82.2	2.09	0.073	4.0	0.0467	460, 461
12	245	2.86	0.328	87.1	2.09	0.092	5.0	0.0516	469, 470
12	246	2.86	0.321	89.2	2.09	0.114	7.0	0.0575	483, 484
12	247	2.86	0.357	80.0	2.09	0.098	8.0	0.0430	490, 491
12	248	2.86	0.399	71.6	2.09	0.083	9.0	0.0316	497, 498
12	249	3.81	0.296	129	6.09	0.072	2.0	0.0182	506, 507
12	250	3.81	0.216	176	6.09	0.164	3.0	0.0310	513, 514
12	251	3.81	0.218	175	6.09	0.186	4.0	0.0297	521, 522
12	252	3.81	0.204	187	6.09	0.239	5.0	0.0385	530, 531
12	253	3.81	0.275	138	6.09	0.143	6.0	0.0162	534, 535
12	254	3.81	0.266	143	6.09	0.166	7.0	0.0187	542, 543
12	255	3.81	0.219	174	6.09	0.278	9.0	0.0435	558, 559
12	256	3.81	0.217	176	3.84	0.133	2.0	0.0625	566, 567
12	257	3.81	0.268	142	3.84	0.107	3.0	0.0340	570, 571
12	258	3.81	0.195	196	3.84	0.234	4.0	0.0738	579, 580
12	259	3.81	0.288	132	3.84	0.120	5.0	0.0255	586, 587
12	260	3.81	0.194	196	3.84	0.288	6.0	0.0895	595, 596
12	261	3.81	0.260	146	3.84	0.173	7.0	0.0361	601, 602
12	262	3.81	0.229	167	3.84	0.240	8.0	0.0607	610, 611
12	263	3.81	0.267	143	3.84	0.187	9.0	0.0379	614, 616
12	264	4.76	0.275	173	5.18	0.083	2.0	0.0257	621, 622
12	265	4.76	0.264	181	5.18	0.111	3.0	0.0234	626, 627
12	266	4.76	0.186	255	5.18	0.255	4.0	0.0514	635, 637
12	267	4.76	0.273	174	5.18	0.133	5.0	0.0186	667, 668
12	268	4.76	0.202	236	5.18	0.267	6.0	0.0455	674, 676
12	269	4.76	0.216	220	5.18	0.251	7.0	0.0391	681, 682
12	270	4.76	0.208	229	5.18	0.291	8.0	0.0486	688, 690
12	271	4.76	0.216	220	5.18	0.284	9.0	0.0456	694, 696
12	272	1.75	0.224	78.0	7.62	0.125	2.0	0.0277	642, 643
12	273	1.75	0.226	77.4	7.62	0.150	3.0	0.0278	645, 646
12	274	1.75	0.237	73.8	7.62	0.158	4.0	0.0267	648, 649
12	275	1.75	0.281	62.3	7.62	0.126	5.0	0.0170	651, 652
12	276	1.75	0.204	85.9	7.62	0.262	6.0	0.0626	655, 656
12	277	1.75	0.294	59.5	7.62	0.136	7.0	0.0179	657, 658
12	278	1.75	0.290	60.4	7.62	0.158	9.0	0.0231	664, 665

Table B3. Laboratory observations of initiation of motion of cylinders placed on smooth and rough beds under currents in the absence of waves: *No.* = reference number, *Obs.* = observation number; *D* = diameter of cylinder in cm, *k* = effective roughness in mm of the far-field bed surface, ρ_o/ρ = object density in (kg/m³) / (1000 kg/m³), $U_{crit}(z_{obs})$ = far field velocity in m/s at height z_{obs} , z_{obs} = observation height in meters above bed, and $\Theta_{U_{crit}}$ = mobility parameter observed at U_{crit} (see text Eq (9)). Additional notes regarding sources of individual parameters in Table B3 and their calculation are provided in Table B4.

<i>No.</i>	<i>Obs.</i>	<i>D</i>	<i>k</i>	<i>D/k</i>	ρ_o/ρ	$U_{crit}(z_{obs})$	z_{obs}	$\Theta_{U_{crit}}$
13	279	4.80	0.358	134	3.17	0.230	0.30	0.0347
13	280	4.80	0.646	74.3	1.63	0.120	0.30	0.0317
13	281	6.00	0.358	168	3.01	0.230	0.30	0.0316
13	282	6.00	0.646	92.8	1.71	0.120	0.30	0.0238
13	283	8.90	0.320	278	3.01	0.260	0.30	0.0299
13	284	8.90	0.646	138	1.57	0.120	0.30	0.0220
13	285	11.50	0.320	359	2.77	0.260	0.30	0.0278
13	286	11.50	0.646	178	1.63	0.120	0.30	0.0164
14	287	10.30	0.270	382	4.52	0.305	0.22	0.0223
14	288	10.30	0.224	459	4.52	0.373	0.22	0.0335
14	289	10.30	0.261	395	4.52	0.316	0.22	0.0240
14	290	10.30	0.286	360	4.52	0.285	0.22	0.0195
14	291	10.30	0.272	379	4.52	0.302	0.22	0.0220
14	292	10.30	0.270	381	4.52	0.304	0.22	0.0223
14	293	10.30	0.271	381	4.52	0.304	0.22	0.0222
14	294	10.30	0.285	362	4.52	0.287	0.22	0.0198
14	295	10.50	0.363	289	1.21	0.220	0.22	0.191
14	296	10.50	0.329	319	1.21	0.245	0.22	0.237
14	297	10.50	0.398	264	1.21	0.198	0.22	0.155
14	298	10.50	0.400	263	1.21	0.197	0.22	0.154
14	299	10.50	0.406	259	1.21	0.194	0.22	0.149
14	300	2.54	0.327	77.6	2.69	0.246	0.22	0.0881
14	301	2.54	0.313	81.3	2.69	0.259	0.22	0.0977
14	302	2.54	0.400	63.5	2.69	0.197	0.22	0.0560
14	303	2.54	0.440	57.7	2.69	0.178	0.22	0.0450
14	304	2.54	0.305	83.3	2.69	0.266	0.22	0.1032
14	305	2.54	0.209	122	7.90	0.404	0.22	0.0595
14	306	2.54	0.223	114	7.90	0.376	0.22	0.0513
14	307	2.54	0.247	103	7.90	0.336	0.22	0.0407
14	308	2.54	0.279	91.0	7.90	0.293	0.22	0.0309
14	309	2.54	0.313	81.2	7.90	0.259	0.22	0.0239
14	310	2.54	0.223	114	7.90	0.376	0.22	0.0513
14	311	10.50	0.332	317	2.42	0.243	0.22	0.0345
14	312	10.50	0.336	313	2.42	0.239	0.22	0.0335

Table B3. Laboratory observations of initiation of motion of cylinders on smooth and rough beds (cont.)

<i>No.</i>	<i>Obs.</i>	<i>D</i>	<i>k</i>	<i>D/k</i>	ρ_o/ρ	$U_{crit}(z_{obs})$	z_{obs}	Θ_{Ucrit}
14	313	10.50	0.381	275	2.42	0.208	0.22	0.0253
14	314	10.50	0.361	291	2.42	0.221	0.22	0.0286
14	315	10.50	0.312	337	2.42	0.260	0.22	0.0396
14	316	2.54	1.93	13.2	2.69	0.470	0.22	0.288
14	317	2.54	1.93	13.2	2.69	0.516	0.22	0.347
14	318	2.54	1.93	13.2	2.69	0.425	0.22	0.236
14	319	2.54	1.93	13.2	2.69	0.458	0.22	0.274
14	320	2.54	1.93	13.2	7.90	0.801	0.22	0.204
14	321	10.50	1.93	54.4	1.21	0.226	0.22	0.197
14	322	10.50	1.93	54.4	1.21	0.229	0.22	0.202
14	323	10.50	1.93	54.4	1.21	0.228	0.22	0.200
14	324	10.50	1.93	54.4	1.21	0.234	0.22	0.212
14	325	10.30	1.93	53.4	4.52	0.710	0.22	0.117
14	326	10.30	1.93	53.4	4.52	0.711	0.22	0.117
14	327	10.30	1.93	53.4	4.52	0.803	0.22	0.149
14	328	10.30	1.93	53.4	4.52	0.767	0.22	0.136
14	329	10.50	2.96	35.5	2.42	0.614	0.22	0.211
14	330	10.50	2.96	35.5	2.42	0.569	0.22	0.181
14	331	10.50	2.96	35.5	2.42	0.552	0.22	0.171
14	332	10.50	2.96	35.5	2.42	0.565	0.22	0.179
14	333	10.50	2.96	35.5	2.42	0.553	0.22	0.172
14	334	10.50	2.96	35.5	1.21	0.229	0.22	0.200
14	335	10.50	2.96	35.5	1.21	0.253	0.22	0.243
14	336	10.50	2.96	35.5	1.21	0.260	0.22	0.256
14	337	10.50	2.96	35.5	1.21	0.225	0.22	0.193
14	338	2.54	2.96	8.6	2.69	0.571	0.22	0.406
14	339	2.54	2.96	8.6	2.69	0.531	0.22	0.352
14	340	2.54	2.96	8.6	2.69	0.497	0.22	0.307
14	341	2.54	2.96	8.6	2.69	0.496	0.22	0.306
14	342	10.62	3.56	29.8	1.21	0.241	0.22	0.218
14	343	10.62	3.56	29.8	1.21	0.236	0.22	0.208
14	344	10.62	3.56	29.8	1.21	0.220	0.22	0.181
14	345	10.62	3.56	29.8	1.21	0.220	0.22	0.182
14	346	10.62	3.56	29.8	1.21	0.215	0.22	0.174
14	347	10.62	3.56	29.8	2.42	0.472	0.22	0.123
14	348	10.62	3.56	29.8	2.42	0.490	0.22	0.133
14	349	10.62	3.56	29.8	2.42	0.435	0.22	0.105
14	350	10.62	3.56	29.8	2.42	0.444	0.22	0.109
14	351	10.62	3.56	29.8	2.42	0.440	0.22	0.107
14	352	10.42	3.56	29.3	4.52	0.760	0.22	0.131
14	353	10.42	3.56	29.3	4.52	0.623	0.22	0.0877

Table B3. Laboratory observations of initiation of motion of cylinders on smooth and rough beds (cont.)

<i>No.</i>	<i>Obs.</i>	<i>D</i>	<i>k</i>	<i>D/k</i>	ρ_o/ρ	$U_{crit}(z_{obs})$	z_{obs}	Θ_{Ucrit}
14	354	2.66	3.56	7.47	2.69	0.578	0.22	0.396
14	355	2.66	3.56	7.47	2.69	0.587	0.22	0.408
14	356	2.66	3.56	7.47	2.69	0.390	0.22	0.181
14	357	2.66	3.56	7.47	2.69	0.563	0.22	0.376
14	358	2.66	3.56	7.47	2.69	0.567	0.22	0.382
14	359	10.62	2.53	42.0	1.21	0.241	0.22	0.220
14	360	10.62	2.53	42.0	1.21	0.204	0.22	0.158
14	361	10.62	2.53	42.0	1.21	0.236	0.22	0.212
14	362	10.62	2.53	42.0	1.21	0.212	0.22	0.171
14	363	10.62	2.53	42.0	1.21	0.220	0.22	0.183
14	364	10.62	2.53	42.0	2.42	0.496	0.22	0.137
14	365	10.62	2.53	42.0	2.42	0.461	0.22	0.119
14	366	10.62	2.53	42.0	2.42	0.516	0.22	0.149
14	367	10.62	2.53	42.0	2.42	0.528	0.22	0.156
14	368	10.62	2.53	42.0	2.42	0.555	0.22	0.172
14	369	10.62	2.53	42.0	2.42	0.433	0.22	0.105
14	370	2.66	2.53	10.5	2.69	0.394	0.22	0.191
14	371	2.66	2.53	10.5	2.69	0.399	0.22	0.196
14	372	2.66	2.53	10.5	2.69	0.411	0.22	0.208
14	373	2.66	2.53	10.5	2.69	0.405	0.22	0.202
14	374	2.66	2.53	10.5	2.69	0.419	0.22	0.216
14	375	10.42	2.53	41.2	4.52	0.683	0.22	0.107
14	376	10.42	2.53	41.2	4.52	0.763	0.22	0.133
14	377	10.42	2.53	41.2	4.52	0.677	0.22	0.105
14	378	10.42	2.53	41.2	4.52	0.903	0.22	0.186
14	379	10.42	2.53	41.2	4.52	0.674	0.22	0.104
14	380	10.42	2.53	41.2	4.52	0.702	0.22	0.113
14	381	2.66	2.53	10.5	7.90	0.737	0.22	0.163
14	382	10.42	1.50	69.5	4.52	0.525	0.22	0.0662
14	383	10.42	1.50	69.5	4.52	0.488	0.22	0.0570
14	384	10.42	1.50	69.5	4.52	0.479	0.22	0.0550
14	385	10.42	1.50	69.5	4.52	0.482	0.22	0.0556
14	386	10.42	1.50	69.5	4.52	0.648	0.22	0.101
14	387	10.42	1.50	69.5	4.52	0.427	0.22	0.0437
14	388	10.42	1.50	69.5	4.52	0.536	0.22	0.0690
14	389	10.62	1.50	70.8	1.21	0.211	0.22	0.175
14	390	10.62	1.50	70.8	1.21	0.203	0.22	0.160
14	391	10.62	1.50	70.8	1.21	0.200	0.22	0.157
14	392	10.62	1.50	70.8	1.21	0.196	0.22	0.150
14	393	10.62	1.50	70.8	1.21	0.187	0.22	0.136
14	394	2.66	1.50	17.7	2.69	0.464	0.22	0.312

Table B3. Laboratory observations of initiation of motion of cylinders on smooth and rough beds (cont.)

<i>No.</i>	<i>Obs.</i>	<i>D</i>	<i>k</i>	<i>D/k</i>	ρ_o/ρ	$U_{crit}(z_{obs})$	z_{obs}	Θ_{Ucrit}
14	395	2.66	1.50	17.7	2.69	0.432	0.22	0.269
14	396	2.66	1.50	17.7	2.69	0.465	0.22	0.313
14	397	2.66	1.50	17.7	2.69	0.371	0.22	0.197
14	398	2.66	1.50	17.7	2.69	0.414	0.22	0.246
14	399	2.66	1.50	17.7	2.69	0.353	0.22	0.178
14	400	2.66	1.50	17.7	2.69	0.322	0.22	0.148
14	401	10.62	1.50	70.8	2.42	0.444	0.22	0.115
14	402	10.62	1.50	70.8	2.42	0.405	0.22	0.0959
14	403	10.62	1.50	70.8	2.42	0.422	0.22	0.104
14	404	10.62	1.50	70.8	2.42	0.435	0.22	0.110
14	405	10.62	1.50	70.8	2.42	0.497	0.22	0.145
14	406	10.62	1.50	70.8	2.42	0.437	0.22	0.112

Table B4. Notes regarding sources of individual parameters in Tables B1 to B3. See Table B1 to B3 and report text for additional definitions of variables.

<i>No.</i>	<i>Obs.</i>	<i>Notes</i>
1-10	1-182	$k = 2.5 d_{bed} = 2.5 d_{50}$ of bed grain distribution following Garcia (2008); $\rho_o = 2700 \text{ kg/m}^3$.
1-11	1-210	For gravel and spheres under steady currents, information regarding flow conditions at initiation of motion were presented in source articles in terms of θ_{crit} , i.e., the Shields parameter characterizing the stress acting on the far-field bed at the time of initiation of motion of the clast or sphere of interest. U_{crit} at a height $z = D$ above the bed was then estimated here based on a log-profile utilizing Eqns. (1), (13) and (14) in the report text with $u_* = (\theta_{crit}/\rho)^{1/2}$. Data included here are limited to $D > 0.5 \text{ cm}$ and $D/d_{bed} \geq 1$.
1-4	1-132	Field observations of natural gravel under steady flow.
1	1-23	Source: Hammond et al. (1984) from Komar (1996) for D, d_{50}, θ_{crit} (Fig.4.16, p.150).
2	24-72	Source: Carling (1983) from Komar (1996) for D, d_{50}, θ_{crit} (Fig.4.16, p.150).
3	73-116	Source: Milhous (1973) from Komar (1996) for D, d_{50}, θ_{crit} (Fig.4.16, p.150).
4	117-132	Source: Mao & Surian (2010) [MS10]. $D/d_{50}, \theta_{crit}$ (Fig.7, p.333). d_{50} here estimated as the mean of the minimum and maximum d_{50} of all transported grains as reported on p.333 of MS10.
5-10	1-132	Laboratory observations of natural gravel under steady flow; here limited to $D > 0.5 \text{ cm}$ and $D/d_{50} \geq 1$.
5	133-138	Source: Kuhnle (1993). d_{50} , (Fig.5, p.1409); $D/d_{50}, \theta_{crit}$ (Fig.6, p.1410).
6	139-159	Source: Patel & Ranga Raju (1999). d_{50} , (Table 1, p.41); D, θ_{crit} (Table 4, p.46).
7	160-162	Source: Wilcock (1987) from Wilcock & Southard (1988) [WS88]. d_{50} (Table 1, p.1138); D, θ_{crit} (Table 5, p.1144).
8	163-165	Source: Day (1980) from WS88. d_{50} (Table 1, p.1138); D, θ_{crit} (Table 5, p.1144).
9	166-179	Source: Misri et al. (1984) from WS88. d_{50} (Table 1, p.1138); D, θ_{crit} (Table 5, p.1145).
10	180-182	Source: Dhamotharan et al. (1980) from WS88. d_{50} (Table 1, p.1138); D, θ_{crit} (Table 5, p.1145).
11	183-210	Source: James (1993). D, ρ_o (Table 2, p.6); $D/d_{bed}, \theta_{crit}$ (Fig.4, p.7). $k = 0.75 d_{bed}$ for bed of closely packed spheres, following Schlichting & Gersten (2000) [SG00] (Fig.17.10, case No.5, p.531). Note that in SG00 Fig.17.10, they define the Nikuradse roughness as $k_s = 25 z_0$ under fully rough turbulence, while we define the Nikuradse roughness to be $k = 30 z_0$. So their finding of $k_s = (0.257/0.41) d_{bed}$ for closely packed spheres translates here to $k = (30/25) (0.257/0.41) d_{bed}$.
12-14	211-315	For these smooth beds cases, $k = 30z_0$, where $z_0 = \nu/(9u_*)$. For steady flow, u_* is determined by fitting observed velocity at height z_{obs} to $U(z_{obs}) = (1/\kappa) \log(z_{obs}/z_0)$. $U(z=D)$ is then extrapolated from $U(z_{obs})$ assuming a log profile. For waves, $u_* = (0.5 f_w)^{1/2} U_w$, where the wave friction factor, f_w is calculated iteratively following Pedocchi & Garcia (2009) (see text Eq. (18)). For waves it is assumed that $U(z=D) = U_w = U(z_{obs})$.
12	211-278	Source: Williams (2001). $D, \rho_o, U_{w,crit}, T$ (pp.90-97); $z_{obs} = 0.4$ to 1.0 cm above top of cylinder (p.36). Each $U_{w,crit}$ is calculated as the average of + and - directed orbital velocity amplitude for two consecutive experimental runs with the lower U_w producing no cylinder movement and the higher U_w producing cylinder movement. Run sequences were included only for cases for which $(onshore\ velocity + offshore\ velocity)/2$ for the cylinder movement case was greater than $(onshore\ velocity + offshore\ velocity)/2$ for the no motion case.
13	279-286	Source: Davis et al. (1999, 2007) [D99, D07]. $z_{obs} = 0.3 \text{ m}$ (D99 Fig.3, p.944); D, ρ_o (D99 Fig 6, p.947; D07 p.1436); U for the lowest velocities with cylinder movement

Table B4. Notes regarding sources of individual parameters in Table B1 to B3 (cont.)

<i>No.</i>	<i>Obs.</i>	<i>Notes</i>
14	287-406	(D99 Fig 6, p.947; D07 p.1436). U_{crit} is taken to be the average of two consecutive experimental runs with the lower U producing no cylinder movement and the higher U producing cylinder movement. The U intervals tested for determining U_{crit} for PVC cylinders were 4 cm/s apart (D99 p.946; D07 p.1436), whereas the U intervals tested for determining U_{crit} for steel cylinders were 2 cm/s apart (D99 Fig 6, p.947; D07 p.1436). Source: Brandt & Rennie (2013) [BR13], Rennie et al. (2017) [R17]. U_{crit} , D , ρ_o (BR13 Table 2, p.5); z_{obs} (R17 p.285). Note that the U_{crit} values in Table 2 of BR13 are averages of several runs for each case. The U_{crit} values presented here in Table B3 are the original velocity data for the individual runs as compiled before averaging (provided by S. Rennie via pers. comm.).
14	316-381	k for smooth cylinders on carpet (Obs. 316-342) was set equal to one half the measured heights of uncompressed carpet fibers because the carpet was observed to compress substantially under the test cylinders (R17 p.287). For sand-roughened cylinders on carpet, k was set to one half the fiber height plus the grain size of the sand glued onto the cylinders ($d_{coat} = 0.6$ mm) (R17 p.287).
14	382-406	For cylinders roughened with a coating of sand of diameter d_{coat} , but placed on a smooth bed, a contribution of $k = 2.5 d_{coat}$ was utilized in the ratio D/k , but the far field k relevant to log-layer structure did not include d_{coat} .

Appendix C. List of Scientific/Technical Publications

1. Articles in peer-reviewed journals and book chapters:

Rennie, S.E., Brandt, A. & Friedrichs, C.T. 2017. Initiation of motion and scour burial of objects underwater. *Ocean Engineering* 131: 282-294.

Friedrichs, C.T., Rennie, S.E. & Brandt, A. 2016. Self-burial of objects on sandy beds by scour: A synthesis of observations. In: Harris, J.M., Whitehouse, R.J.S. & Moxon, S. (eds.), *Scour and erosion*. CRC Press, 179-189.

2. Professional presentations: (All downloadable at <http://www.vims.edu/chsd/>)

Friedrichs, C.T., Rennie, S.E. & Brandt, A. 2017. Simple parameterized models for predicting mobility, burial, and re-exposure of underwater munitions. SERDP and ESTCP Symposium, Washington, DC, 28-30 November.

Friedrichs, C.T., Rennie, S.E. & Brandt, A. 2016. Self-burial of objects on sandy beds by scour: A synthesis of observations. 8th International Conference on Scour and Erosion, Oxford, UK. 12-15 September.

Friedrichs, C.T. 2015. Simple parameterized models for predicting mobility, burial, and re-exposure of underwater munitions. Workshop on Burial and Mobility Modeling of Munitions in the Underwater Environment, Johns Hopkins University Applied Physics Laboratory, Laurel, MD, 8 December.

Friedrichs, C.T. 2015. Factors affecting munitions mobility underwater. Strategic Environmental Research and Development Program/Environmental Security Technology Certification Program (SERDP/ESTCP) Webinar Series, 7 May.

Friedrichs, C.T. 2014. Simple parameterized models for predicting mobility, burial, and re-exposure of underwater munitions. In-Progress Review Meeting for the Munitions Response Program Area, The Potomac Institute for Policy Studies, Alexandria, VA, 21 May.

Friedrichs, C.T. 2013. Simple parameterized models for predicting mobility, burial, and re-exposure of underwater munitions. In-Progress Review Meeting for the Munitions Response Program Area, The Potomac Institute for Policy Studies, Alexandria, VA, 12 February.